THREE ESSAYS ON AGRICULTURAL PRICE VOLATILITY AND THE LINKAGES BETWEEN AGRICULTURAL AND ENERGY MARKETS

By

Feng Wu

A DISSERTATION

Submitted to
Michigan State University
in partial fulfillment of the requirements
for the degree of

DOCTOR OF PHILOSOPHY

Agricultural, Food and Resource Economics

2012

ABSTRACT

THREE ESSAYS ON AGRICULTURAL PRICE VOLATILITY AND THE LINKAGES BETWEEN AGRICULTURAL AND ENERGY MARKETS

By

Feng Wu

This dissertation contains three essays. In the first essay I use a volatility spillover model to find evidence of significant spillovers from crude oil prices to corn cash and futures prices, and that these spillover effects are time-varying. Results reveal that corn markets have become much more connected to crude oil markets after the introduction of the Energy Policy Act of 2005. Furthermore, crude oil prices transmit positive volatility spillovers into corn prices and movements in corn prices become more energy-driven as the ethanol gasoline consumption ratio increases. Based on this strong volatility link between crude oil and corn prices, a new cross hedging strategy for managing corn price risk using oil futures is examined and its performance studied. Results show that this cross hedging strategy provides only slightly better hedging performance compared to traditional hedging in corn futures markets alone. The implication is that hedging corn price risk in corn futures markets alone can still provide relatively satisfactory performance in the biofuel era.

The second essay studies the spillover effect of biofuel policy on participation in the Conservation Reserve Program. Landowners' participation decisions are modeled using a real options framework. A novel aspect of the model is that it captures the structural change in agriculture caused by rising biofuel production. The resulting model is used to simulate the spillover effect under various conditions. In particular, I simulate how increased growth in agricultural returns, persistence of the biofuel production boom, and the volatility surrounding

agricultural returns, affect conservation program participation decisions. Policy implications of these results are also discussed.

The third essay proposes a methodology to construct a risk-adjusted implied volatility measure that removes the forecasting bias of the model-free implied volatility measure. The risk adjustment is based on a closed-form relationship between the expectation of future volatility and the model-free implied volatility assuming a jump-diffusion model. I use a GMM estimation framework to identify the key model parameters needed to apply the model. An empirical application to corn futures implied volatility is used to illustrate the methodology and demonstrate differences between my approach and the model-free implied volatility using observed corn option prices. I compare the risk-adjusted forecast with the unadjusted forecast as well as other alternatives; and results suggest that the risk-adjusted volatility is unbiased, informationally more efficient, and has superior predictive power over the alternatives considered.

ACKNOWLEDGEMENTS

First and foremost I would like to gratefully and sincerely thank my dissertation supervisor, Dr. Zhengfei Guan, for his guidance, understanding, patience, and most importantly, his friendship during my graduate studies. He has supported me throughout my dissertation with his patience and knowledge whilst giving me the freedom to work in my own way. I appreciate all his contributions of time, ideas, and funding to make my Ph.D. experience productive and stimulating. I am also deeply indebted to my major professor Dr. Robert Myers. His insights and incisive analytical skills sharpened my analysis. I have benefitted tremendously from his insightful comments and constructive suggestions at different stages of my research. His encouragement of thinking like an applied economist will never be forgotten. I would also like to express my admiration and appreciation to my other committee members, Richard Baillie and Jinhua Zhao, for their helpful feedback on my research. Lastly, I would like to express my deepest appreciation towards my parents and family who have always been there for me no matter where I am, for unconditional support and patience.

TABLE OF CONTENTS

LIST OF TABLES

LIST OF FIGURES

KEY TO ABBREVIATIONS

BEKK	Baba-Engle-Kraft-Kroner
BS	Black-Scholes
CBOT	Chicago Board of Trade
CRP	Conservation Reserve Program
DM	Diebold-Mariano
EIA	Energy Information Administration
EISA	Energy Independence and Security Act
ERS	Economic Research Service
GBM	geometric Brownian motion
GMM	Generalized Method of Moments
HV	historical volatility
IV	integrated volatility
LCP	linear complementarity problem
MAE	mean absolute errors
MAPE	mean absolute percentage errors
MDM	modified Diebold-Mariano
MF	model-free
MTBE	Methyl Tertiary Butyl Ether
NASS	National Agricultural Statistics Service
NYMEX	New York Mercantile Exchange
QV	quadratic variation
RMSE	root-mean-square-errors

RV	realized volatility
SBC	Schwartz Bayesian Criterion
SD	standard deviations
USDA	U.S. Department of Agriculture
VEC	vector error correction

CHAPTER 1: VOLATILITY SPILLOVER EFFECTS AND CROSS HEDGING IN CORN AND CRUDE OIL FUTURES

1.1 Introduction

U.S. biofuel production has gone through a rapid expansion in response to both higher energy prices making biofuels more cost effective and government policies designed to reduce U.S. dependence on imported crude oil for energy needs (Tyner, 2008). Replacing fossil fuels with biofuels is also regarded by some as having the potential to at least partially address climate change issues as well as energy security. The expansion in biofuel production is expected to persist according to recent studies on the economics of biofuels (Liska et al., 2009; Feng, Rubin, and Babcock, 2010).

Rising biofuel production, particularly the production of corn-based ethanol, is likely to have made corn and crude oil markets more connected, possibly causing volatility spillovers from crude oil markets to corn markets. Zulauf and Roberts (2008) measured corn historical and expected volatilities from 1989 to 2007 and found corn price volatility has increased substantially over this period. Increased corn price volatility presumably results in greater costs for managing risks, such as more costly crop insurance premiums, higher option premiums, and higher hedging costs. Therefore, it is important to understand these new volatility relationships in order to inform and develop appropriate risk management strategies for corn market participants in an era of high biofuel production.

Volatility spillovers have been studied extensively in the finance literature (Bekaert and Harvey, 1997; Ng, 2000; Bekaert, Harvey, and Lumsdaine., 2002; Baele, 2005; and Christiansen, 2007). Many applications separate the shock to an individual country stock or bond return into three components: local, regional, and global. Ng (2000), for example, analyzes the sources of

return volatility of stock markets in the Pacific-Basin and finds transmission from the world and regional markets. However, volatility spillover effects have rarely been studied among commodities and may provide interesting insights into the nature of commodity price volatility and the connections between different markets. In particular, possible volatility spillovers from crude oil markets into corn markets have become an increasingly important issue given the growth in biofuel production.

In this study I examine volatility spillover effects from crude oil prices to corn prices, paying particular attention to the extent to which volatility in corn prices is impacted by external shocks from crude oil markets. More specifically, I construct a volatility spillover model and investigate the effect of shocks from the crude oil futures price on corn cash and futures prices. I compare three model specifications with different assumptions on the spillover effects: constant spillover parameters in the *constant* spillover model; differing spillover parameters before and after the introduction of the Energy Policy Act of 2005 in the *event* spillover model; and time-varying spillover parameters that are allowed to vary with the ratio of fuel ethanol consumption to gasoline consumption in the *substitution* spillover model. The constant spillover model reveals statistically significant volatility spillovers from crude oil prices into corn prices, with similar effects on corn cash and futures prices. The event spillover model shows that spillover intensities have increased significantly since the Energy Policy Act of 2005. In the substitution spillover model, I further examine the impact of fuel substitution on corn price volatility and show that the sign and size of a spillover depend on the magnitude of the ethanol-gasoline consumption ratio.

Given evidence of strong linkages between crude oil and corn markets, this study further examines a new cross hedging strategy to determine whether this would provide improved hedging performance for corn market participants. This cross hedging strategy allows portfolios

of corn cash, corn futures, and crude oil futures. A considerable amount of previous research has focused on optimal hedging strategies using corn futures (e.g., Baillie and Myers, 1991; Myers, 1991; and Moschini and Myers, 2002). However, previous research has not considered the possibility of hedging corn cash positions using both corn and crude oil futures simultaneously in a broader portfolio that allows for volatility spillovers. In this essay I compare the performance of the cross hedging strategy to that of conventional hedging strategies using corn futures only. The comparison sheds light on whether corn futures alone could continue to provide effective risk management for corn market participants in an era of increased biofuel production.

1.2 Trivariate Volatility Spillover Model

The volatility spillover studies of Bekaert and Harvey (1997), Ng (2000), Bekaert, Harvey and Ng (2005), Baele (2005), and Christiansen (2007) all consider volatility spillover effects on international stock and bond markets. For example, Ng (2000) develops a two-factor spillover model in which unexpected shocks to stock returns on any Pacific-Basin market are influenced by news (shocks) originating from two foreign markets. This literature has focused on spillovers in the same type of market (i.e. stock or bond market) at different levels (e.g., local, regional, or global). In this study, however, I investigate spillovers across two types of market, focusing on the impact of external shocks from the crude oil futures market on corn cash and futures prices.[1] The trivariate volatility spillover model has the general form:

[1] Crude oil spot prices could also be included explicitly in my analysis, but my ultimate interest lies in cross hedging a cash corn position in corn and crude oil futures markets. Therefore I restrict the analysis to the three key variables required for this purpose—corn spot prices, corn futures prices, and crude oil futures prices.

$$(1.1)\quad \begin{bmatrix} o_t \\ p_t \\ f_t \end{bmatrix} = \begin{bmatrix} E(o_t|I_{t-1}) \\ E(p_t|I_{t-1}) \\ E(f_t|I_{t-1}) \end{bmatrix} + \begin{bmatrix} \varepsilon_{o,t} \\ \varepsilon_{p,t} \\ \varepsilon_{f,t} \end{bmatrix},$$

$$(1.2)\quad \begin{bmatrix} \varepsilon_{o,t} \\ \varepsilon_{p,t} \\ \varepsilon_{f,t} \end{bmatrix} = \begin{bmatrix} 1 & 0 & 0 \\ \varphi_t & 1 & 0 \\ \omega_t & 0 & 1 \end{bmatrix} \begin{bmatrix} e_{o,t} \\ e_{p,t} \\ e_{f,t} \end{bmatrix},$$

$$(1.3)\quad Cov\begin{pmatrix} e_{o,t}|I_{t-1} \\ e_{p,t}|I_{t-1} \\ e_{f,t}|I_{t-1} \end{pmatrix} = \begin{pmatrix} \sigma^2_{o,t} & 0 & 0 \\ 0 & & \\ 0 & H_t & \end{pmatrix},$$

where o_t, p_t, and f_t denote crude oil futures price, corn cash price, and corn futures price, respectively; I_{t-1} is information available at time $t-1$; $\varepsilon_{o,t}$, $\varepsilon_{p,t}$, and $\varepsilon_{f,t}$ are respective prediction errors in the crude oil futures market, the corn cash market, and the corn futures market; $e_{o,t}$ is an idiosyncratic structural shock to oil futures; $[e_{p,t}, e_{f,t}]'$ is a vector of idiosyncratic structural shocks to corn cash and futures prices that may be mutually correlated but are both uncorrelated with $e_{o,t}$; $\sigma^2_{o,t}$ is a time varying conditional covariance for $e_{o,t}$; and H_t is a time-varying conditional covariance-variance matrix for $[e_{p,t}, e_{f,t}]'$. This model clearly allows oil futures price shocks to spill over into corn markets.

1.2.1 Model Specifications

In equation (1.1), oil futures, corn cash, and corn futures prices are composed of a conditional expectation that needs to be modeled. Here I specify a vector error correction (*VEC*) model for the conditional means:

$$(1.4)\quad \begin{bmatrix} \Delta o_t \\ \Delta p_t \\ \Delta f_t \end{bmatrix} = \begin{pmatrix} \beta_o \\ \beta_p \\ \beta_f \end{pmatrix} + \sum_{i=1}^{n} \Phi_i \begin{bmatrix} \Delta o_{t-i} \\ \Delta p_{t-i} \\ \Delta f_{t-i} \end{bmatrix} + \sum_{i=1}^{2} \Gamma_i \cdot ECT_i + \begin{bmatrix} \varepsilon_{o,t} \\ \varepsilon_{p,t} \\ \varepsilon_{f,t} \end{bmatrix},$$

where Δ is the first-difference operator; Φ_i ($i = 1, \ldots, n$) are three-by-three matrices of coefficients; Γ_i are three-by-one vectors of coefficients; and ECT_i denotes error correction terms to capture up to two cointegration relationships. The specification allows for past oil returns in the mean equations of corn markets and vice versa. In other words, past information about oil or corn prices can influence current price expectations for any of the prices. I also allow for possible seasonality in the conditional means, but empirical results show no significant seasonality so that seasonal variables are not included in the model specification. The specific form for the error correction model depends on the data and will be discussed in the data analysis section below.

I assume the crude oil shocks ($e_{o,t}$) follow a conditional normal distribution and allow its conditional variance ($\sigma_{o,t}^2$) to vary over time in response to changing market conditions. Since it is typically found that negative shocks lead to higher subsequent volatility than positive shocks of an equal magnitude, I follow Glosten, Jagannathan, and Runkle (GJR) (1993) and allow a GARCH process that accounts for an asymmetric volatility effect. The full GJR- GARCH(*m* ,*l*) for $\sigma_{o,t}^2$ takes the form:

$$(1.5)\quad e_{o,t} \Big| I_{t-1} \sim N(0, \sigma_{o,t}^2),$$

$$(1.6)\quad \sigma_{o,t}^2 = \alpha_0 + \sum_{i=1}^{l} \alpha_i e_{o,t-i}^2 + \sum_{i=1}^{l} \lambda_i d_{t-i} e_{o,t-i}^2 + \sum_{i=1}^{m} \tau_i \sigma_{o,t-i}^2 + \varsigma_0 z_t + \sum_{i=1}^{k} \varsigma_i Q_{it},$$

where $d_{t-i}\,(i=1,\ldots,l)$ are dummy variables that take a value of one if $e_{o,t-i}<0$ and zero if $e_{o,t-i}\geq 0$; z_t is the number of days to contract maturity to allow for time-to-maturity effects; and Q_{it} $(i=1,\ldots,k)$ are seasonal dummies..

In equation (1.2), shocks to the corn cash price and corn futures price are allowed to be driven by an external shock from the crude oil market in addition to a purely idiosyncratic component. Volatility spillover effects from the crude oil market to corn cash and futures markets are introduced via the idiosyncratic crude oil shock $e_{o,t}$ while $e_t=[e_{p,t},e_{f,t}]'$ is assumed to be uncorrelated with $e_{o,t}$ and follow a conditional normal distribution with mean zero and time-varying covariance matrix H_t. There are several possible parameterizations of the resulting bivariate GARCH process for $[e_{p,t},e_{f,t}]'$ including the VECH model of Bollerslev, Engle, and Wooldridge (1988), the constant correlation model of Bollerslev (1990), the factor ARCH model of Engle, Ng, and Rothschild (1990), and the Baba-Engle-Kraft-Kroner (BEKK) model defined in Engle and Kroner (1995). The asymmetric version of the BEKK model (Kroner and Ng, 1998) is used here to account for a possibly asymmetric volatility effect, due to the fact that negative shocks might have a bigger impact on future volatility than do positive shocks of the same size. The generalized BEKK(*m*,*l*) model is then specified as:

$$(1.7)\quad [e_{p,t}\quad e_{f,t}]'\,|\,I_{t-1}\sim N(0,H_t),$$

$$(1.8)\quad H_t=C'C+\sum_{i=1}^{l}A_i'e_{t-i}e_{t-i}'A_i+\sum_{i=1}^{l}D_i'\eta_{t-i}\eta_{t-i}'D_i+\sum_{i=1}^{m}B_i'H_{t-i}B_i+G\otimes z_t,$$

where *C*, *A*, *B*, and *D* are lower triangular matrices; *G* is a symmetric matrix; $\otimes$ is a Kronecker product; and z_t is a strictly exogenous variable, representing the number of days to contract maturity. The vector $\eta_t=[\eta_{p,t}\quad \eta_{f,t}]'$ represents the vector of negative shocks with

$\eta_t = \min\{0, e_t\}$. I also allow for possible seasonality in the covariance structure using dummy variables. However, later results indicate that the coefficients on seasonal dummies are small and not statistically significant. Therefore, seasonal variables are excluded from (1.8).

1.2.2 Parameterizations for Volatility Spillovers

Three different parameterizations for the spillover parameters, φ_t and ω_t, are introduced. The first specification assumes that the spillover parameters are constant throughout the entire sample period and investigates whether there are significant volatility spillovers from crude oil prices:

(1.9) $\varphi_t = \varphi$,

(1.10) $\omega_t = \omega$.

However, some studies have found that spillovers vary in intensity in response to various influences, especially to important legislative or policy events. In the present context, the Energy Policy Act of 2005 is particularly important. This Act established the Renewable Fuel standard requiring that transportation fuels sold in the US contain a minimum amount of renewable fuel, and also mandates increasing domestic use of renewable fuels to 7.5 billion gallons by 2012.[2] Subsequent tax incentives, federal and state mandates, and the progressive elimination of MTBE (Methyl Tertiary Butyl Ether) as an additive in many states, have quickly increased the demand for biofuels, particularly corn-based ethanol. The linkage between crude oil prices and corn

[2] Under the act, for the calendar years 2006 through 2012 the applicable volumes of biofuel that must be mixed with gasoline sold in the United States increase from 4, 4.7, 5.4, 6.1, 6.8, 7.1, 7.4, and 7.5 billion gallons, respectively. However, I would argue that these future mandates became known when the act was passed in 2005, and that rational agents would immediately build these expectations into current pricing and price expectations. Therefore, I view the date when the act was passed as the key determinant of the main change in the oil-corn price relationships.

prices is thus likely to have strengthened as a result of the Act. Therefore, I allow the Act to have an impact on spillover effects in the event spillover specification:

(1.11) $\varphi_t = \varphi_0 + \varphi_1 D_t$,

(1.12) $\omega_t = \omega_0 + \omega_1 D_t$,

where D_t is dummy variable which equals 1 for the period after the Act is passed (Jul 29, 2005) and 0 otherwise.

Third, I further relax the assumption of constant spillovers. Other volatility spillover studies have found evidence of time-varying correlations across national stock and bond markets (Ng, 2000; Christiansen, 2007). To explore the possibility of time-varying volatility spillovers further I allow spillover parameters to vary with certain underlying factors. In view of the substitution effect between different types of energy, I might expect corn prices and crude oil prices to become more connected as the ratio of fuel ethanol consumption to gasoline consumption rises. Therefore I use this ratio as an indicator of the size of spillovers between the markets. It is likely that rising ethanol consumption, and thus a high consumption substitution ratio in response to high crude oil prices, will also push up the demand for corn, the major feedstock of ethanol, thereby increasing the integration of crude oil and corn markets. Thus a more appropriate way of investigating the behavior of spillover effects may be to allow the parameters to vary with the ethanol to gasoline consumption ratio. To avoid potential endogeneity problems, I use lagged consumption ratios to capture the time-varying spillovers. The specification of the substitution spillover model is therefore:

(1.13) $\varphi_t = \varphi_0 + \varphi_1 R_{t-1}$,

(1.14) $\omega_t = \omega_0 + \omega_1 R_{t-1}$,

where R_{t-1} is the consumption ratio of the previous period.[3]

1.2.3 Volatility Spillover Ratio

Under the assumption of no correlation between $e_{o,t}$ and $[e_{p,t}, e_{f,t}]'$, the conditional variances of corn cash and futures prices are given by:

$$(1.15)\quad E(\varepsilon_{p,t}^2 \mid I_{t-1}) = H_t^{11} + \varphi_t^2 \sigma_{o,t}^2 ,$$

$$(1.16)\quad E(\varepsilon_{f,t}^2 \mid I_{t-1}) = H_t^{22} + \omega_t^2 \sigma_{o,t}^2 ,$$

where H_t^{ij} is the element in the *i*-th row and the *j*-th column of H_t. The signs and significance of φ_t and ω_t determine whether volatility spillover effects from crude oil markets are present in corn markets. To measure the proportion of the forecast error variance of corn markets that is accounted for by crude oil volatility spillover effects, I define spillover ratios for corn cash and futures prices as:

$$(1.17)\quad SR_{p,t} = \frac{\varphi_t^2 \sigma_{o,t}^2}{H_t^{11} + \varphi_t^2 \sigma_{o,t}^2} \in [0,1],$$

$$(1.18)\quad SR_{f,t} = \frac{\omega_t^2 \sigma_{o,t}^2}{H_t^{22} + \omega_t^2 \sigma_{o,t}^2} \in [0,1].$$

[3] Using lagged consumption ratios in the substitution spillover model is mainly intended to avoid potential endogeneity and thus simplify joint estimation of eqs. (1.2), (1.7), (1.8), (1.13), and (1.14). However, this treatment may raise issues regarding the specification of dynamics. I replaced lagged consumption ratios with contemporaneous ratios and re-estimated eqs. (1.2), (1.13), and (1.14) using an IV regression (the instrument is lagged consumption ratios) with robust standard errors. Coefficient estimates for consumption ratios are similar to those in the substitution spillover model.

These ratios summarize the relative importance of shocks in crude oil markets on volatility in corn markets at different points in time.

1.3 Data and Estimation

Weekly data are used in the study, covering the period from January 2, 1992 to June 30, 2009. All price data are the mid-week closing price (Thursday) and include 883 observations. Corn cash price p_t is the average of the low and high bids for #2 yellow corn from mid-states Terminals, Toledo, Ohio. The prices were obtained from quotes in the Livestock and Grain Market News Portal, USDA. The corn futures price f_t is for the nearest expiration contract[4] on the CBOT. The crude oil futures price o_t is for the nearest expiration contract[5] on light, sweet crude oil traded on NYMEX. Fuel ethanol consumption data (in thousands of gallons) are obtained from the energy review of the Energy Information Administration (EIA). Gasoline consumption refers to U.S. total gasoline sales/deliveries of prime suppliers and these data are from the Petroleum Marketing Monthly of EIA. Figure 1.1 plots the movement of the event dummy and the ethanol-gasoline consumption ratio variables. The ratio exhibits a strong upward trend with an average increase of 16.84%. Since ratios were higher during the latter half of the sample, its correlation coefficient with the event dummy is fairly high (0.87). The presence of such co-movement should not be surprising since the Act also drives the energy substitution ratio.

[4] The last trade date for corn futures contracts is the business day prior to the 15th calendar day of the contract month.

[5] For crude oil, each contract expires on the third business day prior to the 25th calendar day of the month preceding the delivery month. If the 25th calendar day of the month is a non-business day, trading ceases on the third business day prior to the business day preceding the 25th calendar day. After a contract expires, the nearest expiration contract for the remainder of that calendar month is the second following month.

Figure 1.1. Movement of the Event Dummy and the Ethanol-Gasoline Consumption Ratio Variables ("For interpretation of the references to color in this and all other figures, the reader is referred to the electronic version of this dissertation.")

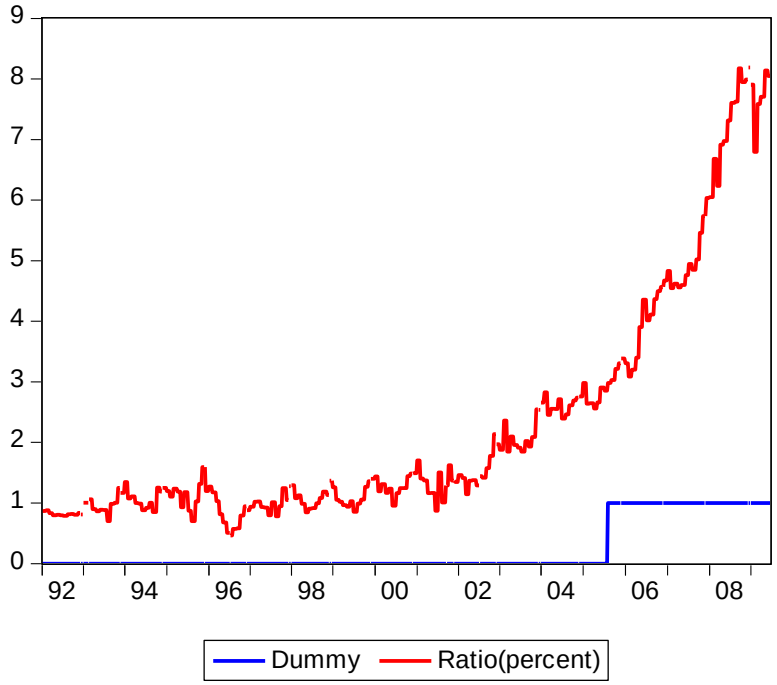

Table 1.1 presents summary statistics for weekly price series over the sample period and for three sub-periods, separated by two important dates, the first being July 29, 2005 when the Energy Policy Act of 2005 was passed, and the second being July 3, 2008 when the crude oil price climbed to its historical record high. The correlation matrices show that the connection between corn prices and crude oil prices changes from a weak negative into a strong positive relationship. The skewness and excess kurtosis measures show that the price change distributions are asymmetric and fat-tailed. Formal testing rejects the null hypothesis of unconditional normality at the 5% level of significance.[6]

[6] The Shapiro–Wilk test is used to test the null hypotheses that each sample series of price changes is normally distributed. The test statistics for the change of corn cash, corn futures, and crude oil futures prices are 0.87, 0.84 and 0.86, respectively. The *p*-values show all the null hypotheses are rejected at the 5% significant level.

Table 1.1. Descriptive Statistics and Correlation Analysis

Descriptive Statistics				Correlation			
Jan2, 1992- Jul 28, 2005 (689 obs.)							
	p_t	f_t	o_t		p_t	f_t	o_t
Mean	2.3980	2.4695	25.0246	p_t	1.0000		
Std. dev.	0.5950	0.5369	10.0282	f_t	0.9809	1.0000	
Min	1.5800	1.7625	10.7200	o_t	-0.1985	-0.2099	1.0000
Max	5.4300	5.4000	67.4900				
Aug 4, 2005-Jul 3, 2008(150 obs.)							
	p_t	f_t	o_t		p_t	f_t	o_t
Mean	3.4136	3.5877	77.6336	p_t	1.0000		
Std. dev.	1.3864	1.3927	22.0097	f_t	0.9965	1.0000	
Min	1.5250	1.8825	50.4800	o_t	0.8183	0.8271	1.0000
Max	7.1950	7.5375	145.2900				
Jul 10, 2008-Jun 30, 2009(44 obs.)							
	p_t	f_t	o_t		p_t	f_t	o_t
Mean	4.0865	4.1960	65.1375	p_t	1.0000		
Std. dev.	0.6022	0.6898	25.4375	f_t	0.9903	1.0000	
Min	3.1800	3.1825	33.9800	o_t	0.8968	0.9263	1.0000
Max	5.7050	5.9775	121.1800				
Full Sample (883 obs.)							
	p_t	f_t	o_t		p_t	f_t	o_t
Mean	2.6546	2.7455	35.9604	p_t	1.0000		
Std. dev.	0.9329	0.9278	24.9612	f_t	0.9904	1.0000	
Min	1.5250	1.7625	10.7200	o_t	0.5849	0.6318	1.0000
Max	7.1950	7.5375	145.2900				
Skewness	-1.0072	-0.9383	-0.9976				
Kurtosis	12.9611	13.0195	12.9390				

Notes: skewness and kurtosis are presented for the weekly change in the price series.

As with most weekly asset price data, Augmented Dickey-Fuller tests and Phillips-Perron tests could not reject the unit root hypothesis in any of the three price series. Johansen tests with and without trend specifications show that there is no evidence of cointegration between crude oil futures and either corn cash or futures prices, which suggests no long-run equilibrium relationship between crude oil prices and corn prices. Johansen tests also suggest a cointegrating relationship of order one between corn cash and futures prices, as confirmed in other research (Beck, 1994). The exact form of the Johansen cointegration test depends on the specification of deterministic components of the system. Here I include a linear trend to account for carrying charges and changes in convenience yield over time to maturity. Table 1.2 presents these Johansen cointegration test results. Neither the trace statistics nor the maximum eigenvalue statistics in the first difference reject one cointegrating relationship at the 5% level.[7] An error correction model is therefore chosen for the mean equations for corn cash and futures prices.

Table 1.2. Johansen Cointegration Test

Null (H_0)	Alternative (H_1)	$\lambda_{\max}$	λ_{trace}
Corn cash and futures			
Rank = 0	Rank $\geq$ 1	27.08**	33.32**
Rank $\leq$ 1	Rank $\geq$ 2	6.24	6.24
Corn cash and crude oil futures			
Rank = 0	Rank $\geq$ 1	17.82	11.16
Rank $\leq$ 1	Rank $\geq$ 2	6.65	6.65
Corn futures and crude oil futures			
Rank = 0	Rank $\geq$ 1	18.20	11.46
Rank $\leq$ 1	Rank $\geq$ 2	6.74	6.74

Note: ** denotes rejection of the null hypothesis at the 5% significance levels. $\lambda_{\max}$ critical values at the 5% significant level under the two null hypotheses are 18.96 and 12.52, while λ_{trace} critical values at the same level are 25.32 and 12.25, respectively.

[7] Under other trend specifications, the two statistics in the first difference do not reject one cointegrating rank at the 5% level, either.

Given the large number of parameters that would have to be estimated in the spillover model, I follow a two-step procedure similar to that implemented by Bekaert and Harvey (1997), Ng (2000), and Baele (2005).[8] In the first step the vector error correction model (equation (1.4)) is estimated to obtain estimates of the forecast errors $(\varepsilon_{o,t}, \varepsilon_{p,t}, \varepsilon_{f,t})$ for oil futures, corn cash, and futures prices. In the second step, the first stage residuals are used as data in joint maximum likelihood estimation of the trivariate spillover model (Equations (1.2), (1.7) and (1.8)), assuming the purely idiosyncratic shock vector has a bivariate conditional normal distribution with mean zero and time-varying variance matrix. I report the Bollerslev-Wooldridge robust quasi-maximum likelihood covariance matrix, which is robust to misspecification of the distribution of the error term. For the event or substitution spillover model, equations (1.11)-(1.12) or equations (1.13)-(1.14) are substituted into equation (1.2) and the same maximum likelihood estimation procedure is implemented.

Based on results from the unit root and cointegration analysis, equation (1.4) is estimated by restricting one cointegration relationship between corn cash and corn futures prices and zero adjustment parameter for the oil price ($\Gamma_1^{11} = 0$). The estimation is implemented by Engel-Granger two-step procedure to *VEC*(10) which renders all residuals white noise and results are given in Table 1.3. The *Q*-statistics at lags from 1 to 53 confirm that there is no significant autocorrelation at the 1% level in the residuals. The results show that the crude oil returns series has statistically significant autocorrelations at lags 1, 4, and 8. The Wald statistic for the joint significance of all lagged oil price changes indicates that they have significant explanatory power for future oil price returns. These results suggest that the oil futures price does not follow a

[8] It may be more desirable to estimate the system jointly, but this is often not feasible due to the large number of parameters to be estimated in spillover models. The two-step method yields consistent but not necessarily efficient estimates (Ng, 2000).

martingale. Sadorsky (2002) suggests this is due to futures markets not being unbiased due to the existence of a risk premium. Also, it is found that the corn futures price has a similar characteristic. In the last row of the table, I also give results for estimation of the cointegration relationship between corn cash and futures prices.

Table 1.3. Vector Error Correction Model for Oil Futures, Corn Cash, and Futures Prices

$$\begin{bmatrix} \Delta o_t \\ \Delta p_t \\ \Delta f_t \end{bmatrix} = \begin{pmatrix} \beta_o \\ \beta_p \\ \beta_f \end{pmatrix} + \sum_{i=1}^{10} \Phi_i \begin{bmatrix} \Delta o_{t-i} \\ \Delta p_{t-i} \\ \Delta f_{t-i} \end{bmatrix} + \begin{pmatrix} 0 \\ \Gamma_{12} \\ \Gamma_{13} \end{pmatrix} \cdot ECT + \begin{bmatrix} \varepsilon_{o,t} \\ \varepsilon_{p,t} \\ \varepsilon_{f,t} \end{bmatrix}$$

Δo_t	Coe.	t statistic	Δp_t	Coe.	t statistic	Δf_t	Coe.	t statistic
β_o	0.0339	0.4716	β_p	0.0013	0.2966	β_f	0.0010	0.2337
$\Phi_1^{1,1}$	-0.0794	-2.1819	$\Phi_1^{2,1}$	-0.0065	-3.0305	$\Phi_1^{3,1}$	-0.0073	-3.3807
$\Phi_2^{1,1}$	0.0698	1.9076	$\Phi_2^{2,1}$	-0.0047	-2.1765	$\Phi_2^{3,1}$	-0.0042	-1.9086
$\Phi_3^{1,1}$	-0.0344	-0.9416	$\Phi_3^{2,1}$	0.0022	1.0219	$\Phi_3^{3,1}$	0.0021	0.9531
$\Phi_4^{1,1}$	0.1026	2.8190	$\Phi_4^{2,1}$	0.0018	0.8549	$\Phi_4^{3,1}$	0.0015	0.7016
$\Phi_5^{1,1}$	0.0107	0.2922	$\Phi_5^{2,1}$	-0.0007	-0.3343	$\Phi_5^{3,1}$	0.0010	0.4729
$\Phi_6^{1,1}$	-0.0204	-0.5615	$\Phi_6^{2,1}$	0.0013	0.6085	$\Phi_6^{3,1}$	0.0000	-0.0133
$\Phi_7^{1,1}$	0.0556	1.5345	$\Phi_7^{2,1}$	0.0029	1.3760	$\Phi_7^{3,1}$	0.0044	2.0530
$\Phi_8^{1,1}$	0.1041	2.8514	$\Phi_8^{2,1}$	-0.0013	-0.5870	$\Phi_8^{3,1}$	-0.0009	-0.3986
$\Phi_9^{1,1}$	0.0121	0.3351	$\Phi_9^{2,1}$	-0.0030	-1.4304	$\Phi_9^{3,1}$	-0.0004	-0.2024
$\Phi_{10}^{1,1}$	-0.0101	-0.2802	$\Phi_{10}^{2,1}$	-0.0004	-0.1847	$\Phi_{10}^{3,1}$	0.0001	0.0251
$\Phi_1^{1,2}$	-1.9699	-1.4182	$\Phi_1^{2,2}$	0.3988	4.8895	$\Phi_1^{3,2}$	0.3230	3.9047
$\Phi_2^{1,2}$	-0.8845	-0.6300	$\Phi_2^{2,2}$	-0.3411	-4.1373	$\Phi_2^{3,2}$	-0.3748	-4.4816
$\Phi_3^{1,2}$	-1.9306	-1.3842	$\Phi_3^{2,2}$	-0.0470	-0.5743	$\Phi_3^{3,2}$	0.0536	0.6447
$\Phi_4^{1,2}$	0.5977	0.4270	$\Phi_4^{2,2}$	0.2922	3.5555	$\Phi_4^{3,2}$	0.2500	2.9996
$\Phi_5^{1,2}$	0.8436	0.5986	$\Phi_5^{2,2}$	0.0006	0.0067	$\Phi_5^{3,2}$	-0.0708	-0.8429
$\Phi_6^{1,2}$	-3.3482	-2.3739	$\Phi_6^{2,2}$	0.0616	0.7438	$\Phi_6^{3,2}$	-0.0257	-0.3059

Table 1.3. (Cont'd)

Δo_t	Coe.	t statistic	Δp_t	Coe.	t statistic	Δf_t	Coe.	t statistic
$\Phi_7^{1,2}$	0.7887	0.5557	$\Phi_7^{2,2}$	0.0026	0.0311	$\Phi_7^{3,2}$	-0.0546	-0.6463
$\Phi_8^{1,2}$	-0.9950	-0.7084	$\Phi_8^{2,2}$	-0.1911	-2.3174	$\Phi_8^{3,2}$	-0.0675	-0.8072
$\Phi_9^{1,2}$	2.4941	1.7713	$\Phi_9^{2,2}$	0.1386	1.6767	$\Phi_9^{3,2}$	0.1837	2.1900
$\Phi_{10}^{1,2}$	-2.0340	-1.4420	$\Phi_{10}^{2,2}$	-0.1369	-1.6529	$\Phi_{10}^{3,2}$	-0.0968	-1.1524
$\Phi_1^{1,3}$	4.3851	3.1326	$\Phi_1^{2,3}$	-0.3186	-3.8766	$\Phi_1^{3,3}$	-0.2125	-2.5490
$\Phi_2^{1,3}$	2.4240	1.7130	$\Phi_2^{2,3}$	0.3999	4.8137	$\Phi_2^{3,3}$	0.4179	4.9581
$\Phi_3^{1,3}$	2.8348	2.0042	$\Phi_3^{2,3}$	0.0514	0.6187	$\Phi_3^{3,3}$	-0.0288	-0.3414
$\Phi_4^{1,3}$	-1.1809	-0.8359	$\Phi_4^{2,3}$	-0.2653	-3.1986	$\Phi_4^{3,3}$	-0.2290	-2.7215
$\Phi_5^{1,3}$	0.9783	0.6899	$\Phi_5^{2,3}$	0.0444	0.5336	$\Phi_5^{3,3}$	0.0903	1.0686
$\Phi_6^{1,3}$	3.9776	2.8076	$\Phi_6^{2,3}$	-0.1222	-1.4689	$\Phi_6^{3,3}$	-0.0252	-0.2989
$\Phi_7^{1,3}$	0.4389	0.3068	$\Phi_7^{2,3}$	0.0110	0.1307	$\Phi_7^{3,3}$	0.0371	0.4353
$\Phi_8^{1,3}$	2.2964	1.6324	$\Phi_8^{2,3}$	0.2482	3.0050	$\Phi_8^{3,3}$	0.1703	2.0325
$\Phi_9^{1,3}$	-3.8311	-2.7160	$\Phi_9^{2,3}$	-0.1201	-1.4497	$\Phi_9^{3,3}$	-0.1985	-2.3630
$\Phi_{10}^{1,3}$	3.9367	2.7638	$\Phi_{10}^{2,3}$	0.3006	3.5945	$\Phi_{10}^{3,3}$	0.2600	3.0651
			Γ_1^{12}	-0.0102	-2.4647	Γ_1^{13}	-0.0015	-0.3532

p_t	Coe.	t statistic
f_t	1.0202	158.7372
Trend	-0.0002	-8.4505
Cons.	-0.0811	-4.5569

Note: Φ_l^{ij} is the element in the *i*-th row and the *j*-th column of Φ_l ($l = 1, \cdots, 10$)

1.4 Spillover Model Results

The spillover models are estimated under different spillover parameterizations. This section presents and discusses the estimation results with a BEKK (1, 1) process for H_t.

1.4.1 The Constant Spillover Model

I first constrain all spillover parameters to be constant over time. The estimation results are presented in Table 1.4.[9] First, D(1,1) is negative and statistically significant at the 1% level, which supports the existence of asymmetric volatility in the corn cash price. Second, all elements in matrix *G* are insignificant at the 5% level, which suggests no time-to-maturity effects in corn price volatilities. Third, estimated coefficients in the ARCH and GARCH matrices (*A* and *B*) are also significant and have large magnitudes, which suggests volatility persistence.

In the spillover functions I find significant volatility spillover effects from crude oil prices to corn prices (φ and ω are positive and statistically significant at the 1% level). The positive sign shows evidence of increased volatility of corn prices due to spillovers from crude oil prices. Robust Wald tests reject the joint hypothesis of no spillover effects, $H_0 : \varphi = \omega = 0$, at the 1% level. Also, results do not reject the null hypothesis, $H_0 : \varphi = \omega$, at the 1% level, suggesting that volatilities for corn cash and futures prices are influenced by crude oil prices to the same extent.

[9] Test results show that the estimated BEKK model captures all dynamics in the means and variances of corn prices. The estimated residuals are serially uncorrelated and have no GARCH effects. The null hypothesis that the Ljung-Box *Q*-statistics of the standardized residuals and the squared standardized residuals are equal to zero is not rejected.

Table 1.4. Estimation of the Constant Volatility Spillover Model

$$\begin{bmatrix} \varepsilon_{o,t} \\ \varepsilon_{p,t} \\ \varepsilon_{f,t} \end{bmatrix} = \begin{bmatrix} 1 & 0 & 0 \\ \varphi_t & 1 & 0 \\ \omega_t & 0 & 1 \end{bmatrix} \begin{bmatrix} e_{o,t} \\ e_{p,t} \\ e_{f,t} \end{bmatrix},$$

$$[e_{p,t}, e_{f,t}]' | I_{t-1} \sim N(0, H_t),$$

$$H_t = C'C + A'e_{t-1}e_{t-1}^{'}A + B'H_{t-1}B + D'\eta_{t-1}\eta_{t-1}^{'}D + G \otimes z_t .$$

	Coefficient	Std. Error	z-Statistic	p-value
φ	0.0088	0.0014	6.3661	0.0000
ω	0.0099	0.0014	6.8722	0.0000
C(1,1)	0.0003	0.0001	2.5410	0.0111
C(1,2)	0.0003	0.0001	2.5391	0.0111
C(2,2)	0.0003	0.0001	1.9556	0.0505
A(1,1)	0.0881	0.0120	7.3203	0.0000
A(1,2)	0.0746	0.0100	7.4230	0.0000
A(2,2)	0.0900	0.0132	6.8326	0.0000
D(1,1)	-0.0475	0.0133	-3.5655	0.0004
D(1,2)	-0.0253	0.0133	-1.9053	0.0567
D(2,2)	-0.0088	0.0175	-0.5053	0.6133
B(1,1)	0.9084	0.0116	78.2287	0.0000
B(1,2)	0.9040	0.0116	77.6592	0.0000
B(2,2)	0.8769	0.0148	59.1153	0.0000
G(1,1)	0.0000	0.0000	-1.0406	0.2981
G(1,2)	0.0000	0.0000	-0.7638	0.4450
G(2,2)	0.0000	0.0000	0.2262	0.8210
Log-likelihood		2342.4140		
SBC		-5.2405		

Before estimating the time series of the spillover ratios from equations (1.17)-(1.18), I first estimate the conditional variance of the crude oil shock from equations (1.5) and (1.6). The results of the TGARCH(1,1) model are presented in Table 1.5. As expected, I find time-to-maturity effects and seasonality. But there are no significant asymmetric effects in the volatility of crude oil futures prices. On average over the sample period, the crude oil volatility spillover effect makes up from 0 to 23.572% of the conditional variance of the corn cash market shocks, while it makes up a bigger proportion (between 0 and 30.52%) of the corn futures prices (Table

1.6). The mean energy spillover ratios are 2.89% and 3.49% for corn cash and futures prices, respectively.

Table 1.5. Univariate TGARCH (1, 1) Models for Crude Oil Futures Price

$$\sigma_{o,t}^2 = \alpha_0 + \alpha_1 e_{o,t-1}^2 + \lambda_1 d_{t-1} e_{o,t-1}^2 + \tau_1 \sigma_{o,t-1}^2 + \varsigma_0 z_t + \sum_{i=1}^{51} \varsigma_i Q_{it}$$

	Coefficient	Std. Error	z-Statistic	p-value
α_0	3.8134	2.3882	1.5968	0.1103
α_1	0.2161	0.0470	4.5965	0.0000
λ_1	0.1172	0.0668	1.7548	0.0793
τ_1	0.5793	0.0566	10.2351	0.0000
ς_0	-0.0422	0.0113	-3.7397	0.0002

Note: seasonal variables are weekly dummies with the total number of 51 and their coefficient estimates are not reported in the table to save space.

Table 1.6. Summary Statistics of Spillover Ratio for Three Models

	Constant Spillover		Event Spillover				Sub. Spillover	
			Before the Act		After the Act			
	Cash	Futures	Cash	Futures	Cash	Futures	Cash	Futures
Mean	0.0289	0.0349	0.0108	0.0170	0.0953	0.0940	0.0310	0.0344
Median	0.0211	0.0267	0.0078	0.0127	0.0812	0.0780	0.0040	0.0096
Maximum	0.2357	0.3052	0.1068	0.1821	0.2780	0.2884	0.5656	0.4834
Minimum	0.0001	0.0001	0.0000	0.0000	0.0124	0.0100	0.0000	0.0000
Std. Dev.	0.0242	0.0290	0.0100	0.0158	0.0563	0.0550	0.0609	0.0554

In sum, the volatility spillover effect from crude oil prices is statistically significant but accounts for a relatively small proportion of total volatility in corn prices. Figure 1.2 shows the time series evolution of spillover ratios for the corn market.[10] There are some relatively high spillovers after 2005. However, the overall spillover effect throughout the sample period is relatively small in many periods.

[10] Spillover ratios spike in early 2003. This abrupt shock captures the impact of the Iraq War.

Figure 1.2. Spillover Ratios for Corn Cash (*SRP*) and Futures (*SRF*) Markets – the Constant Spillover Model

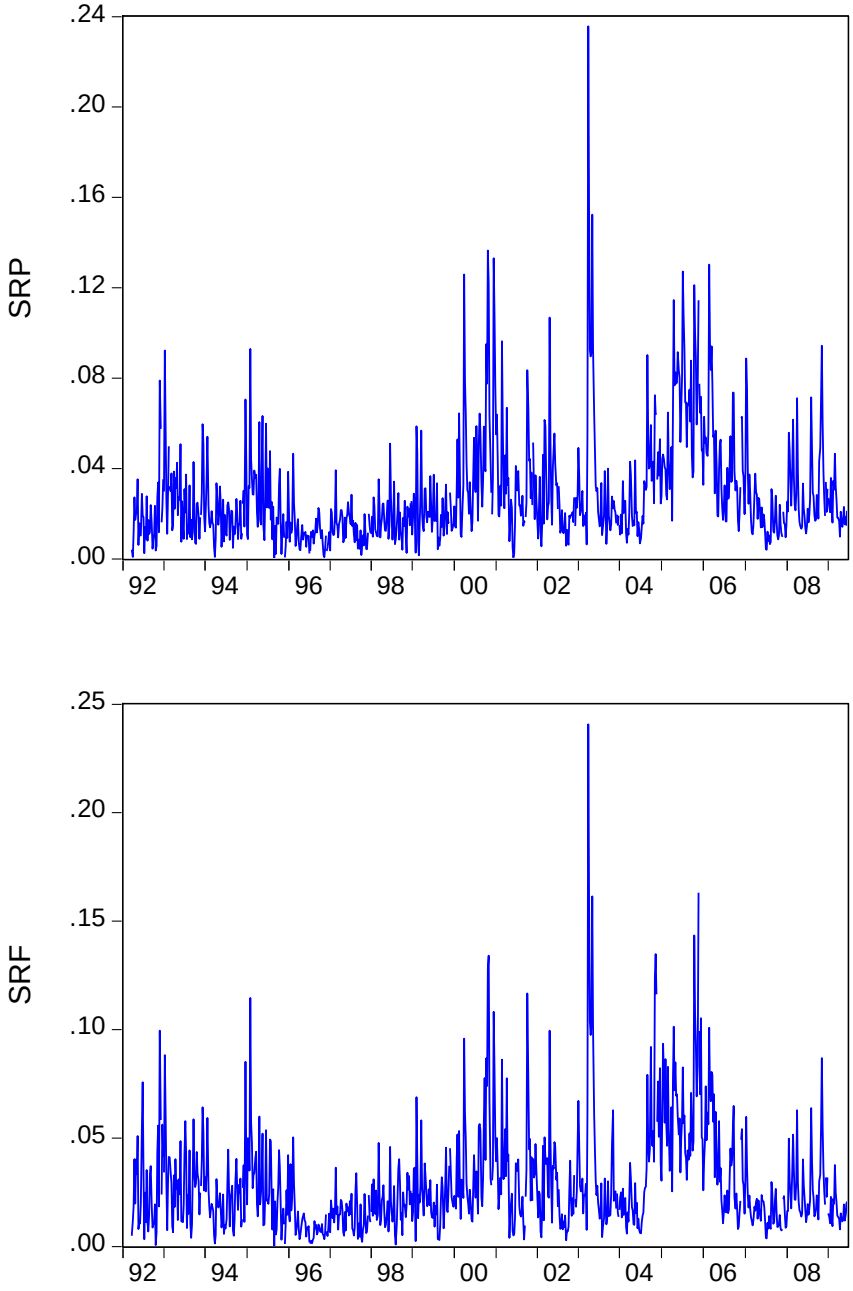

1.4.2 The Event Spillover Model

The event spillover model accounts for changes brought about by the introduction of the Energy Policy Act of 2005, allowing spillover parameters to take on different values before and after the event. The estimation results are presented in Table 1.7. Results show that for the sample period before the Act was introduced energy volatility spillovers (φ_0 and ω_0) are significant at conventional significance levels. However, results also point to a stronger positive spillover effect after the introduction of the Act. Both φ_1 and ω_1 are statistically significant at the 5% level. The Wald test of the hypothesis $H_0 : \varphi_1 = \omega_1$ cannot be rejected, suggesting the crude oil market has similar spillover effects on corn cash and futures markets. It is interesting to see that the introduction of the Act dramatically increased the connection between the crude oil market and the corn market. The crude oil price now plays a more important role in corn price movements. As a result, corn producers are now being exposed to an additional source of uncertainty from energy spillovers. A closer examination shows that the average spillover ratio in the cash corn market before the introduction of the Act was 1.08% whereas it became 9.53% thereafter, a jump of more than 8 times the original level (Table 1.6). The spillover ratio for corn futures was also 1.70% before the introduction but increased to 9.40% thereafter, a jump of more than 5 times. Figure 1.3 clearly shows the dramatic changes. The spillover ratio gets close to 28% at times after the introduction of the Act.

Table 1.7. Estimation of the Event Spillover Effect Model

$$\begin{bmatrix} \varepsilon_{o,t} \\ \varepsilon_{p,t} \\ \varepsilon_{f,t} \end{bmatrix} = \begin{bmatrix} 1 & 0 & 0 \\ \varphi_t & 1 & 0 \\ \omega_t & 0 & 1 \end{bmatrix} \begin{bmatrix} e_{o,t} \\ e_{p,t} \\ e_{f,t} \end{bmatrix},$$

$$\varphi_t = \varphi_0 + \varphi_1 D_t,$$

$$\omega_t = \omega_0 + \omega_1 D_t,$$

$$[e_{p,t}, e_{f,t}]' \big| I_{t-1} \sim N(0, H_t),$$

$$H_t = C'C + A' e_{t-1} e_{t-1}' A + B' H_{t-1} B + D' \eta_{t-1} \eta_{t-1}' D + G \otimes z_t.$$

	Coefficient	Std. Error	z-Statistic	p-value
φ_0	0.0054	0.0022	2.4790	0.0132
φ_1	0.0098	0.0045	2.1699	0.0300
ω_0	0.0071	0.0022	3.1814	0.0015
ω_1	0.0081	0.0042	1.9417	0.0522
C(1,1)	0.0003	0.0001	2.1107	0.0348
C(1,2)	0.0003	0.0003	1.0262	0.3048
C(2,2)	0.0002	0.0004	0.6040	0.5459
A(1,1)	0.0851	0.2021	0.4211	0.6737
A(1,2)	0.0717	0.2624	0.2733	0.7846
A(2,2)	0.0865	0.3264	0.2651	0.7910
D(1,1)	-0.0443	0.4350	-0.1018	0.9189
D(1,2)	-0.0243	0.5588	-0.0434	0.9654
D(2,2)	-0.0063	0.7081	-0.0089	0.9929
B(1,1)	0.9087	0.0396	22.9462	0.0000
B(1,2)	0.9058	0.0250	36.2360	0.0000
B(2,2)	0.8784	0.0164	53.6951	0.0000
G(1,1)	0.0000	0.0000	-0.4593	0.6460
G(1,2)	0.0000	0.0000	-0.1615	0.8717
G(2,2)	0.0000	0.0000	0.2354	0.8139
Log-likelihood		2345.953.464		
SBC		-5.2331		

Figure 1.3. Spillover Ratios for Corn Cash (*SRP*) and Futures (*SRF*) Markets – the Event Spillover Model

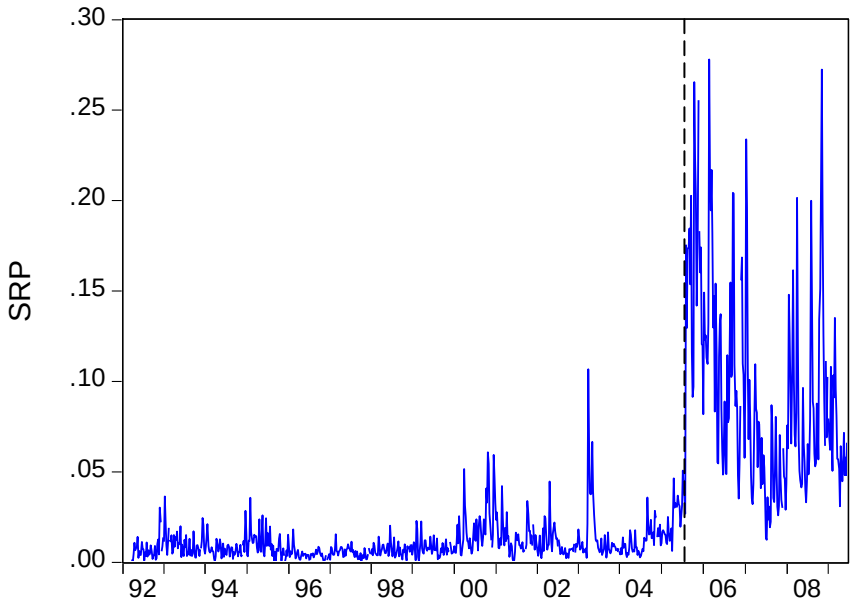

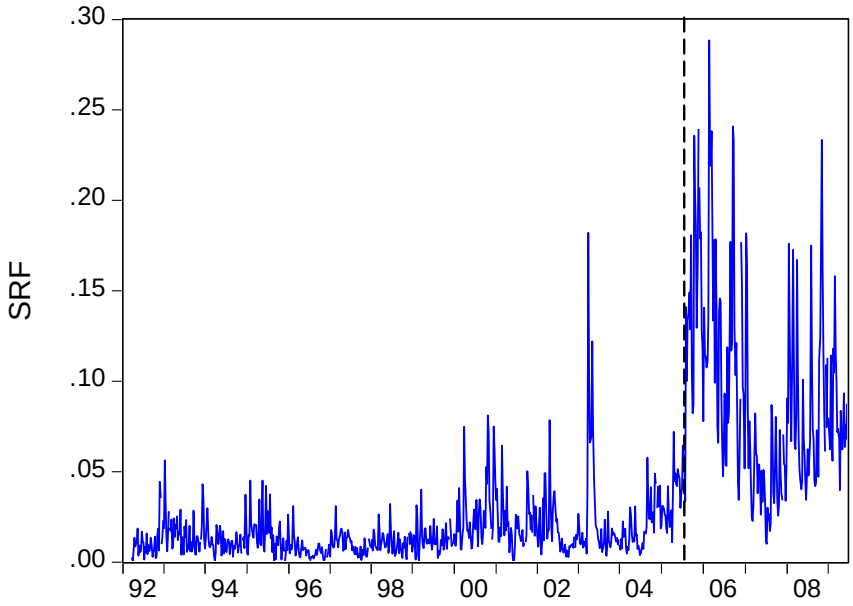

1.4.3 The Substitution Spillover Model

The substitution spillover model investigates the time-varying impact of the fuel consumption ratio on volatility spillovers. Results in Table 1.8 provide insights into how the consumption ratio has impacted volatility spillovers into the corn market. The results show that the crude oil price does not always have significant spillover effects on corn prices. The sign and size of the spillover effect depends on the magnitude of the consumption substitution ratio. Parameter estimates for φ_0 and ω_0 are not significantly different from zero, while φ_1 and ω_1 are positive and significant at the 1% level. A higher consumption ratio implies that ethanol has become a more important substitute for gasoline, and thus the connection between oil and corn markets increases. Looking at the most recent portion of the sample (Figure 1.4), the spillover remained in the high range in 2008 and spiked at more than 48% when the consumption ratio rose to close to 8%. It dipped to an average of 15% when the consumption ratio decreased after 2009 during the deep economic recession. At low consumption ratios, the connection between crude oil and corn markets is essentially cut off as biofuel-based demand for corn is sluggish, but when the consumption ratio reached its maximum value, crude oil prices accounted for more than 40% of total corn price volatility (Figure 1.4), which suggests that crude oil markets have become a much more important factor in explaining corn price movements during these periods. It is clear that the relative influence of the crude oil market varies with consumption ratios and changes over time.

I also go one step further to estimate a more general spillover model that nests the event spillover and consumption substitution specifications. That is, the spillover parameters are allowed to vary with both the event dummy and the consumption substitution ratio variables. The results (they are not reported to save space) show that the event dummy coefficient estimates are

insignificant while the consumption ratio coefficient estimates are positive and significant at the 1% level. This is not surprising given that the high correlation between two variables. The consumption substitution ratio captures the effect of the Energy Policy Act of 2005 so that adding the event dummy variable to the substitution model does not increase explanatory power. Furthermore, the fit of the model does not improve, as shown by an increased Schwartz Bayesian Criterion (SBC).

Table 1.8. Estimation of the Substitution Spillover Effect Model

$$\begin{bmatrix} \varepsilon_{o,t} \\ \varepsilon_{p,t} \\ \varepsilon_{f,t} \end{bmatrix} = \begin{bmatrix} 1 & 0 & 0 \\ \varphi_t & 1 & 0 \\ \omega_t & 0 & 1 \end{bmatrix} \begin{bmatrix} e_{o,t} \\ e_{p,t} \\ e_{f,t} \end{bmatrix},$$

$$\varphi_t = \varphi_0 + \varphi_1 R_{t-1}, \quad \omega_t = \omega_0 + \omega_1 R_{t-1},$$

$$[e_{p,t}, e_{f,t}]' | I_{t-1} \sim N(0, H_t),$$

$$H_t = C'C + A' e_{t-1} e_{t-1}^{'} A + B' H_{t-1} B + D' \eta_{t-1} \eta_{t-1}^{'} D + G \otimes z_t .$$

	Coefficient	Std. Error	z-Statistic	p-value
φ_0	-0.0006	0.0028	-0.2058	0.8370
φ_1	0.0032	0.0006	5.1188	0.0000
ω_0	0.0021	0.0028	0.7604	0.4470
ω_1	0.0027	0.0005	5.1931	0.0000
C(1,1)	0.0002	0.0001	1.4461	0.1481
C(1,2)	0.0001	0.0001	1.3917	0.1640
C(2,2)	0.0001	0.0001	1.1897	0.2341
A(1,1)	0.0793	0.0113	7.0242	0.0000
A(1,2)	0.0666	0.0085	7.8549	0.0000
A(2,2)	0.0803	0.0098	8.2059	0.0000
D(1,1)	-0.0562	0.0129	-4.3486	0.0000
D(1,2)	-0.0423	0.0122	-3.4604	0.0005
D(2,2)	-0.0334	0.0150	-2.2303	0.0257
B(1,1)	0.9242	0.0101	91.8567	0.0000
B(1,2)	0.9258	0.0082	112.4387	0.0000
B(2,2)	0.9035	0.0095	94.9563	0.0000
G(1,1)	0.0000	0.0000	0.0191	0.9847
G(1,2)	0.0000	0.0000	0.3959	0.6922
G(2,2)	0.0000	0.0000	0.9785	0.3278
Log-likelihood		2349.7980		
SBC		-5.2419		

Figure 1.4. Spillover Ratios for Corn Cash (SRP) and Futures (SRF) Markets – the Substitution Spillover Model

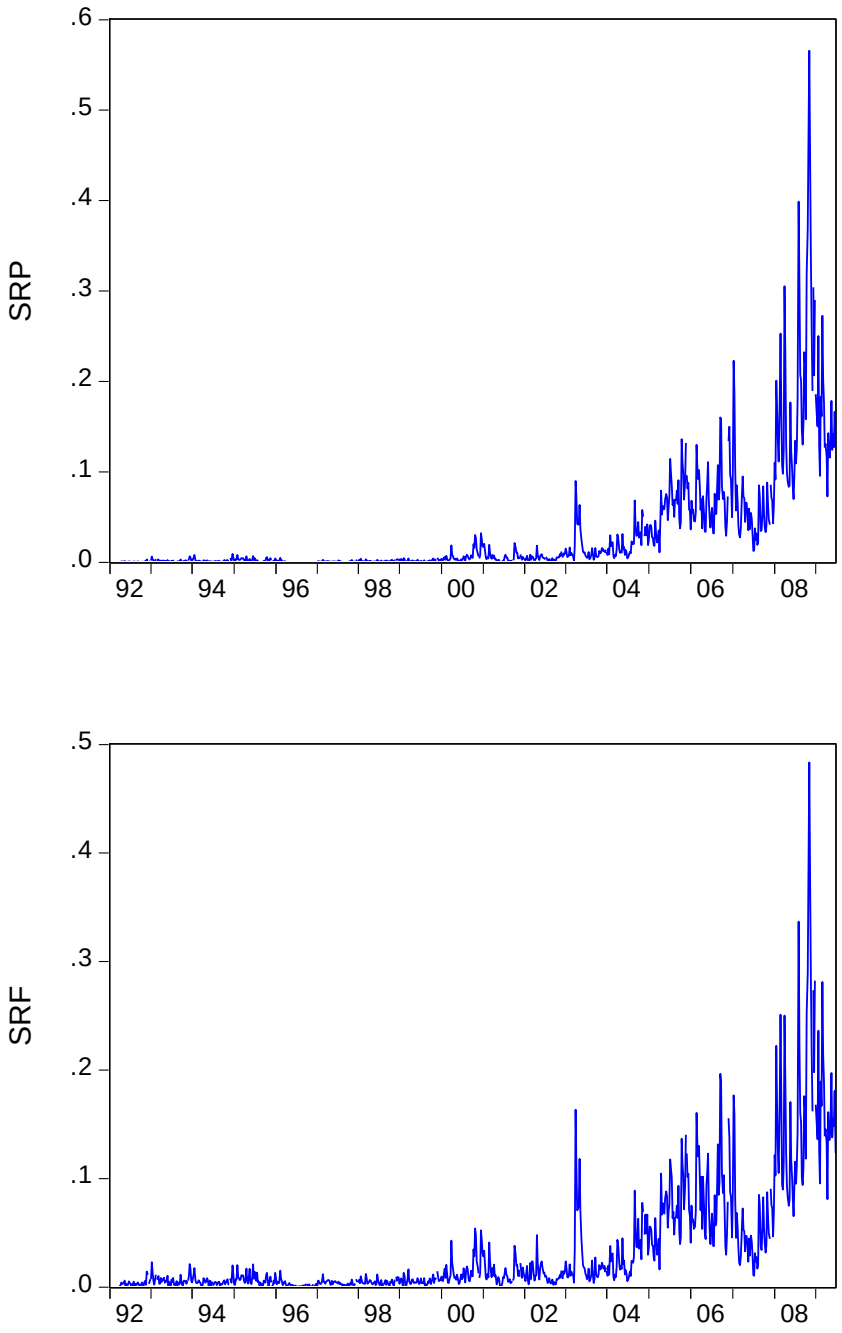

1.5 Implications for Hedging Strategies

1.5.1 Optimal Hedging

The additional source of uncertainty resulting from the strong connection between crude oil and corn prices during some periods may present a new challenge to corn market participants. Producers and traders may need to re-evaluate their risk management strategy to cope with this additional source of risk. Naturally, hedgers may be tempted to exploit the information linkage between crude oil and corn prices by examining a cross hedge strategy of simultaneously using corn futures and crude oil futures to hedge cash corn price risk. This section examines whether such a strategy would significantly improve hedging performance.

Consider an investor with a fixed corn cash position who wishes to hedge this cash position in both corn and crude oil futures markets. I use a one-period portfolio selection framework. Assume the investor aims to maximize expected utility from the end-of-period portfolio profit:

$$(1.19) \quad \max_{b_{t-1},a_{t-1}} E[U(\pi_t)|I_{t-1}]$$

subject to

$$(1.20) \quad \pi_t = (p_t - p_{t-1})q_{t-1} + (f_t - f_{t-1})b_{t-1} + (o_t - o_{t-1})a_{t-1}$$

where π_t is end-of-period profit; initial and end-of-period prices (corn cash, corn and oil futures) are subscripted by t-1 and t, respectively; q_{t-1} is a fixed quantity of cash corn purchased; and b_{t-1} and a_{t-1} are the quantities of corn and crude oil futures purchased (sold if negative). Assuming the joint distribution of (π_t, p_t, f_t, o_t) conditional on I_{t-1} is multivariate normal, the optimal hedge ratio of the cross hedge can be derived as (see appendix A for details):

$$(1.21) \quad \begin{bmatrix} -b_{t-1}/q_{t-1} \\ -a_{t-1}/q_{t-1} \end{bmatrix} = \frac{1}{m_t^{22}m_t^{33} - m_t^{23}m_t^{32}} \begin{bmatrix} m_t^{12}m_t^{33} - m_t^{13}m_t^{32} \\ m_t^{13}m_t^{22} - m_t^{12}m_t^{23} \end{bmatrix},$$

where m_t^{ij} is the element in the *i*-th row and the *j*-th column of M_t, the conditional covariance matrix of $(p_t, f_t, o_t)'$.

Equations (1.16) and (1.6) specify models for m_t^{22} and m_t^{33}. From the spillover effect model, I can also infer other elements of the covariance matrix:

$$(1.22) \quad m_t^{13} = E(\varepsilon_{p,t}\varepsilon_{o,t}\Big|I_{t-1}) = \varphi_t\sigma_{o,t}^2 ,$$

$$(1.23) \quad m_t^{23} = E(\varepsilon_{f,t}\varepsilon_{o,t}\Big|I_{t-1}) = \omega_t\sigma_{o,t}^2 ,$$

$$(1.24) \quad m_t^{12} = E(\varepsilon_{p,t}\varepsilon_{f,t}\Big|I_{t-1}) = H_t^{12} + \varphi_t\omega_t\sigma_{o,t}^2 .$$

The resulting covariance matrix M_t is used to compute the optimal hedge ratio vector for cross hedging.

1.5.2 Comparisons of Hedging Performance

In order to compare the performance of different hedging strategies, I first break the full sample into two parts for purposes of in-sample and out-of-sample evaluation. In-sample evaluation covers the period from January 2, 1992 to March 22, 2007. Out-of-sample data are from March 29, 2007 to June 30, 2009, and includes 100 observations. Assume an investor holds one bushel of cash corn (i.e., q_{t-1} = 1) continuously over the sample period, which is hedged by selling nearest expiration futures contracts of corn and crude oil. The futures position is adjusted on a weekly basis conditional on all past information. As the futures contract matures, futures positions are rolled over into the next expiration contract.[11] Performance is evaluated in terms of

[11] Rolling cost is not considered in the performance evaluation because all hedging strategies involve contract rolling.

the effects on the variance of the investor's portfolio return. The performance comparisons are conducted under three different hedging rules: no hedge, traditional hedge with only corn futures,[12] and the cross hedge using corn and crude oil. For out-of-sample performance evaluation, I implement dynamic forecasts. That is, the model is re-estimated each time when a new data point is observed and included in the estimation, and the optimal hedge ratio is then re-calculated. This process continues until 100 forecasts have been generated.

Ex-ante evaluations of hedge performance are used to construct the ex-ante conditional standard deviation of portfolio returns for each date based on the spillover model.[13] I compute the percentage reduction in the conditional standard deviation under two hedging rules, the traditional hedge and the cross hedge, all compared to a no-hedge outcome. The average percentage reduction is computed over the sample period.[14] In the in-sample case, the cross hedge reduces the conditional standard deviation by 53.10% compared to no hedging while the traditional hedge provides similar hedging performance, reducing the conditional standard deviation by 51.87%. Since traders are more concerned with the future performance than past, out-of-sample forecasts are a more useful way of analyzing hedging performance and are of more interest (Haigh and Holt, 2002). In the out-of-sample case, the cross hedge reduces the conditional standard deviation by 48.10%, slightly better than the traditional hedge performance reduction of 47.95% (see Table 1.9). Therefore I conclude that the cross hedge strategy performs marginally better compared to the traditional hedge with only corn futures.

---

[12] I use the spillover empirical model to estimate the components of the traditional hedge formula. The formula can be found in Myers (1991).

[13] The computations are based on the constant spillover model. Similar results can be obtained from the event and substitution spillover models.

[14] I did not compare the *ex-ante* conditional means of return because they are the same, which is implied by the assumption that the expected return from holding futures is zero (Myers, 1991).

Ex-post evaluations of hedge performance are undertaken by constructing the actual ex-post portfolio returns using observed prices and comparing their standard deviations over the relevant period. In the in-sample case, the cross hedge performs slightly better than any other strategy in terms of risk reduction. The standard deviation falls 42.22% under a cross hedge, while the traditional hedge provides a 42.21% reduction. In the out-of-sample case, cross hedging offers a little more risk reduction (72.15%) than the traditional hedge (71.93%). Similarly, ex-post performance of cross hedge is also slightly improved.

Table 1.9. In- and Out-of-sample Hedging Performance

	In-sample s. d.	Out-of-sample s. d.
Ex-ante		
No hedge	8.5539	14.3200
Biv. hedge	4.1171(-51.87%)	7.4530(-47.95%)
Cross hedge	4.0121(-53.10%)	7.4321(-48.10%)
Ex-post		
No hedge	9.7713	28.1070
Biv. hedge	5.6460(-42.21%)	7.8886(-71.93%)
Cross hedge	5.6457(-42.22%)	7.8293(-72.15%)

Note: all standard deviations are scaled by 0.01. Numbers in parentheses are percentage deviations from the no hedge strategy.

Our results show that a cross hedging strategy using oil and corn futures contributes only a small improvement over hedging based solely on corn futures. However, this is exactly what I would expect if the corn futures market is efficient and incorporates all relevant information, including information contained in oil prices. The fact that crude oil and corn prices are related, and there is volatility spillover between the markets, does not necessarily distort the relationship between corn cash and futures prices which may (and should, if the market is operating efficiently) continue to be strongly correlated. Cross hedging would only be expected to result in improved hedging performance if corn futures price movements deviate significantly from corn cash price movements, so that corn futures alone become an imperfect hedging vehicle for corn

cash price risk. So I view the fact that cross hedging does not improve hedging performance, despite the connection and volatility spillover between oil and corn prices, as evidence that the corn futures market continues to operate efficiently and effectively. In short, the futures market is not detached from the cash market in a time of increased volatility from the biofuel boom.

Despite the fact that cross hedging does not improve hedging performance our results do show that with the increasing use and production of biofuel, a stronger connection between crude oil and corn markets is being established, particularly in times of high oil prices and relatively high ethanol use. The Energy Independence and Security Act (EISA) of 2007 has mandated increased biofuel production (36 billion gallons by 2022) so the connection between crude oil and corn markets will likely continue to grow in the future, the implications of which deserve to be examined further. In addition, understanding the nature of the spillover and its pattern is critical for forecasting price movements, for production and investment planning, and for risk management in a broader context beyond hedging portfolio management.

1.6 Conclusions

This paper investigates the magnitude and changing nature of volatility spillover effects from crude oil markets to corn markets. I find that volatility spillovers from crude oil prices are significant and have similar impacts on corn cash and futures prices. The relative importance of spillovers jumps significantly after the introduction of the Energy Policy Act of 2005. Also, more substantial volatility spillovers occur in periods of high ethanol-gasoline consumption ratios. The emerging connection between energy and corn prices is exposing agriculture to additional risk, which implies agricultural risk management may be more costly and potentially calls for new strategies for risk management. Given the statistically significant spillovers from the crude oil

market, corn market participants perhaps should consider pursuing a cross hedge with crude oil. This study shows that such a cross hedge has slightly better performance than traditional hedging strategies, but the improvement is not large, which indicates that the corn futures market continues to provide a reliable, efficient way to manage the risk of cash corn price movements. The findings in this study suggest that corn market participants can still rely on corn futures markets to hedge risk and achieve a relatively satisfactory performance, even when there are significant spillovers from the energy market.

APPENDIX A

APPENDIX A: DERIVATION OF EQUATION 1.21

The derivation is based on the relation $Cov[g(x), y] = E[g'(x)]Cov(x, y)$, if the random variables *x* and *y* are jointly normally distributed, and g is a differentiable function. Assuming the joint distribution of (π_t, p_t, f_t, o_t) conditional on I_{t-1} is multivariate normal, the first order conditions are

$$\text{(A.1)} \quad M_t \begin{bmatrix} q_{t-1} \\ b_{t-1} \\ a_{t-1} \end{bmatrix} = -\frac{U'}{U''} \begin{bmatrix} \mu_t^p \\ \mu_t^{f_c} \\ \mu_t^{f_o} \end{bmatrix},$$

where M_t is the covariance matrix of $(p_t, f_t, o_t)'$ conditional on the information set; and μ_t^p, μ_t^f and μ_t^o are the conditional expected returns from holding cash and futures positions, respectively. It is often assumed that the expected return to trading futures is approximately zero ($\mu_t^f = \mu_t^o = 0$). Then

$$\text{(A.2)} \quad \begin{bmatrix} b_{t-1} \\ a_{t-1} \end{bmatrix} = \frac{1}{(M_t^{-1})^{11}} \begin{bmatrix} (M_t^{-1})^{21} \\ (M_t^{-1})^{31} \end{bmatrix} q_{t-1},$$

where $(M_t^{-1})^{ij}$ is the element in the *i*-th row and the *j*-th column of the inverse covariance matrix, M_t^{-1}.

The optimal hedge ratio is the proportion of the long cash position which should be covered by a short position in corn and crude oil futures. So the optimal hedge ratio can be written as,

$$\text{(A.3)} \quad \begin{bmatrix} -b_{t-1}/q_{t-1} \\ -a_{t-1}/q_{t-1} \end{bmatrix} = \frac{1}{m_t^{22} m_t^{33} - m_t^{23} m_t^{32}} \begin{bmatrix} m_t^{12} m_t^{33} - m_t^{13} m_t^{32} \\ m_t^{13} m_t^{22} - m_t^{12} m_t^{23} \end{bmatrix}$$

REFERENCES

REFERENCES

Baele, L. 2005. Volatility spillover effects in European equity markets: evidence from a regime switching model. Journal of Financial and Quantitative Analysis 40, 373-401.

Baillie, R. T., Myers, R. J. 1991. Bivariate GARCH estimation of the optimal commodity futures hedge. Journal of Applied Econometrics 6, 109–124.

Beck, S. E. 1994. Cointegration market efficiency in commodities futures markets. Applied Economics 26, 249-257.

Bekaert, G., Harvey, C. R. 1997. Emerging equity market volatility. Journal of Financial Economics 43, 29–77.

Bekaert, G., Harvey, C. R., Lumsdaine, R. L. 2002. Dating the integration of world equity markets. Journal of Financial Economics 65, 203-247.

Bekaert. G., Harvey, C. R., Ng, A. 2005. Market integration and contagion. Journal of Business 78, 1-31.

Bollerslev, T. 1990. Modeling the coherence in short-run nominal exchange rates: a multivariate generalized ARCH approach. Review of Economics and Statistics 72, 498–505.

Bollerslev, T., Engle, R. F., Wooldridge, J. M. 1988. A capital asset pricing model with time varying covariances. Journal of Political Economy 96, 116–131.

Christiansen, C. 2007. Volatility-spillover effects in European bond markets. European Financial Management 13, 923–948.

Engle, R. F., Kroner, K. F. 1995. Multivariate simultaneous generalized ARCH. Econometric Theory 11,122–150.

Engle, R. F., Ng, V. K., Rothschild, M. 1990. Asset pricing with a Factor-ARCH covariance structure: empirical estimates for treasury bills. Journal of Econometrics 45, 213–237.

Feng, H., Rubin, O. D., Babcock, B. A. 2010. Greenhouse gas impacts of ethanol from Iowa corn: life cycle assessment versus system wide approach. Biomass and Bioenergy 34, 912-921.

Glosten, L. R., Jagannathan, R. Runkle, D. 1993, On the relation between the expected value and the volatility of the nominal excess return on stocks. Journal of Finance 48, 1779-1801.

Haigh, M. S., Holt, M. T. 2002. Crack spread hedging: accounting for time-varying volatility spillovers in the energy futures markets. Journal of Applied Econometrics 17, 269–289.

Liska, A. J., Yang, H. S., Bremer, V. R., Klopfenstein, T. J., Walters, D. T., Erickson, G. E., Cassman, K. G. 2009. Improvements in life cycle energy efficiency and greenhouse gas emissions of corn-ethanol. Journal of Industrial Ecology 13, 58–74.

Kroner, K. F., Ng, V. K. 1998. Modeling asymmetric comovement of asset returns. Review of Financial Studies 11, 8I7-844,

Moschini, G., Myers, R. J. 2002. Testing for constant hedge ratios in commodity markets: a multivariate GARCH approach. Journal of Empirical Finance 9, 589-603.

Myers, R. J. 1991. Estimating time-varying optimal hedge ratios on futures markets. The Journal of Futures Markets 11, 39–53.

Ng, A. 2000. Volatility spillover effects from Japan and the US to the Pacific-Basin. Journal of International Money and Finance 19, 207–233.

Sadorsky, P. 2002. Time-varying risk premiums in petroleum futures prices. Energy Economics 24, 539–556.

Tyner, W. E. 2008. The US ethanol and biofuels boom: its origins, current status, and future prospects. BioScience 58, 646-653.

Zulauf, C., Roberts, M. 2008. Price variability: corn, soybeans, wheat, 1989-2007. Unpublished economic report, The Ohio State University, Columbus, Ohio.

CHAPTER 2: SPILLOVER EFFECTS OF BIOFUEL POLICY ON THE CONSERVATION PROGRAM

2.1 Introduction

Over the past several decades, public awareness and concerns of environmental issues, including environmental degradation and global warming, have prompted the U.S. government to make the environment a priority policy area and promote policies that address public interests in these areas, particularly in environmental conservation and greenhouse gas emissions. The Conservation Reserve Program (CRP), enacted in 1985, is by far the most important U.S. conservation program in terms of scale and budget. The CRP aims to provide environmental benefits (e.g., to reduce erosion, improve water quality, establish wildlife habitat, and sequester carbon) through retiring environmentally sensitive cropland from production, and in exchange, give participants a dependable source of income in the form of CRP land rental payments. The program's economic and environmental benefits have been well documented (see, e.g., Young and Osborn, 1990; Wu, 2000; Wu, Zilberman, and Babcock, 2001; Wu and Lin, 2010). In its first twenty years of implementation, the program has prevented an estimated 450 million tons of soil from erosion and sequestered 50 million tons of carbon dioxide per year (USDA-FSA, 2007).

Another policy initiative that has profound environmental and economic impacts is the 2005 and 2007 Energy Acts (2005 Energy Policy Act and 2007 Energy Independence and Security Act (EISA)), which set a roadmap for bioenergy production and biofuel mandates in the United States. This policy was designed to mitigate greenhouse gas emissions and to reduce U.S. dependency on energy import. The policy has created tremendous demand and supply of biofuels in the country and caused structural changes in agricultural commodity markets and farming returns (USDA-ERS, 2007; Collins, 2008; Lipsky, 2008; Frank and Garcia, 2010). Supported by

ethanol tax credits and mandates on biofuel consumption under the 2005 and 2007 Acts, annual ethanol production and, consequently, the acreage of corn, the major feedstock of ethanol in the U.S. have increased rapidly. While the desire to reduce greenhouse gas emission was an important driver of the production and consumption of biofuels, the ethanol-driven structural changes in U.S. agriculture have been pressuring lands out of conservation. As of 2009, CRP enrollment stood at 31.2 million acres, approximately 5 million acres lower than in 2007 (USDA-FSA, 2010). Exiting conservation programs results in increasing greenhouse gas emissions from land use changes, thus compromising the initial goal of the conservation program as well as that of the biofuel policy. This research studies the spillover effect of biofuel policy on conservation participation and the implications of potential policy options, illustrating the nature, mechanism, and extent of competition and spillover between government policies.

To analyze the effect of biofuel policy, an understanding of landowners' conservation participation decision process is important. When making participation decision, landowners trade off the cost and benefit of participation; the factors, such as annual program land rental payments, revenue and cost of crop production, all affect landowners' participation decision (e.g., Parks and Kramer, 1995; Lubowski, Plantinga, and Stavins, 2008; Suter, Poe, and Bills, 2008; Change and Boisvert, 2009). Biofuel production has triggered a sharp increase in the opportunity cost of giving up agricultural production. Since the Energy Policy Act was passed in 2005, farming returns have experienced a sharp increase; and agriculture has entered a high growth stage, departing from the historical equilibrium growth rate. The prospect and persistence of the biofuel driven agricultural boom have direct impact on landowners' decisions. Another important factor that impact participation decision is risk and uncertainty (Capozza and Li, 1994; Dixit and Pindyck, 1994; Schatzki, 2003; Isik and Yang, 2004); this is particularly important in the current

context of ethanol-driven structural changes. Faced with risk and uncertainty, landowners may choose to wait for more information about future returns and thus delay participation. Though participation in the CRP offers landowners a stable stream of cash flows from government payments over the contracted years, once enrolled in the CRP, the land will be locked up for 10 or 15 years, so the participation decision is essentially irreversible during the fixed contract period. In particular, landowners who participate in the CRP may be losing out economically due to higher forgone farming returns in the future, especially in an environment of increasing ethanol production.

In this study I propose a two-stage Gordon growth process to model the structural change in farming returns and investigate the impact of biofuel production on conservation participation in the real options decision framework. Traditionally, the uncertain farming return is assumed to follow a geometric Brownian motion (GBM), in which the location (mean) of the distribution is assumed to be fixed (see, e.g., Dixit and Pindyck, 1994). Under the biofuel-driven structural changes, however, the assumption of *constant* growth of farming returns would be inappropriate. It is more realistic to assume that the growth rate of agricultural returns in the biofuel era may be different than in the past. In this study I assume a two-stage process, in which the current high growth will eventually settle in to a long-term equilibrium growth as the ethanol industry matures or as a result of policy changes, for instance, repealing of the ethanol tax credit in the future.

I further assume that the duration of high growth is random due to exogenous policy uncertainty, for example, repealing ethanol tax credit or removing ethanol import tariff. Unlike the traditional GBM model's assumption of a known growth rate which implies that decision makers have full information over the entire stochastic process, under the regime of two-stage

growth and random duration of high growth, I assume decision makers observe only historical information and make decisions basing on their expectations, which is more realistic and consistent with the real world decision process. This incomplete information and expectation formation are particularly relevant at a time of structural change where past observations only contain partial information about the future growth rate. This parameter uncertainty causes an extra layer of uncertainty compared to the GBM assumption and has important implications for decision making. To our knowledge, this issue has not been addressed in modeling land use decisions. The model I propose in this study assumes a geometric Brownian motion with a *stochastic* growth rate (Gennotte, 1986; Brennan, 1998; Xia, 2001; Abasov, 2005), in which landowners continuously update their expectations, conditional on new information arriving at the time of the decision. The expectation formation with information updating is modeled using a non-linear Kalman filtering approach (Kalman, 1960).

Based on the proposed model, I derive thresholds of farming returns (profit per acre) under different growth expectations that would make land conversion attractive. The model is then used to investigate the impacts of the structural change and biofuel production on program participation using Monte Carlo simulations. I further analyze the sensitivity of the land-use conversion thresholds to changes in the policy and economic environment and examine the landowner's response to changes in market conditions, including the expected duration of the biofuel boom and the uncertainty surrounding future agricultural returns. The comparative static analysis of conversion thresholds and the Monte Carlo simulations of program participation rates provide a number of important new insights with significant policy implications.

2.2 Landowner's Decision under Uncertainty

The CRP provides an annual per-acre rental payment to landowners to take highly erodible or environmentally sensitive cropland out of production. The payment is fixed over the contracted period once the land is enrolled. The program also provides cost-share assistance to participants who establish approved resource-conserving vegetative covers on eligible cropland. The cost-share assistance can be an amount no more than 50 percent of the participants' costs in establishing covers. In some cases, other financial incentive payments (e.g. one-time signup payments) are also offered. Landowners who decide to enroll in the program must enter into a $\overline{T}$ year contract (10 or 15 years).

Consider a landowner facing a decision to convert a unit of land from crop production to conservation.[15] I assume that the participation decision is made in a continuous-time framework. Defining the farming return as R_t, the expected discounted farming return forgone over the $\overline{T}$ year horizon is:

$$(2.1) \quad V(R_t) = E_t \int_{t}^{t+\overline{T}} R_t e^{-\rho t} dt ,$$

where ρ is the continuous discount rate.

After participation, the annual rental payment Q is fixed. The expected land rental payment received over the $\overline{T}$ years of the CRP contract is:

[15] To accommodate the likelihood of increased biofuel production, I limit my discussion to a single switching decision from cropland to the CRP. After the contract expires, the landowner is faced with an opposite land conversion decision – stay in the CRP or conversion back to production. My model could also be extended to address this problem, but such an extension would be outside the scope of the current study.

$$(2.2) \qquad V(Q) = \int_{t}^{t+\bar{T}} Qe^{-\rho t} dt - (1-k)C + \pi = \frac{Q(1-e^{-\rho \bar{T}})}{\rho} - (1-k)C + \pi,$$

where C is the total land cover establishment cost when participating in the CRP, k is the portion paid by the government as an incentive for participation, and π is the additional financial incentive, e.g., a one-time sign-up incentive payment. This payment is made as soon as the contract has been signed and approved.

Denote $M(R_t, Q) = V(Q) - V(R_t)$ as the benefit from land conversion at time t. The minimum requirement for conversion is that $M(R_t, Q)$ be positive. The conversion decision can be characterized as an optimal timing problem given uncertain market conditions, in which landowners choose when to stop waiting and participate in the CRP. The optimal stopping problem can be represented as:

$$(2.3) \qquad J(R_t) = \max_T E_t[e^{-\rho(T-t)} M(R_T, Q)],$$

which reflects the landowner's choice of the optimal conversion time, $T \geq t$, to maximize the discounted expected conversion benefit at t.

2.3 Structural Change and Parameter Uncertainty

The participation problem is similar to an American put option: landowners have an option to put the land into conservation, with discounted total rental payments over the contract period as the exercise price. Valuation of American put options usually assumes the underlying asset return follows a geometric Brownian motion (GBM) (Carey and Zilberman, 2002; Isik and Yang, 2004):

$$(2.4) \qquad dR_t = \theta R_t dt + \sigma R_t dW_t,$$

where θ is a drift term, σ is a constant volatility parameter, and W_t is a standard Brownian motion, defined on a complete probability space.

This model incorporates the strong assumption that the parameters of the process are known. That is, all possible sources of uncertainty that affect the farming return are summarized in the form of a log-normal distribution with a *known*, *constant* growth rate θ and a volatility parameter σ, which, in practice, must be estimated from historical farming returns data. These assumptions are often plausible. Given the current structural changes in farming returns, however, these assumptions would be too restrictive and likely do not hold; and assuming a constant, known farming return growth rate may result in substantial error (Gennotte, 1986).

It is more realistic to assume that the growth rate of agricultural returns in the biofuel era may be different than in the past, and that landowners' expectations about growth vary at different points in time. To capture the impact of structural change on expectations about future agricultural returns, I assume the growth rate (θ) is stochastic and unobservable. I use a two-stage stochastic Gordon growth process to model θ_t, assuming an initial high growth (α) stage, followed by an average growth (β) stage as the ethanol industry matures and reaches a long-run equilibrium. The two-stage assumption is reasonable given the biofuel boom, and the anticipated technological breakthroughs in more cost-effective production of cellulosic ethanol, the second generation biofuel.

In the generalized farming return model, θ_t is specified as:

(2.5) $\quad \theta_t \in \{\alpha, \beta\}, \quad \alpha > \beta,$

where α and β are the growth rates of the two states. The duration of state α, denoted T_α, follows an exponential distribution with parameter λ:

(2.6) $prob(T_\alpha \geq t) = \exp(-\lambda t)$.

To estimate θ_t, I use the Kalman filter information updating algorithm, which is a recursive algorithm that continuously updates model estimates using new information. The Kalman filter minimizes the estimated error variance and generates more efficient parameter estimates compared to other estimation procedures (Kalman, 1960). I allow landowners to update their information and thus learn about the true parameter distribution with each new farming return realization. At time t, there is an initial prior about the growth rate. As new farming returns are observed over time, this prior distribution is updated. Liptser and Shiryayev (1977) derive the basic equation of optimal nonlinear filtering in a partially observable random process.

Specifically, the conditional probability of the growth rate reverting to the long-term average β is defined as:

(2.7) $p_t = prob(\theta_t = \beta \left| \Omega_t^R \right.)$.

Based on the information set Ω_t^R available to landowners at time t,[16] landowners form expectations about the value of θ_t,

(2.8) $m_t = E(\theta_t \left| \Omega_t^R \right.) = (1 - p_t)\alpha + p_t \beta$.

Given parameter uncertainty, the Brownian motion W_t is also unobserved. I define a process based on the observed farming return R_t and its expected growth rate m_t as:

(2.9) $d\overline{W}_t = \frac{1}{\sigma}(\frac{1}{R_t} dR_t - m_t dt)$.

[16] In the landowner's information set, the agricultural return R_t is observable, while its growth rate θ_t is not.

Liptser and Shiryayev (1977) show that $\overline{W}_t$ is a standard Brownian motion with respect to the information set Ω_t^R. Rearranging (2.9), I obtain:

$$(2.10) \quad dR_t = R_t m_t dt + R_t \sigma d\overline{W}_t .$$

Substituting (2.4) into (2.9) and rearranging yields

$$(2.11) \quad d\overline{W}_t = dW_t + \frac{1}{\sigma}(\theta_t - m_t)dt .$$

Landowners seek to extract information on the expected growth rate from observed past returns, and keep updating the expectation when new return realizations come along. The conditional mean m_t evolves according to (see Appendix B for the derivation):

$$(2.12) \quad dm_t = \lambda(\beta - m_t)dt + \frac{1}{\sigma}(\alpha - m_t)(m_t - \beta)d\overline{W}_t .$$

Combining (2.3), (2.10), and (2.12), I arrive at the following decision model:

$$(2.13) \quad \begin{cases} J(R_t, m_t) = \max_T E_t[e^{-\rho(T-t)} M(R_T, Q)] \\ dR_t = R_t m_t dt + R_t \sigma d\overline{W}_t \\ dm_t = \lambda(\beta - m_t)dt + \frac{1}{\sigma}(\alpha - m_t)(m_t - \beta)d\overline{W}_t \end{cases} .$$

In this framework, landowners maximize option value *J* by choosing the optimal time *T* to enter into the CRP contract. Landowners continuously update their estimate of the growth rate of farming returns based on new return realizations. With the uncertain growth rate, there is no analytical solution to the decision problem. The problem is therefore formulated as a linear complementarity problem (LCP), and solved numerically using an implicit finite difference approach (Wilmott, Howison, and Dewynne, 1993).

2.4 Linear Complementarity Problem

Under known regularity conditions, there will be a critical return R^* for a given initial expected growth rate, such that participating in the CRP is optimal if $R_t < R^*$, while continuing in farming is optimal if $R_t \geq R^*$. The solution to the participation problem involves finding this threshold R^*. Using Ito's lemma, I derive a partial differential equation in a continuous region of the farming return (see Appendix C for the derivation):

$$\begin{aligned} &\rho J - R_t m_t J_R - \lambda(\beta - m_t) J_m - \frac{1}{2} R_t^2 \sigma^2 J_{RR} \\ &- \frac{1}{2\sigma^2}(\alpha - m_t)^2 (m_t - \beta)^2 J_{mm} - R_t(\alpha - m_t)(m_t - \beta) J_{Rm} = 0 \end{aligned}, \tag{2.14}$$

where J denotes the put option value, J_R, J_{RR} denotes, respectively, the first and second derivatives of J with respect to R_t, and J_{Rm} denotes the cross derivative of J with respect to R_t and m_t.

I solve the optimal stopping problem (2.13) numerically using an LCP algorithm. This technique is often used to solve American options due to the existence and uniqueness of solutions (Wilmott, Howison, and Dewynne, 1993), but to our knowledge this technique has not been used previously to solve an optimal land conversion problem with a structural change in the return process. Define the left-hand side of (2.14) as HJ:

$$HJ = \rho J - \left[\begin{aligned} &R_t m_t J_R + \lambda(\beta - m_t) J_m + \frac{1}{2} R_t^2 \sigma^2 J_{RR} + \\ &\frac{1}{2\sigma^2}(\alpha - m_t)^2 (m_t - \beta)^2 J_{mm} + R_t(\alpha - m_t)(m_t - \beta) J_{Rm} \end{aligned} \right], \tag{2.15}$$

where ρJ is the opportunity cost of holding the option (i.e., the required return for holding it). The expression within the square parentheses represents the expected return from waiting due to the change in the option value. Then, the LCP can be specified as:

$$(2.16)\quad \begin{cases} HJ \geq 0 \\ J \geq M(R_t, Q) \\ HJ \cdot \left[J - M(R_t, Q) \right] = 0 \end{cases} .$$

This LCP describes the strategy with regard to holding versus exercising the option. The inequality $HJ \geq 0$ states that the required return for holding the option must be at least as great as the expected return of holding it. If HJ >0, the required return for holding the option exceeds the expected return, and it is optimal to exercise the option immediately. If HJ =0, the required return equals the expected return, and the landowner can either hold the option or exercise it, depending on the second inequality in (2.16). The inequality $J \geq M(R_t, Q)$ indicates that the option value should be at least as large as the intrinsic value of participating immediately in the CRP. When $J > M(R_t, Q)$, holding the option is optimal. If HJ =0 and $J = M(R_t, Q)$, then landowners are indifferent between participation and non-participation. The equality of $HJ \cdot \left[J - M(R_t, Q) \right] = 0$ excludes the possibility of both HJ >0 and $J > M(R_t, Q)$.

Because of the uncertainty regarding the growth rate of the farming return in our model, the optimal participation problem does not have a closed-form solution. However, it is possible to solve the problem numerically. The numerical algorithm for determining the value of the option involves the discretization of the LCP in (2.16) using an implicit finite difference method (see Appendix D for the derivation). For a numerical solution of the LCP, I must specify the boundary conditions. [17]

[17] In my model, the LCP is time-independent, or of the elliptic type. However, in practice, it appears that there is no satisfactory method dealing with elliptic LCPs. Following Abasov (2005), I introduce an artificial time variable into the partial differential inequalities of the elliptic LCP and solve the resulting parabolic LCP. Therefore, a terminal condition (with respect to the time variable) is required to implement this method.

Boundary condition 1. It can be seen from (2.10) that once R_t reaches zero, it will stay there because of $dR_t = 0$. Therefore, it is optimal to exercise the option immediately for landowners, in which case:

(2.17) $J(0, m_t, t) = M(0, Q)$.

Boundary condition 2. At a very high farming return $R_{\max}$, the put option is deeply out of the money and I can simply set the option value equal to zero: [18]

(2.18) $J(R_{\max,} m_t, t) = 0$.

Boundary condition 3. Since I are searching for a solution on a rectangular domain in the space of (R_t, m_t), I apply two other boundary conditions, $m_{\min} = \beta$ and $m_{\max} = \alpha$. In particular, I use boundary condition BC2 on $m_{\min}$ and $m_{\max}$ (Tavella and Randall, 2000).[19]

Terminal condition. The terminal condition follows from the observation that at $t = \infty$ there is no uncertainty about the true value of the growth rate. As a result, m_t becomes a constant. Hence, $J(R_t, m, \infty)$ is the solution of the one-dimensional problem:

$$(2.19) \quad \begin{cases} J(R_t, m, \infty) = \max_T E_t[e^{-\rho(T-t)} M(R_T, Q)] \\ dR_t = R_t m dt + R_t \sigma d\overline{W}_t \end{cases},$$

which can be solved in closed-form. In this case, the put option value will be (see Appendix E for the derivation):

---

[18] In the numerical implementation, $R_{\max}$ is set to be three times the average farming return.

[19] The boundary conditions proposed by Tavella and Randall (2002) are to apply the pricing equation itself as a boundary condition, rather than to appeal to other financial arguments. BC1 postulates a linear dependence of the option value on the underlying variable, while BC2 discretizes the drift and volatility with second order one-sided differential operators. BC2 yields smaller errors when I compute the option value using a finite difference method.

$$(2.20)\quad J(R_t, m, \infty) = \begin{cases} M(R^*, Q)\left(\frac{R_t}{R^*}\right)^{\gamma} & R_t \geq R^* \\ M(R_t, Q) & R_t \leq R^* \end{cases}$$

where $R_t^* = \frac{\gamma}{\gamma - 1} \cdot \frac{(\rho - m)V(Q)}{(1 - e^{-(\rho - m)\bar{T}})}$ and $\gamma = \frac{-(m - \frac{1}{2}\sigma^2) - \sqrt{(m - \frac{1}{2}\sigma^2)^2 + 2\rho\sigma^2}}{\sigma^2}$.

2.5 Data and Parameter Estimation

To analyze the landowners' decision, I need to first estimate parameters in the proposed land-use decision model, which include the growth rates and volatility of farming returns, namely, α, β, and σ. In addition, I also need to derive the distribution parameter λ associated with the high grown duration.

2.5.1 Data on Farming Returns

Assume that a representative landowner in the U.S. is making a decision to convert croplands to conservation.[20] Annual per-acre cropland returns are calculated as the weighted average of the net returns of three major crops — corn, soybean, and wheat.[21] The weight is the percentage of planted acreage for each crop relative to their total planted acreage. Data on marketing-year-average prices and national level yields used to calculate the value of production are from the National Agricultural Statistics Services (NASS), USDA. Per-acre crop production costs are from the Economic Research Service (ERS), USDA, which include operating costs and

[20] USDA defines CRP eligible land as "cropland (including field margins) … physically and legally capable of being planted in a normal manner to an agricultural commodity".

[21] In 1975-2009, combined corn, soybean, and wheat acreage on average accounts for 62% of the U.S. total cropland.

allocated overhead, excluding the opportunity cost of land.[22] The net cropland return is the gross value of production less crop production costs. Government payments are also important to landowners when making land-use decisions. Therefore, per-acre government payments are also estimated and included in cropland returns. National direct government payments by program are available from the ERS, USDA (payments for conservation programs are excluded in the calculation).[23] Per-acre government payments received for crop production are calculated by dividing direct government payments by total cropland acreage reported in the *Major land Uses* series of the ERS, USDA. The calculated annual cropland returns from 1975 to 2009 form a sample of 35 observations.

2.5.2 Parameter Estimation

In July 2005, the 2005 Energy Policy Act was passed.[24] As a result, biofuel production increases considerably from 2006, which led to an increased demand for and higher prices of agricultural commodities. Recent studies also recognize biofuel production as the major driver of a structural change of commodity prices and farming returns. Frank and Garcia (2010) identified

[22] The cost and return accounts were categorized into cash and economic costs for all commodities from 1975 to 1994. Beginning 1995, the accounts were revised to conform to methods recommended by the American Agricultural Economics Association Task Force on Commodity Costs and Returns, which recommended that the cost and return accounts be divided into operating costs and allocated overhead costs. To be consistent throughout, I adjusted the account item "taxes and insurance" from 1975 to 1994 according to the new method. I took the difference at the transition (between 1994 and 1995); the ratio of the difference to the balance is assumed to apply to all previous years and was used in the adjustment. The comparison of USDA's former and new cost of production estimation methodology can be found at: http://www.ers.usda.gov/data/costsandreturns/compare.htm.

[23] Payments include receipts from deficiency payments, marketing loan gains, indemnity programs, disaster payments, and production flexibility contract payments, etc.

[24] This Act established the Renewable Fuel standard requiring that transportation fuels sold in the United States contain a minimum amount of renewable fuel.

a structural change in 2006 for agricultural commodity prices using data from 1998 to 2009 and found that the agricultural markets, especially the corn market, have been more energy-driven since 2006. A report from USDA evaluated the effects of biofuel production on farm income and predicted that biofuel production would substantially improve net farm income during 2007-2016 (USDA-ERS, 2007). Given this evidence I assume that a shift of farming returns to high growth occurred in 2006 and use annual returns before 2006 to estimate the low growth rate β.

When the farming return follows a GBM, the logarithm of the return can be described as:

(2.21) $d\ln(R_t) = (\beta - 0.5\sigma^2)dt + \sigma dW_t$.

To verify whether $\ln(R_t)$ follows the process described above, (2.21) must be approximated in discrete time. The discretized version of (2.21) can be written as:

(2.22) $\ln(R_t) - \ln(R_{t-1}) = (\beta - 0.5\sigma^2)\Delta t + \sigma\varepsilon_t\sqrt{\Delta t}$,

where ε_t is a normally distributed random variable with mean 0 and variance 1.

I performed an augmented Dickey–Fuller test with a trend on the logarithm of the return series to investigate whether the data-generating process is nonstationary. The null hypothesis of unit root cannot be rejected at standard significant levels. Therefore, the analysis will be undertaken assuming that the farming return follows a GBM. The maximum-likelihood estimates of the drift β and the variance σ^2 for farming return R_t will be $\beta = \phi + 0.5\varphi^2$ and $\sigma = \varphi$, where ϕ is the mean and φ is the standard deviation of the series of $\ln(R_t) - \ln(R_{t-1})$. I obtain β=4% and $\sigma = 0.26$ from this estimation.

Based on (2.6), the expected time of staying in the high growth state is $1/\lambda$, after which the ethanol industry attains equilibrium and agricultural returns revert to their long-term growth rate. Tokgoz et al. (2008) predict that the long-run equilibrium of the ethanol industry may be

achieved in 2016-17. Therefore, I assume that $\lambda = 1/7$, which is equivalent to assuming that the high growth (α) stage will continue for an *average* of 7 more years (2010-2016). The high growth rate α is computed based on annual farming returns from 2006 to 2009 and the report of USDA Agricultural Projections to 2016 conducted in 2010. This report shows that although increases in corn-based ethanol production in the United States are projected to slow, the demand for ethanol remains high. This affects the production, use, and pricing of farm commodities throughout the sector. Consequently, although net farm income initially declines from the highs of 2007 and 2008, it remains historically strong and will rebound according to the projections. With the projected price and yield data for corn, soybean, and wheat, the production costs, and the proportion of planted areas of these crops, I estimate the higher growth rate α to be 8.5%.[25]

For other parameters, a discount rate ρ of 6% is used,[26] and the government's cost share proportion (k) for establishing land cover is 50%. The cost C depends on the land cover. In general, the cost is \$60/acre/year. In the "continuous contract" category (e.g., with wetland and buffer), participants also receive a sign-up incentive payment (π) equal to \$10/acre/year upon enrollment in the program. The annual rental payment is set at \$65 according to recent CRP reports and statistics.

2.6 Results

The option value, $J(R_t, m_t)$, is determined using the numerical method described in Appendix D. Figure 2.1 plots the value of the option to participate in the CRP under any two

[25] Since the number of observations are small, I use the simple average of annual growth rates to proxy for α.

[26] The discount rate is the same as or close to the rate used in the literature (Ince and Moiseyev, 2002; Insley, 2002; De La Torre Ugarte et al., 2003; Insley and Rollins, 2005).

different expected growth rates ($m_t = 0.049$ or $m_t = 0.085$) for the baseline case where $\alpha = 8.5\%$, $\beta = 4\%$, λ =1/7, k =0.5, C =60, $\sigma = 0.26$, $\rho = 0.06$, $\bar{T} = 15$, $Q = 65$, and $\pi = 0$. This figure shows that the option value increases (decreases) as the farming return or its expected growth rate decreases (increases).

Figure 2.1. Option Value of Land Conversion Opportunity under Two Different Expected Growth Rates (the Baseline Case)

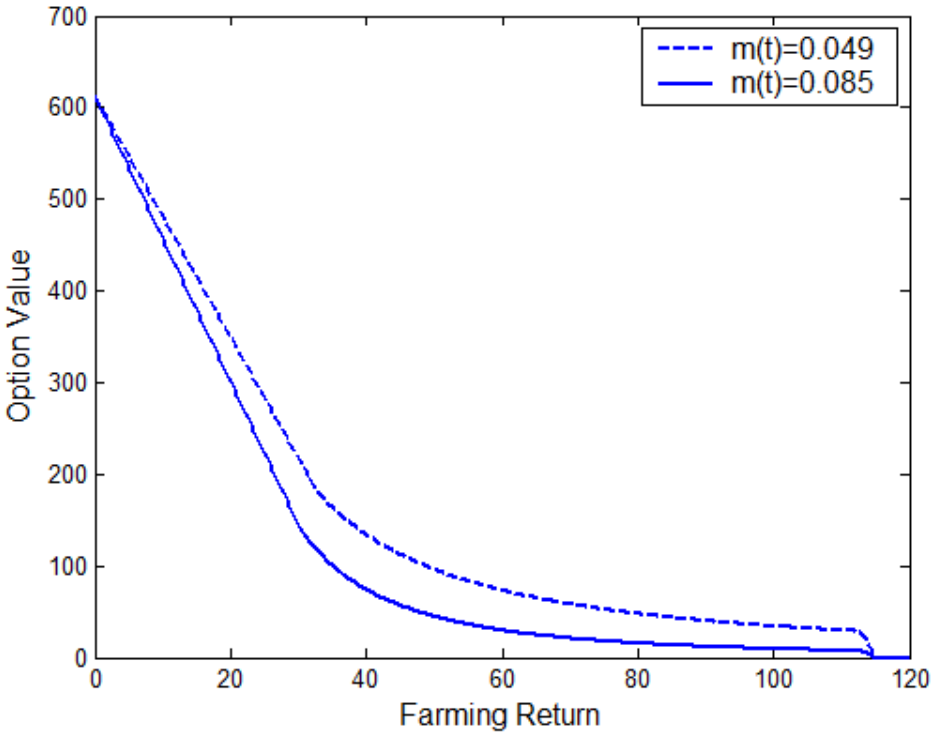

Table 2.1 shows the option value on the grid. The highlighted cells represent combinations of the farming return and its expected growth rate, for which the landowner is indifferent between waiting and participating immediately in the CRP. The numbers below these highlighted cells give the value of continuing to hold the option to convert the land, while the numbers in the upper part of the table give the value of participating immediately in the program. Together, these combinations specify the critical farming return as a function of the expected

growth rate. Farming returns lower than the threshold will make the CRP attractive enough for landowners to stop waiting and participate in the CRP. On the other hand, farming returns higher than the threshold make the CRP less attractive, and landowners will choose to wait.

Table 2.1. Option Value of Participation in the CRP for the Baseline

R / m	*0.04*	*0.0445*	*0.049*	*0.0535*	*0.058*	*0.0625*	*0.067*	*0.0715*	*0.076*	*0.0805*	*0.085*
0.00	612.9	612.9	612.9	612.9	612.9	612.9	612.9	612.9	612.9	612.9	612.9
0.25	609.7	609.6	609.5	609.5	609.4	609.3	609.3	609.2	609.1	609.1	609.0
0.50	606.4	606.3	606.2	606.1	605.9	605.8	605.7	605.5	605.4	605.2	605.1
0.75	603.2	603.0	602.8	602.6	602.4	602.2	602.0	601.8	601.6	601.4	601.2
⋮	⋮	⋮	⋮	⋮	⋮	⋮	⋮	⋮	⋮	⋮	⋮
30.25	222.0	214.5	207.0	199.3	191.4	183.4	175.3	167.0	158.5	149.9	141.2
30.50	218.7	211.2	203.6	195.8	187.9	179.9	171.7	163.3	154.8	146.1	**137.3**
30.75	215.5	207.9	200.3	192.4	184.4	176.3	168.0	159.6	151.0	**142.3**	134.7
31.00	212.3	204.6	196.9	189.0	181.0	172.8	164.4	155.9	**147.3**	139.4	132.2
31.25	209.0	201.4	193.5	185.6	177.5	169.2	160.8	**152.2**	144.2	137.0	129.8
31.50	205.8	198.1	190.2	182.2	174.0	165.7	**157.2**	149.0	141.8	134.7	127.5
31.75	202.6	194.8	186.8	178.7	170.5	**162.1**	153.9	146.7	139.5	132.4	125.2
32.00	199.3	191.5	183.5	175.3	**167.0**	158.8	151.6	144.4	137.3	130.1	123.0
32.25	196.1	188.2	180.1	**171.9**	163.8	156.6	149.4	142.2	135.0	127.9	120.9
32.50	192.9	184.9	**176.8**	168.8	161.6	154.4	147.2	140.0	132.9	125.8	118.8
32.75	189.6	**181.6**	173.9	166.7	159.5	152.3	145.1	137.9	130.8	123.7	116.7
33.00	**186.4**	179.0	171.8	164.6	157.4	150.2	143.0	135.8	128.7	121.7	114.7
33.25	184.1	177.0	169.8	162.6	155.3	148.1	141.0	133.8	126.7	119.7	112.8
⋮	⋮	⋮	⋮	⋮	⋮	⋮	⋮	⋮	⋮	⋮	⋮

Note: threshold returns under different growth rate expectations can be easily detected from highlighted cells.

Our main findings can be summarized as follows. 1) The option value decreases when farming returns R_t and the expected growth rate m_t increase, as illustrated in Figure 2.1; the

threshold return R_t^* declines when the expected growth rate increases, making conversion more difficult. 2) The option value increases with λ (recall that $1/\lambda$ represents the average time of staying in the high growth state), which means that the longer the high growth state is expected to persist, the lower is the value of the option. This suggests that the threshold at which the landowner is likely to enroll in the CRP is lower in a time of extended high growth, and hence landowners are less likely to participate. These results are intuitive: higher farming returns, higher expected growth rates, and a longer time of remaining in the high growth state all reduce the incentive for conservation. This is consistent with the observation of reduced participation in the last few years when farming returns grew rapidly.

The land-use decisions model developed in this study and the decision thresholds calculated can be used to simulate CRP participation probability. I conducted Monte Carlo simulations to investigate the enrollment probability for a piece of land with the baseline characteristics as discussed above. I use the Euler method to simulate the dynamics of farming return (eq. 2.10) and growth rate (eq. 2.12). The farming return and growth rate dynamics are simulated over a 5-year horizon from 2010. The initial farming return in 2009 is assumed to be \$104 per acre;[27] and the initial growth rate expectation is set at 7.30%, which is the mean growth rate for 2009 according to the dynamics of eq. 2.12, implying that the landowner believes that the growth rate has a 27% chance of reverting to the long-term average according to eq. 2.8. The conversion thresholds (i.e., the highlighted boundaries in Table 2.1) are used as the decision criteria: at a certain growth rate expectation, if the simulated farming return is lower than the

[27] Since the land eligible for CRP participation generally has lower productivity, the initial farming return for CRP land is the general cropland return multiplied by a coefficient of 0.68, which is the average ratio of rental payments of CRP land to the cash rent of the general cropland, assuming proportional downward adjustment.

threshold anytime in the 5-year horizon, the land would be enrolled into the conservation program but otherwise would stay in farming. The results of 20,000 Monte Carlo replications show that in 5 years the land with the baseline characteristics discussed would have a 3.19% probability of being enrolled in the CRP. To get a feel for the sensitivity of participation to initial farming returns, I conducted an additional simulation setting the initial farming return at a low value of $90 per acre, which resulted in a participation rate of 4.96%. A rough estimate of the elasticity of the participation probability with respect to farming returns is -4.1, which indicates that participation is very sensitive to changes in initial farming returns.

To evaluate the impact of structural change, I perform another simulation assuming $\alpha = \beta = 4.0\%$, which is equivalent to assuming the traditional geometric Brownian motion without parameter uncertainty. Accordingly, the initial farming return in 2009 is set at $66, which is calculated using the realized farming return in 2005 and an annual growth of 4%, adjusted for the lower productivity of CRP lands. New conversion thresholds are derived and used in the Monte Carlo simulation. The simulation result shows that the participation rate rises to 15.92%, which is five times the baseline case of 3.19%. That is, structural change has reduced participation probability by 80 percent. This shows that incorrectly ignoring uncertainty in growth rates surrounding future agricultural returns can have a huge impact on estimated participation.

Though biofuel production is a major source of structural change, other factors may also be important. Based on the evidence from the literature, I assume that biofuel production accounted for 60 percent of the increase in corn prices, 40 percent of the increase in soybean prices, and 26 percent of the increase in wheat prices (Collins, 2008; Lipsky, 2008). Assuming the same effect on net returns for each crop and using historical average planted ratios of each

crop as weights, biofuel production contributes roughly 40% of the jump in growth from 4% to 8.5%. To separate the impact of biofuel production on CRP participation, I re-simulate the participation probability excluding biofuel production's effect on the growth rate. For this purpose, I reset $\alpha = 6.7\%$ (keeping $\beta = 4\%$) and re-calculate the land conversion threshold returns under different growth expectations. With an adjusted initial growth rate of 6% (similarly, assuming the landowner holds the same 27% belief on the probability of the growth rate reverting to the long-term average) and an adjusted initial farming return of $74 for 2009, the simulation results show that the participation rate would be 9.92% in the next 5 years, which is more than three times higher than the baseline case of 3.19%.[28] That is, of the entire structural change impact (an 80 percent drop from 15.92% to 3.19%), biofuel production accounts for approximately half of the reduction. Further simulation shows that, to offset the participation loss due to the biofuel impact, the government would need to raise the per-acre rental payment by $25, which means an increase of nearly 40%.

The negative effect of the biofuel boom on participation is intuitive. Policies designed to support biofuel production would create incentives to move resources into biofuels. For example, the 2005 Energy Policy Act mandates 7.5 billion gallons of renewable fuel to be added to gasoline by 2012. Subsequent tax incentives and subsidies (e.g. federal tax credits of 51 cents a gallon for ethanol blenders) have paved the way for the increase in biofuel production. The growing demand for biofuels has decreased participation in the CRP, as shown by our simulations. This unintended consequence on conservation programs will counteract the emission reduction benefits of biofuel and thus need to be taken into consideration in the evaluation of biofuel programs and policy designs. Also, it raises the question of whether corn

[28] The initial farming return of $74 is calculated using the realized farming return in 2005 and an annual growth of 6%, adjusted for the lower productivity of CRP lands.

ethanol production could lead to effective net greenhouse gas emission reductions compared to the reductions achieved by the CRP itself (Searchinger et al., 2008; Piñeiro et al., 2009).

2.7 Sensitivity Analysis

A sensitivity analysis is undertaken to determine landowners' response to changes in various parameters. In particular, I analyze landowners' response to market conditions.

2.7.1 Length of the High Growth State, $1/\lambda$

In this section I investigate the impact of high growth duration on conservation participation. Figure 2.2 shows the return boundaries under different expectations of the high growth duration, namely, 4, 7, 12 and 20 years. For example, if the landowner expects the growth rate to be at 7.15% and persist for 12 years (corresponding to the 2022 target set in the 2007 energy act), he would be willing to participate in the CRP at a lower, $30.25/acre farming return. The Monte Carlo simulation result shows that the participation probability in a 5-year horizon reduces from 3.19% to 2.53% when the high growth duration extends from 7 years to 12 years. Persistence of the biofuel boom has a clear impact on the length of the high growth state and therefore would lead to decreased conservation participation. Figure 2.2 also shows that the lower the initial growth rate expectation, the less sensitive is the boundary to the duration of the high growth state.

Figure 2.2. Farming Threshold Returns (R^*) versus Growth Rate Expectations (m_t) under Different Durations of the High Growth State

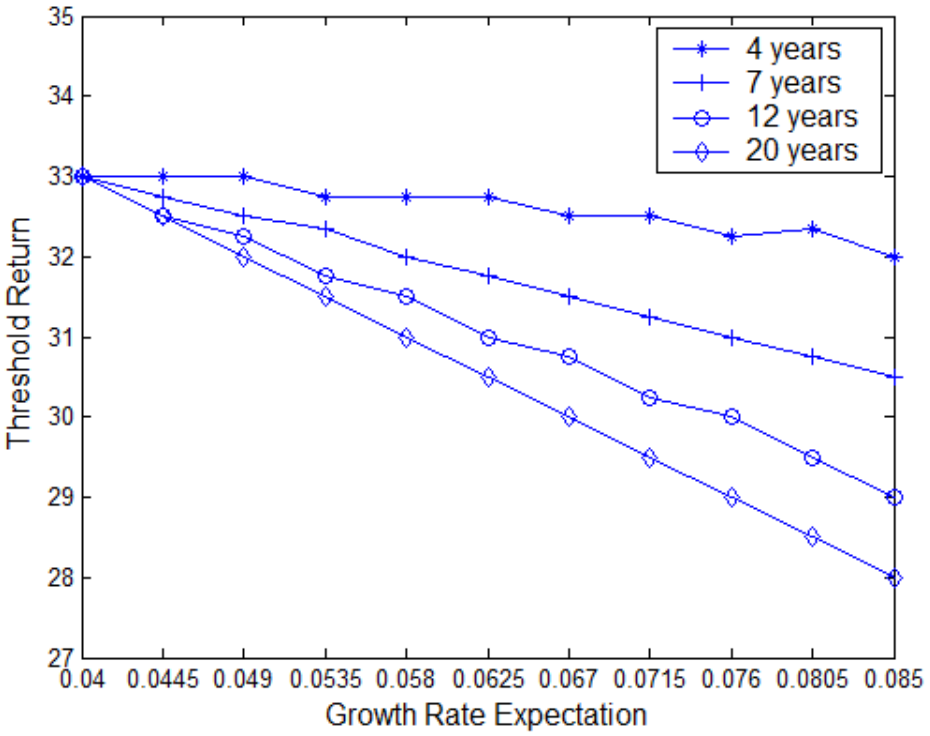

The durations of biofuel boom and in turn the high growth in farming returns are to a large extent dependent on a long list of incentives that the State and Federal governments have instated to support ethanol production since the 1970s and protections from the U.S. trade barriers. The most prominent among them are the Federal ethanol tax credit and ethanol import tariff. While the tax credit goes to ethanol refiners, farmers have benefited because with sufficiently high competition among blenders, the corn price increases by almost the full amount of the credit (Elobeid et al., 2007). Also, imposing an import tariff raises domestic ethanol and corn prices. However, to date rising food prices, the desperation to reduce federal budget deficits, and criticisms to corn-based ethanol from environmental organizations have led to the debate of eliminating ethanol tax credits and import tariffs. Elobeid and Tokgoz (2008) simulated the

effect of removing the tax credit and trade distortions and found that corn demand and prices would decline substantially. Importantly, the ethanol industry may end its boom sooner and farming returns may return to its long-run equilibrium in a shorter duration. In that case, I have a larger λ value and would expect an increase in program participation as simulated in Figure 2.2.

2.7.2 The Effect of Volatility, σ

I further study the effect of uncertainty on the participation threshold. I keep other parameters in the baseline unchanged while varying the standard deviation of the logarithm of farming returns. The impact of changes in volatility is illustrated in Figure 2.3.

Figure 2.3. Farming Threshold Returns (R^*) versus Growth Rate Expectations (m_t) under Different Volatility Parameters

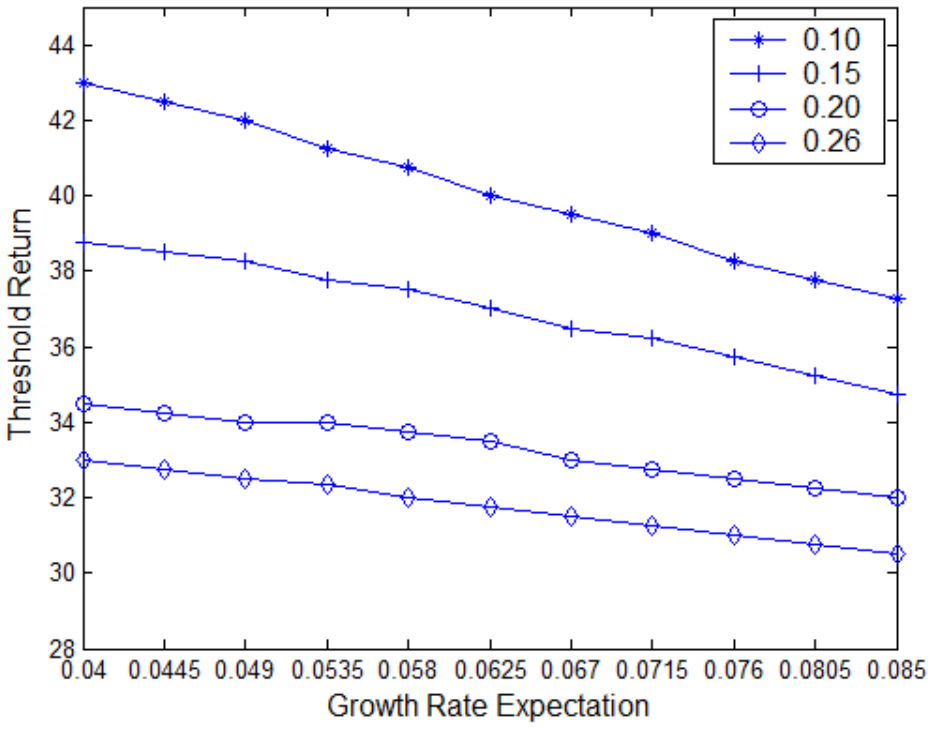

Figure 2.3 shows that volatility in the farming return contributes to a decrease in the participation threshold. As expected, when the volatility of the farming return increases, the option value increases, and the threshold decreases, indicating the landowner would wait for a lower farming return realization before committing to land conversion. For example, when volatility changes from 0.2 to 0.26, the participation threshold decreases from $32.75/acre to $31.25/acre at the 7.15% growth rate expectation. The decrease in the threshold value may have a negative effect on participation. However, besides lowering the critical trigger value, higher volatility may also make the farming return more likely to reach the critical value, which would have a positive effect on participation. To determine the overall effect of volatility, I examine the probability of participation with Monte Carlo simulation. The simulation results show that when volatility increases from 0.20 to 0.26, the probability of participation actually moves up, from 0.63% to 3.19%, which suggests that risk in agriculture would induce conservation. The implication is that reducing risk and uncertainty in agricultural returns, for example, with programs on farm income stabilization, may have a negative impact on CRP participation and environmental conservation.

One could also consider the effect of uncertainty on the reverse land use decision to convert from CRP land back to crop production. Higher uncertainty in crop returns should increase the value of the option to convert from CRP back to crop production which should contribute to an increase in the threshold (R^*) above which farming returns must go before the landowner will convert back to farming. As a result, when all other conditions are kept unchanged, landowners would need a higher realized return from farming in order to convert, and therefore would be more likely to delay the decision to return to crop production. However, besides increasing the critical trigger value, higher volatility may also make the farming return

more likely to reach the critical value, which would have a positive effect on the overall probability of converting back to farming. Determining the net effect of increased uncertainty in farming returns on the net probability of converting from CRP back to crop farming would require a complete numerical analysis of the reverse conversion decision, which was not undertaken here.

2.8 Conclusions

Biofuel policies have spurred biofuel production and have been pressuring land out of conservation programs, offsetting the emission reduction goal of the biofuel policy and increasing the potential for environmental degradation. This essay proposes a general land-use decision model to analyze the spillover effect of biofuels policy on conservation program participation. The proposed model captures the biofuel-driven structural changes in the agricultural sector and is used to simulate landowners' conservation participation decision under different layers of uncertainty and investigates factors that affect this decision. I derived the threshold conditions that would trigger participation in conservation. The decision model provides a useful tool for quantifying the spillover effect, determining optimal land use, and for policy makers to develop informed and more cost-effective environmental policies. Methodologically, I derived numerical solutions to the land-use decision problem under parameter uncertainty using a technique that can handle a fairly general class of specifications for the source of uncertainty. More specifically, I use a nonlinear Kalman filter approach to addressing parameter uncertainty, which continuously updates information observed by landowners and estimates the random growth rate of farming returns with minimum error. The

real options problem is formulated as a linear complementarity problem and solved with a fully implicit finite difference approach.

I find a strong negative effect of biofuel production on conservation enrollment. Overall, the structural changes have reduced the chance of CRP participation by 80 percent, and one half of this reduction appears to stem from biofuel production. Our simulation results further suggest that, to offset the participation loss caused by biofuel production, the government would have to increase the per-acre rental payment by 40%. Our results show that higher farming returns, higher expected growth rates, and a longer time of remaining in the high growth state all reduce the incentive for conservation due to the decreasing value of the conservation option for landowners. I also found that, though higher volatility of agricultural return reduces the decision threshold of farming returns, its overall effect on participation is positive, which implies that government programs aiming to reduce farm income risk would have a negative effect on conservation participation.

APPENDIX B

APPENDIX B: DERIVATION OF EQUATION 2.12

Let $d\xi_t = A_t(\theta_t, \xi)dt + B_t(\xi)dW_t$, where the unobservable component θ_t is described by a continuous-time Markov chain with transition matrix $\lambda_{\alpha\beta}(t)$ and state space E with states α and β. Let $\pi_\beta(t) = prob(\theta_t = \beta | \Omega_t^\xi)$. According to Lipster and Shiryayev (1977) Theorem 9.1, $\pi_\beta(t)$ satisfies the following equation:

(B.1) $$d\pi_\beta(t) = \sum_{\gamma \in E} \lambda_{\gamma\beta}(t)\pi_\gamma(t)dt + \pi_\beta(t)\frac{A_t(\beta,\xi) - \bar{A}_t(\xi)}{B_t(\xi)}d\bar{W}_t,$$

where $\bar{A}_t(\xi) = \sum_{\gamma \in E} A_t(\gamma,\xi)\pi_\gamma(t)$ and $d\bar{W}_t = \frac{1}{B_t(\xi)}d\xi_t - \frac{A_t(\xi)}{B_t(\xi)}dt$.

In our setup, $dR_t = \theta_t R_t dt + \sigma R_t dW_t$, and $p_t = prob(\theta_t = \beta | \Omega_t^R)$, which means that $A_t(\theta_t, \xi) = \theta_t R_t$, $B_t(\xi) = \sigma R_t$, and $\bar{A}_t(\xi) = p_t \beta R_t + (1 - p_t)\alpha R_t$. From our Markov system, I can derive that $\lambda_{\alpha\beta} = \lambda$ and $\lambda_{\beta\beta} = 0$ under state space $E = \{\alpha, \beta\}$. An application of Theorem 9.1 yields:

(B.2) $$dp_t = \lambda(1 - p_t)dt + \frac{p_t(1-p_t)(\beta - \alpha)}{\sigma}d\bar{W}_t,$$

where $d\bar{W}_t = dW_t + \frac{1}{\sigma}(\theta_t - m_t)dt$.

Plugging $p_t = \frac{m_t - \alpha}{\beta - \alpha}$ into the above equation yields:

(B.3) $$dm_t = \lambda(\beta - m_t)dt + \frac{1}{\sigma}(\alpha - m_t)(m_t - \beta)d\bar{W}_t.$$

APPENDIX C

APPENDIX C: DERIVATION OF EQUATION 2.14

The derivation is through Ito's Lemma. I know that $dR_t = m_t R_t dt + \sigma R_t d\overline{W}_t$ and $dm_t = \lambda(\beta - m_t)dt + \frac{1}{\sigma}(\alpha - m_t)(m_t - \beta)d\overline{W}_t$. Taking the square of the first equation obtains:

(C.1) $(dR_t)^2 = (R_t m_t dt)^2 + 2R_t^2 m_t \sigma dt d\overline{W}_t + R_t^2 \sigma^2 (d\overline{W}_t)^2$.

I already know that $(dt)^2$ and cross product $dtd\overline{W}_t$ are equal to zero in the mean square sense, and $(d\overline{W}_t)^2 = dt$, therefore:

(C.2) $E(dR_t)^2 = R_t^2 \sigma^2 dt$.

Similarly, I obtain:

(C.3) $E(dm_t)^2 = \frac{1}{\sigma^2}(\alpha - m_t)^2 (m_t - \beta)^2 dt$,

(C.4) $E(dR_t dm_t) = R_t(\alpha - m_t)(m_t - \beta)dt$.

Applying Ito's Lemma to $J(R_t, m_t)$, I can derive a partial differential equation:

(C.5) $dJ(R_t, m_t) = J_R dR_t + J_m dm_t + \frac{1}{2}\left[J_{RR}(dR_t)^2 + J_{mm}(dm_t)^2 + 2J_{Rm}dR_t dm_t)\right]$.

Substituting C.2, C.3, and C.4 into C.5, I obtain:

(C.6) $E[dJ(R_t, m_t)] = \left[\begin{array}{l} R_t m_t J_R + \lambda(\beta - m_t)J_m + \frac{1}{2}R_t^2 \sigma^2 J_{RR} \\ + \frac{1}{2\sigma^2}(\alpha - m_t)^2 (m_t - \beta)^2 J_{mm} + R_t(\alpha - m_t)(m_t - \beta)J_{Rm} \end{array}\right] dt$.

The Bellman equation for eq. 2.13 is expressed as:

(C.7) $\rho J(R_t, m_t)dt = E\left[dJ(R_t, m_t)\right]$.

Therefore,

$$\text{(C.8)} \quad \rho J - \left[\begin{array}{l} R_t m_t J_R + \lambda(\beta - m_t) J_m + \frac{1}{2} R_t^2 \sigma^2 J_{RR} \\ + \frac{1}{2\sigma^2} (\alpha - m_t)^2 (m_t - \beta)^2 J_{mm} + R_t (\alpha - m_t)(m_t - \beta) J_{Rm} \end{array} \right] = 0 .$$

APPENDIX D

APPENDIX D: DISCRETIZATION OF THE LCP

This Appendix describes the numerical approach used to solve the LCP for valuing the option to participate in the CRP. For a general discussion of numerical methods of option valuation, refer to Wilmott, Howison, and Dewynne (1993). A finite difference scheme is used in this paper, which involves reducing a continuous partial differential equation to a discrete set of difference equations. Two basic finite difference methods are the implicit method and the explicit method. When applied to the partial differential equation, backward and forward difference approximations for the derivative of option value with respect to time lead to implicit and explicit finite-difference schemes, respectively (Wilmott, Howison, and Dewynne, 1993). The implicit finite-difference method is robust because it can overcome the stability and convergence problems that plague the explicit finite-difference method. In this paper, I use an implicit difference scheme—the Crank-Nicolson scheme.

To explain the three-dimensional (R, m, t) discretization for eq. 2.15, consider a three-dimensional space formed by the farming return R, the growth rate m, and time t. I divide the R-axis into equally-spaced nodes a distance ΔR apart, the m-axis into equally-spaced nodes a distance Δm apart, and the t-axis into equally spaced nodes a distance Δt apart. This divides the (R, m, t) space into a grid, where grid points have the form $(s\Delta R, n\Delta m, i\Delta t)$. I then compute the option value J at these points:

(D.1) $$R = \{R_0, R_1, R_2, \cdots, R_S\},\ m = \{m_0, m_1, m_2, \cdots, m_N\}, t = \{t_0, t_1, t_2, \cdots, t_I\}.$$

The finite difference method involves replacing partial derivatives by approximations based on Taylor expansions near the point of interest. At any point on the grid $(R, m, t) = (R_s, m_n, t_i)$, the value of the option is denoted as $J_{s,n,i}$. A formula for approximating

the partial derivatives using the implicit difference method can be found in Wilmott, Howison, and Dewynne (1993). Replacing these derivatives in eq. 2.15 yields a series of difference equations:

$$\text{(D.2)}\quad HJ_i = \begin{bmatrix} a_{s-1,n-1}J_{s-1,n-1} + a_{s-1,n}J_{s-1,n} + a_{s-1,n+1}J_{s-1,n+1} + a_{s,n-1}J_{s,n-1} + a_{s,n}J_{s,n} \\ + a_{s,n+1}J_{s,n+1} + a_{s+1,n-1}J_{s+1,n-1} + a_{s+1,n}J_{s+1,n} + a_{s+1,n+1}J_{s+1,n+1} \end{bmatrix}^i,$$

Where $a_{s-1,n-1} = -\dfrac{R_{s-1}(\alpha - m_{n-1})(m_{n-1} - \beta)}{4\Delta R \Delta m}$, $a_{s-1,n} = \dfrac{R_{s-1}m_n}{2\Delta R} - \dfrac{R_{s-1}^2\sigma^2}{2\Delta R^2}$,

$$a_{s-1,n+1} = \frac{R_{s-1}(\alpha - m_{n+1})(m_{n+1} - \beta)}{4\Delta R \Delta m},$$

$$a_{s,n-1} = -\frac{(\alpha - m_{n-1})^2(m_{n-1} - \beta)^2}{2\sigma^2 \Delta m^2} - \frac{\lambda(m_{n-1} - \beta)}{2\Delta m},$$

$$a_{s,n} = \frac{(\alpha - m_n)^2(m_n - \beta)^2}{2\sigma^2 \Delta m^2} + \rho + \frac{R_s^2\sigma^2}{2\Delta R^2},$$

$$a_{s,n+1} = -\frac{(\alpha - m_{n+1})^2(m_{n+1} - \beta)^2}{2\sigma^2 \Delta m^2} + \frac{\lambda(m_{n+1} - \beta)}{2\Delta m},$$

$$a_{s+1,n-1} = \frac{R_{s+1}(\alpha - m_{n-1})(m_{n-1} - \beta)}{4\Delta R \Delta m},$$

$$a_{s+1,n} = -\frac{R_{s+1}m_n}{2\Delta R} - \frac{R_{s+1}^2\sigma^2}{2\Delta R^2},\ a_{s+1,n+1} = -\frac{R_{s+1}(\alpha - m_{n+1})(m_{n+1} - \beta)}{4\Delta R \Delta m}.$$

The superscript i on the right-hand side means that all variables within the square parentheses are evaluated at t_i.

The difference equation must also be specified when the growth rate is at its maximum and minimum values. I use BC2 boundary condition on $m_{\min} = \beta$ and $m_{\max} = \alpha$ (Tavella and Randall, 2000). The one-sided difference for J_{mm} (the second derivative of J with respect to

m) and the forward-backward difference for J_{Rm} (the cross derivative of J with respect to R and m) are used at $m_{\max} = \alpha$:

$$\text{(D.3)} \quad J_{mm} = \left[\frac{J_{s,n} - 2J_{s,n-1} + J_{s,n-2}}{\Delta m^2} \right]^i, \; J_{Rm} = \left[\frac{J_{s,n} - J_{s-1,n} - J_{s,n-1} + J_{s-1,n-1}}{\Delta m \Delta R} \right]^i.$$

Then, in eq. 2.15,

$$\text{(D.4)} \quad HJ_i = \begin{bmatrix} a_{s-1,n-1}J_{s-1,n-1} + a_{s-1,n}J_{s-1,n} + a_{s,n-2}J_{s,n-2} \\ + a_{s,n-1}J_{s,n-1} + a_{s,n}J_{s,n} + a_{s+1,n}J_{s+1,n} \end{bmatrix}^i,$$

where $a_{s-1,n-1} = -\dfrac{R_{s-1}(\alpha - m_{n-1})(m_{n-1} - \beta)}{\Delta R \Delta m}$,

$$a_{s-1,n} = \frac{R_{s-1}(\alpha - m_n)(m_n - \beta)}{\Delta R \Delta m} + \frac{R_{s-1}m_n}{2\Delta R} - \frac{R_{s-1}^2\sigma^2}{2\Delta R^2},$$

$$a_{s,n-2} = -\frac{(\alpha - m_{n-2})^2(m_{n-2} - \beta)^2}{2\sigma^2\Delta m^2} - \frac{\lambda(m_{n-2} - \beta)}{2\Delta m},$$

$$a_{s,n-1} = \frac{(\alpha - m_{n-1})^2(m_{n-1} - \beta)^2}{\sigma^2\Delta m^2} + \frac{R_s(\alpha - m_{n-1})(m_{n-1} - \beta)}{\Delta R \Delta m},$$

$$a_{s,n} = -\frac{(\alpha - m_n)^2(m_n - \beta)^2}{2\sigma^2\Delta m^2} + \rho + \frac{R_s^2\sigma^2}{\Delta R^2} + \frac{\lambda(m_n - \beta)}{2\Delta m} - \frac{R_s(\alpha - m_n)(m_n - \beta)}{\Delta R \Delta m},$$

$$a_{s+1,n} = -\frac{R_{s+1}m_n}{2\Delta R} - \frac{R_{s+1}^2\sigma^2}{2\Delta R^2}.$$

Similarly, the one-sided difference for J_{mm} and the forward-backward difference for J_{Rm} are used at $m_{\min} = \beta$:

$$\text{(D.5)} \quad J_{mm} = \left[\frac{J_{s,n+2} - 2J_{s,n+1} + J_{s,n}}{\Delta m^2} \right]^i, \; J_{Rm} = \left[\frac{J_{s,n+1} - J_{s,n} - J_{s-1,n+1} + J_{s-1,n}}{\Delta m \Delta R} \right]^i.$$

Then, in eq. 2.15,

(D.6) $$HJ_i = \begin{bmatrix} a_{s-1,n}J_{s-1,n} + a_{s-1,n+1}J_{s-1,n+1} + a_{s,n}J_{s,n} \\ + a_{s,n+1}J_{s,n+1} + a_{s,n+2}J_{s,n+2} + a_{s+1,n}J_{s+1,n} \end{bmatrix}^i,$$

where $a_{s-1,n} = -\frac{R_{s-1}(\alpha - m_n)(m_n - \beta)}{\Delta R \Delta m} + \frac{R_{s-1}m_n}{2\Delta R} - \frac{R_{s-1}^2\sigma^2}{2\Delta R^2}$,

$$a_{s-1,n+1} = \frac{R_{s-1}(\alpha - m_{n+1})(m_{n+1} - \beta)}{\Delta R \Delta m},$$

$$a_{s,n} = -\frac{(\alpha - m_n)^2(m_n - \beta)^2}{2\sigma^2\Delta m^2} + \rho + \frac{R_s^2\sigma^2}{\Delta R^2} + \frac{\lambda(m_n - \beta)}{2\Delta m} + \frac{R_s(\alpha - m_n)(m_n - \beta)}{\Delta R \Delta m},$$

$$a_{s,n+1} = \frac{(\alpha - m_{n+1})^2(m_{n+1} - \beta)^2}{\sigma^2\Delta m^2} - \frac{R_s(\alpha - m_{n+1})(m_{n+1} - \beta)}{\Delta R \Delta m},$$

$$a_{s,n+2} = -\frac{(\alpha - m_{n+2})^2(m_{n+2} - \beta)^2}{2\sigma^2\Delta m^2}, a_{s+1,n} = -\frac{R_{s+1}m_n}{2\Delta R} - \frac{R_{s+1}^2\sigma^2}{2\Delta R^2}.$$

Equations D.2, D.4 and D.6 form a system of equations, which can be written in matrix form and solved by iteration (Insley, 2002).

APPENDIX E

APPENDIX E: DERIVATION OF EQUATION 2.20

The simple optimal stopping problem without parameter uncertainty is:

$$\text{(E.1)} \quad \begin{cases} J(R_t, m, \infty) = \max_T E_t[e^{-\rho(T-t)} M(R_T, Q)] \\ dR_t = R_t m dt + R_t \sigma d\overline{W}_t \end{cases}.$$

Using Ito's lemma, the fundamental differential equation of this optimal stopping problem is an ordinary differential equation:

$$\text{(E.2)} \quad \frac{1}{2} R_t^2 \sigma^2 J_{RR} + R_t m J_R - \rho J = 0,$$

where J_R and J_{RR} are the first and second derivatives of J with respect to R_t.

Let R^* represent the threshold value, which triggers participation in the CRP. This ordinary differential equation is solved subject to the following boundary conditions. First, the continuity condition is:

$$\text{(E.3)} \quad J(R^*) = M(R^*, Q) = V(Q) - \frac{R^*(1 - e^{-(\rho - m)\overline{T}})}{\rho - m}.$$

Second, the smooth pasting condition is:

$$\text{(E.4)} \quad J_R(R^*) = M_R(R^*, Q) = -\frac{(1 - e^{-(\rho - m)\overline{T}})}{\rho - m}.$$

In addition, I have:

$$\text{(E.5)} \quad J(\infty, m, \infty) = 0,$$

which says that when the farming return approaches infinity, the land conversion option is worthless. The general form of the solution to equations is

$$\text{(E.6)} \quad J(R_t, m, \infty) = \begin{cases} M(R^*, Q)\left(\frac{R_t}{R^*}\right)^{\gamma} & R_t \geq R^* \\ M(R_t, Q) & R_t \leq R^* \end{cases},$$

where $\gamma = \frac{-(m-\frac{1}{2}\sigma^2)-\sqrt{(m-\frac{1}{2}\sigma^2)^2+2\rho\sigma^2}}{\sigma^2}$, which is the negative root of the fundamental quadratic equation $\frac{1}{2}\sigma^2\gamma(\gamma-1)+m\gamma-\rho=0$, and the threshold $R_t^* = \frac{\gamma}{\gamma-1}\cdot\frac{(\rho-m)\cdot V(Q)}{(1-e^{-(\rho-m)\bar{T}})}$.

REFERENCES

REFERENCES

Abasov, T. M. 2005. Dynamic learning effect in corporate finance and risk management. PhD dissertation, University of California, Irvine.

Brennan, M. J. 1998. The role of learning in dynamic portfolio decisions. European Finance Review 1, 295–306.

Capozza, D., Li, Y. 1994. The intensity and timing of investment, the case of land. American Economic Review 84(4), 889-904.

Carey, M. J., Zilberman, D. 2002. A model of investment under uncertainty, modern irrigation technologies and emerging markets in water. American Journal of Agricultural Economics 84, 171-183.

Change, H., Boisvert, R. N. 2009. Distinguishing between whole-farm vs. partial-farm participation in the Conservation Reserve Program. Land Economics 85(1), 144–161.

Collins, K. 2008. The role of biofuels and other factors in increasing farm and food prices, a review of recent development with a focus on feed grain markets and market prospects. Unpublished, Kraft Foods Global, Inc.

De La Torre Ugarte, D. G., Walsh, M. E., Shapouri, H., Slinsky, S. P. 2003. The economic impacts of bioenergy crop production on U.S. agriculture. Washington DC, U. S. Department of Agriculture, Agricultural Economic Report No. 816, February.

Dixit, A. R., Pindyck, R. S. 1994. Investment under uncertainty. Princeton, Princeton University Press.

Elobeid, A., Tokgoz, S. 2008. Removing distortions in the US ethanol market, what does it imply for the United States and Brazil? American Journal of Agricultural Economics 90, 918-932.

Elobeid, A., Tokgoz, S., Hayes, D. J., Babcock, B. A., Hart, C. E. 2007. The long-run impact of corn-based ethanol on the grain, oilseed, and livestock sectors with implications for biotech crops. AgBioForum 10, 11-18.

Frank, J., Garcia, P. 2010. How strong are the linkages among agricultural, oil, and exchange rate markets? Proceedings of the NCCC-134 Conference on Applied Commodity Price Analysis, Forecasting, and Market Risk Management. St. Louis, MO.

Gennotte, G. 1986. Optimal portfolio choice under incomplete information. The Journal of Finance 3, 733-746.

Ince, P. J., Moiseyev, A. N. 2002. Forestry implications of agricultural short-rotation woody crops in the USA. In L. Teeter, B. Cashore, and D. Zhang, ed. Forest policy for private forestry, global and regional challenges. New York, CABI Publishing, pp. 177-188.

Insley, M., 2002. A real options approach to the valuation of a forestry investment. Journal of Environmental Economics and Management 44(3), 471-492.

Insley, M., Rollins, K. 2005. On solving the multirotational timber harvesting problem with stochastic prices, a linear complementarity formulation. American Journal of Agricultural Economics 87, 735-755.

Isik, M., Yang, W. 2004. An analysis of the effects of uncertainty and irreversibility on farmer participation in the Conservation Reserve Program. Journal of Agricultural and Resource Economics 29(2), 242-259.

Lipsky, J. 2008. Commodity prices and global inflation. remarks at the Council on foreign relations, New York City, May 8, 2008.

Liptser R. S., Shiryayev, A. N. 1977. Statistics of random processes I, general theory. New York, Springer-Verlag.

Lubowski, R. N., Plantinga, A. J., Stavins, R. N. 2008. What drives land-use changes in the United States? a national analysis of landowner decisions. Land Economics 84(4), 529-550.

Kalman, R. E. 1960. A new approach to linear filtering and prediction problems. Journal of Basic Engineering 82, 35–45.

Parks, P. J., Kramer, R. A. 1995. A policy simulation of the Wetlands Reserve Program. Journal of Environmental Economics and Management 28(2), 223–240.

Piñeiro, G., Jobbágy, E. G., Baker, J., Murray, B. C., Jackson, R. B. 2009. Set-asides can be better climate investment than corn ethanol. Ecological Applications 19(2), 277-282.

Schatzki, T. 2003. Options, uncertainty and sunk costs, an empirical analysis of land use change. Journal of Environmental Economics and Management 46 (1), 86–105.

Searchinger, T., Heimlich, R., Houghton, R. A., Dong, F., Elobeid, A., Fabiosa, J., Tokgoz, S., Hayes, D., Yu, T. 2008. Use of U.S. croplands for biofuels increases greenhouse gases through emissions from land-use change. Science 319, 1238 – 1240.

Suter, J. F., Poe, G. L., Bills, N. L. 2008. Do landowners respond to land retirement incentives? evidence from the Conservation Reserve Enhancement Program. Land Economics 84 (1), 17–30.

Tavella, D. A., Randall, C. 2000. Pricing financial instruments, the finite difference method. New York, Wiley.

Tokgoz, S., Elobeid, A., Fabiosa, J., Hayes, D. J., Babcock, B. A., Yu, T., Dong, F., Hart, C. E. 2008. Bottlenecks, drought, and oil price spikes, impact on U.S. ethanol and agricultural sectors. Review of Agricultural Economics 30, 1-19.

U.S. Department of Agriculture. 2007. Agricultural baseline projections, baseline presentation, 2007-2016. Economic Research Service (ERS), Washington DC, February.

U.S. Department of Agriculture. 2007. Conservation Reserve Program, summary and enrollment statistics FY 2006. Farm Service Agency (FSA), Washington DC, May.

U.S. Department of Agriculture. 2010. Conservation Reserve Program, monthly summary – August 2010. Farm Service Agency (FSA), Washington DC, September.

U.S. Department of Agriculture. 2010. Acreage. National Agricultural Statistics Service (NASS), Washington DC, September.

Wilmott, P., Howison, S., Dewynne, J. 1993. Option pricing, mathematical models and computation. Oxford, Oxford Financial Press.

Wu, J. 2000. Slippage effects of the Conservation Reserve Program. American Journal of Agricultural Economics 82, 979-992.

Wu, J., Zilberman, D., Babcock, B. A. 2001. Environmental and distributional impacts of conservation targeting strategies. Journal of Environmental Economics and Management 41(3), 333-350.

Wu, J., Lin, H. 2010. The effect of the Conservation Reserve Program on land values. Land Economics 86 (1), 1–21.

Xia, Y. 2001. Learning about predictability, the effects of parameter uncertainty on dynamic asset allocation. Journal of Finance 56, 205-246.

Young, C. E., Osborn, C. T. 1990. The Conservation Reserve Program, an economic assessment. Washington DC, U.S. Department of Agriculture, Agricultural Economic Report No. 626, February.

CHAPTER 3: THE RISK-ADJUSTED IMPLIED VOLATILITY AND ITS FORECAST PERFORMANCE IN CORN FUTURES

3.1 Introduction

The question of whether implied volatility provides unbiased and informationally efficient forecasts of future realized volatility has been studied extensively in the empirical finance and time series econometrics literature. The typical test employed in the literature takes the regression form:

$$v_{t,t+\Delta} = \gamma_0 + \gamma_{IM}\sigma^{IM}_{t,t+\Delta} + \gamma_{AV}\sigma^{AV}_{t,t+\Delta} + \epsilon_{t+\Delta}, \quad (3.1)$$

where $v_{t,t+\Delta}$ is realized volatility over the period t to $t+\Delta$, $\sigma^{IM}_{t,t+\Delta}$ is implied volatility over the same period, and $\sigma^{AV}_{t,t+\Delta}$ is an alternative predictor typically generated from historical information. The objective of the test is to establish whether implied volatility is unbiased (γ_0=0 and γ_{IM}=1) and subsumes all information contained in historical volatility (hereafter *HV*) (γ_{AV}=0). While there is some inconsistency in previous results on informational efficiency,[29] the general result is that the Black-Scholes (hereafter *BS*) implied volatility, a frequently used measure in the literature, is a biased forecast of future volatility in the sense that estimated γ_0 is different from zero and estimated γ_{IM} is significantly less than unity. More recent studies corrects various data and methodological problems in earlier research (see, e.g., Canina and Figlewski, 1993; Christensen and Prabhala, 1998; Ederington and Guan, 2002; Jiang and Tian, 2005). These studies collectively found that the *BS* implied volatility is informationally efficient

[29] Using the Black-Scholes volatility implied in at-the-money options, the test results in the literature are mixed. For example, Canian and Figlewski (1993) found the *BS* implied volatility does not incorporate information contained in *HV* while Jorion (1995) and Szakmary *et al.* (2003) reported evidence that the implied volatility is a more efficient forecast than *HV*.

but biased. The bias was explained by arguing that tests based on the *BS* implied volatility are joint tests of market efficiency and the *BS* option pricing model, and so necessarily suffer from bias due to model misspecification. In view of limitations of the *BS* option pricing model, a model-free (hereafter *MF*) implied volatility measure that does not require any particular option-pricing model has recently been proposed in the literature (Britten-Jones and Neuberger, 2000; Jiang and Tian, 2005; Carr and Wu, 2009). The *MF* implied volatility is computed from a set of options with strikes instead of only at-the-money options, and shown by Britten-Jones and Neuberger (2000) to equal the risk-neutral expectation of future volatility under diffusion assumptions. Since the *MF* implied volatility does not incur any model misspecification error, it would seem to be more likely to be an unbiased estimate of realized volatility than the *BS* implied volatility. But Jiang and Tian (2005) found that the *MF* implied volatility is also biased. So the existence of bias continues to be a puzzle.

Lamoureux and Lastrapes (1993) were the first to suggest that a risk premium could be responsible for the bias in implied volatility forecasts. The risk premium explanation has also been investigated in more recent studies (Chernov, 2007; Doran and Ronn, 2008). For example, Chernov (2007) argued that implied volatility is derived in a risk-neutral environment while realized volatility is based on observed market outcomes. Since a risk premium can cause a disparity between observed and risk-neutral probability measures, it will inevitably result in a disparity between realized and implied volatilities.

One way to resolve the bias puzzle is to incorporate the possibility of risk premiums into the implied volatility forecast. Chernov (2007) found that the disparity between realized volatility and at-the-money implied volatility approximately equals a function of the latent spot volatility, and he suggested using spot volatility as an additional predictive variable in the test

regression. Although at-the-money options are generally more actively traded than other options, and are certainly a good measure to start with, the test may be still subject to model misspecification errors because his approximation formula is only valid in a fairly restricted model for price dynamics.[30]

In this research I focus on the *MF* implied volatility but propose a risk-adjusted model-free implied volatility that may help correct the bias in traditional implied volatility forecasts. To make the risk adjustment I convert the risk-neutral model-free implied volatility into a forecast under an observed probability measure which incorporates a risk premium. This method was first proposed by Becker, Clements, and Coleman-Fenn (2009). However, their risk adjustment model was derived only for a general diffusion processes. Here I go further and generate the risk-adjusted volatility forecast in the framework of a jump-diffusion model of asset returns. The jump-diffusion model is more general and capable of better capturing empirically relevant features of observed asset return dynamics. I derive the risk adjustment model with an exact, closed-form expression between the expectation of future volatility under the observed probability measure and the *MF* implied volatility. The jump-diffusion risk-adjusted model immediately explains the typical finding of a downward bias for the *MF* implied volatility. Similar to prior studies on implied volatility forecasts, the new model indicates that the volatility risk premium contributes to the forecast bias. But more importantly, jump risk premiums are also shown to play a role in the forecast bias.

I estimate the model parameters of interest and use them to convert the risk-neutral measure into its observational equivalent. I rely on standard Generalized Method of Moments

[30] Chernov (2007) showed that extending the approximation formula to more full models, for example, the stochastic volatility with jumps in return and volatility models, hinges on an additional assumption that the risk-neutral expectation of jump in returns is equal to zero. But such an assumption contradicts empirical results.

(GMM) estimation of the cross conditional moments between risk-neutral and observed expectations of volatility. The method is easier to implement than other alternatives which rely on computationally difficult joint estimation of both underlying asset returns and option prices (see, e.g., Jones, 2003; A ť-Sahalia and Kimmel, 2007). Bollerslev, Gibson, and Zhou (2010) used two basic moment conditions in a stochastic volatility model to extract the volatility risk premium. I extend the Bollerslev, Gibson, and Zhou framework to a jump-diffusion model to identify the parameters needed. The extended framework not only generalizes their original moment conditions but also augments moment conditions that involve the jump component of the process. Through a simulation experiment, the framework is shown to perform well with a small sample size of volatility in non-overlapping two-month intervals.

The empirical application addresses corn futures. However, unlike stock index markets, commodity markets have no available *MF* implied volatilities, which poses a significant challenge to estimation.[31] In this study I rely on Jiang and Tian (2005) method to construct the *MF* implied volatility using observed corn options. Meanwhile, I extend the estimation model to highlight the key seasonality feature in agricultural commodities. Using corn futures and options data from 1986 to 2010, I find that statistically significant risk premiums exist in the corn market, which supports our risk premium-based explanation of the bias. Furthermore, these estimates are robust with respect to microstructure market noise that may invalidate our underlying semi-martingale assumption at high sampling frequencies.

Finally, I investigate the forecasting ability of corn risk-adjusted (hereafter *AD*) *MF* implied volatility using three criteria: unbiasedness, informational efficiency relative to alternative forecasts, and superiority in predictive power. Evaluations are conducted against three

[31] For example, the VIX Index, an implied volatility measure based on S&P 500 stock index option prices, is available from January 1990.

alternative predictors of volatility: a) *HV*, b) the *BS* implied volatility, and c) the risk-neutral *MF* implied volatility. Our results support that the *AD* implied volatility is unbiased while the unadjusted *MF* implied volatility is biased, consistent with our theoretical prediction. The results also provide evidence for informational efficiency of the corn option market because both the *MF* implied volatilities subsume information contained in the *BS* implied volatility and *HV*. More importantly, I find that the *AD* implied volatility provides a more precise forecast compared to alternative forecasts.

The rest of this paper is organized as follows. In section 3.2, I propose a stochastic-volatility jump-diffusion model and derive the explicit expression between the expectation of future volatility and the *MF* implied volatility. In section 3.3, I outline basic moment conditions, calculate volatility measures, construct the GMM framework to estimate the parameters of interest, and provide finite sample simulation evidence on the performance of the estimator. Section 3.4 presents the corn dataset used for this study, reports the empirical estimates from applying the estimation procedure to corn data set spanning twenty-three years, and evaluates the robustness of these estimates. In section 3.5, forecast performance of the new implied volatility is examined. Section 3.6 provides concluding comments.

3.2 Model Specifications and Volatility Forecast

3.2.1 Price Dynamics

Asset prices are assumed to follow a jump-diffusion model and the asset volatility is allowed to be stochastic. Specifically, the dynamics of logarithmic asset prices *S* under the observed probability measure *P* are:

$$dlnS_t = udt + \sqrt{V_t}dB_{1t} + \ln(1 + J_t)\, dN_t - \lambda\mu dt, \tag{3.2}$$

(3.3) $dV_t = k(\theta - V_t)dt + \sigma(V_t)dB_{2t},$

where u denotes the drift term; k is speed of volatility mean reversion; θ is the long-term volatility mean; $\sigma(V_t)$ is the volatility of volatility; B_{1t} and B_{2t} are two correlated Wiener processes with the correlation coefficient equal to ρ; N_t is a Poisson process with intensity λ and distributed independently of B_{1t} and B_{2t}; and $\ln(1 + J_t)$ is a normally distributed random variable with mean $\mu = \ln(1 + \mu_J) - \sigma_J^2/2$ and variance σ_J^2. Consequently, the expected percentage jump size is $E(J_t) = \mu_J$. The term $\lambda\mu dt$ is the compensation for the instantaneous change as a result of a jump so that $\ln(1 + J_t)\, dN_t - \lambda\mu dt$ has its mean equal to 0. The general specification in equations (3.2) and (3.3) nests many well-known models. The Hull and White (1987) or Heston (1993) version of the model follows from setting no jump and $\sigma(V_t) = \sigma V_t$ or $\sigma\sqrt{V_t}$. The Bates (2000) version is also a special case of our model if a square-root volatility process is specified.

Assuming no arbitrage, the corresponding dynamics under a risk-neutral probability measure *Q* are:[32]

(3.4) $dlnS_t = \left[-\frac{V_t}{2} - \mu_J^*\lambda^*\right]dt + \sqrt{V_t}dB_{1t}^* + \ln(1 + J_t^*)dN_t^*,$

(3.5) $dV_t = k^*(\theta^* - V_t)dt + \sigma(V_t)dB_{2t}^*,$

where $k^* = k + \delta$ with δ being a volatility risk premium; $\theta^* = k\theta/k^*$; B_{1t}^* and B_{2t}^* are two new correlated Wiener processes under measure *Q* with the same correlation coefficient ρ. N_t^* is

[32] The detailed derivation can be found in Appendix A of Pan (2002).

a new Poisson process with intensity λ^*; and $\ln(1+J_t^*)$ has a new mean $\mu^* = \ln(1+\mu_J^*) - \sigma_J^2/2$ but its variance remains unchanged at σ_J^2. Note that the differences in jump parameters are related to jump risk premiums (including jump size and intensity premiums), but I do not explicitly present the premiums in the model since the adjustment can be done without completely specifying each premium.[33] Under arbitrage-free assumptions, the expected return from holding futures contracts should be zero under the *Q* measure, that is, $E_t^Q\left(\frac{dS_t}{S_t}\right) = 0$. This can be easily verified by Ito's lemma applied to equation (3.4).

3.2.2 The Model

Under the specifications of eq. (3.2), the variance over the trading period $(t, t+\Delta)$ is measured by the quadratic variation (hereafter *QV*):

$$QV_{t,t+\Delta} = IV_{t,t+\Delta} + \int_t^{t+\Delta} \ln(1+J_t)^2\, dN_t, \quad (3.6)$$

where the integrated volatility[34] (hereafter *IV*), $IV_{t,t+\Delta} = \int_t^{t+\Delta} V_u du$, denotes the contribution from the continuous price path, while the second term accounts for the variance contributed from the jumps. The expected *QV* under the *P* measure is:

$$E_t^P\left(QV_{t,t+\Delta}\right) = E_t^P\left(IV_{t,t+\Delta}\right) + \varphi\Delta, \quad (3.7)$$

[33] The explicit relationship between model parameters under the observed and risk-neutral probability measures can be found in Doran and Ronn (2008).

[34] Following the recent literature I will interchangeably use variance and volatility here and throughout the paper unless specifically noted.

where $\varphi = \lambda(\mu^2 + \sigma_J^2)$, is the expected squared jump value. The *QV* can be estimated by a nonparametric estimator, namely, the realized volatility (hereafter *RV*), which will be discussed in the section on volatility measures.

Next I introduce the *MF* implied volatility. Suppose call options with a continuum of strike prices for a given maturity are traded on an underlying asset. Britten-Jones and Neuberger (2000) defined the *MF* implied volatility from the time t to $t + \Delta$ as the integral of call option prices over an infinite range of strike prices

$$MF_{t,t+\Delta} = 2\int_0^\infty \frac{C(t+\Delta,K)-\max(0,S_t-K)}{K^2}\,dK, \tag{3.8}$$

where $C(t + \Delta, K)$ denotes the price of a call option maturing at time $t + \Delta$ with an strike price K. Obviously, unlike the conventional concept of implied volatility, the *MF* implied volatility does not involve any specific underlying option pricing model. Britten-Jones and Neuberger (2000) showed that the *MF* implied volatility is the risk-neutral expected *IV* under diffusion assumptions. Jiang and Tian (2005) demonstrated that the relationship is still approximately valid even if the underlying asset price process accommodates jumps. In the following, I will derive an exact expression between the expected *QV* and the *MF* implied volatility in our jump-diffusion models. The expression facilitates transforming the risk-neutral *MF* implied volatility into its equivalent in the observed measure. First I derive an explicit theoretical relationship between the *MF* implied volatility and the risk-neutral expected *IV*. As shown in Appendix F, the exact equation is

$$E_t^Q\left(IV_{t,t+\Delta}\right) = MF_{t,t+\Delta} - \phi\Delta, \tag{3.9}$$

where $\phi = 2\lambda^*(\mu_J^* - \mu^*)$ is a composite parameter associated with jumps. This equation generalizes the derivation by Britten-Jones and Neuberger (2000), because the *MF* implied

volatility would be equal to the risk-neutral expected *IV* in the absence of jumps ($\phi = 0$). When there are jumps, the *MF* implied volatility becomes a jump-adjusted risk-neutral expected *IV*.

Utilizing the results in Bollerslev and Zhou (2006), I derive the critical expression between the expected *QV* and the *MF* implied volatility (see Appendix F),

$$E_t^P\left(QV_{t,t+\Delta}\right) = A_\Delta MF_{t,t+\Delta} - A_\Delta \phi\Delta + B_\Delta + \varphi\Delta, \tag{3.10}$$

where

$$A_\Delta = \frac{\left(1-e^{-k\Delta}\right)k^*}{\left(1-e^{-k^*\Delta}\right)k},$$

and

$$B_\Delta = \theta\left[\Delta - \frac{1}{k}\left(1-e^{-k\Delta}\right)\right] - A_\Delta\theta^*\left[\Delta - \frac{1}{k^*}\left(1-e^{-k^*\Delta}\right)\right].$$

The bias puzzle can be immediately explained by eq. 3.10. Two potential sources of bias can be identified when using the *MF* implied volatility to forecast future volatility. First, the negative volatility risk premium δ reduces the degree of mean reversion in the risk-neutral volatility process relative to that of the actual volatility process ($k^* < k$), which in turn causes the ratio A_Δ to become less than unity; Second, the jump risk premiums have effects on the intercept via ϕ and φ. In a simulation study Doran and Ronn (2008) demonstrated that the volatility risk premium can explain the difference between the *BS* implied volatility and *RV* at the at-the-money point, while the jump risk premiums are responsible for the bias in out-of-the-money options. Their conclusion echoes our findings because the *MF* implied volatility aggregates information across options.

3.3 Estimation

Eq. 3.10 shows that the risk-neutral *MF* implied volatility can be linked in a closed-form expression to the expected *QV* under the observed measure. The expression thus provides a fundamental tool to transform the *MF* implied volatility into its risk-adjusted counterpart. Instead of identifying each separate model parameter needed for the adjustment, it is more convenient to directly estimate the key parameters (k, θ, δ) in the stochastic volatility model, along with the composite parameters for jumps (ϕ, φ), because this process avoids the joint estimation of both the underlying asset return and specific option pricing models. In particular, let $\xi = (k, \theta, \delta, \phi, \varphi)$ denote the parameter vector of interest. I estimate ξ using the joint time-series data $\{S_t, C_t\}$ on futures and options. Since the affine structure of $\{\ln S_t, V_t\}$ allows us to generate a rich set of moment conditions, I can use GMM estimation to estimate parameters. In the remainder of this section I will first provide a detailed description of the relevant moment conditions. Then I discuss nonparametric estimators for unobserved volatility variables. Finally, the finite sample properties of the parameter estimators are established in simulation experiments.

3.3.1 Moment Conditions

The first moment condition for the *IV* has previously been derived by Bollerslev and Zhou (2002). The conditional moment of the *IV* under the *P* measure satisfies

(3.11) $$E_t^P\left(IV_{t+\Delta,t+2\Delta}\right) = \alpha_\Delta E_t^P\left(IV_{t,t+\Delta}\right) + \beta_\Delta,$$

where the coefficients $\alpha_\Delta = e^{-k\Delta}$ and $\beta_\Delta = \theta\Delta(1 - e^{-k\Delta})$ are functions of the underlying parameters k and θ. The equation establishes the link between the expectation of the *IV* in the *P* measure and its lagged value.

The second moment condition links the expected *IV* with the *MF* implied volatility.

(3.12) $$E_t^P\left(IV_{t,t+\Delta}\right) = A_\Delta MF_{t,t+\Delta} - A_\Delta\phi\Delta + B_\Delta,$$

where A_Δ and B_Δ are functions of the underlying parameters k, θ, and δ. This equation is derived in the Appendix F.

The third moment condition relates to jumps in asset returns. Since the difference between the *QV* and the *IV* offers a simple nonparametric estimator for the jump component in total price variation (Barndorff-Nielsen and Shephard, 2006), I use the following moment to estimate the average jump component:

$$E_t^P\left(QV_{t,t+\Delta}\right) = E_t^P\left(IV_{t,t+\Delta}\right) + \varphi\Delta. \quad (3.13)$$

3.3.2 Volatility Measures

The *QV* and its separate components, such as *IV*, are not directly observable. I resort to recently popularized model-free nonparametric consistent estimators. As demonstrated in Anderson and Bollerslev (1998), the volatility calculated from high-frequency return data provides a good ex-post measure of the actual volatility and is a better measure than that estimated from daily data. I first estimate the *QV* using the *RV*. The *RV* is quantified by summing the squared high frequency returns over the $[t, t+\Delta]$ time interval:

$$RV_{t,t+\Delta} = \sum_{i=1}^{n} r^2_{t+\frac{i}{n}(\Delta)}, \quad (3.14)$$

where $r_{t+\frac{i}{n}\Delta} = lnS_{t+\frac{i}{n}\Delta} - lnS_{t+\frac{i-1}{n}\Delta}$ denotes the corresponding discrete-time within-day returns, and n refers to the number of return observations over the trading period. It is known that the *RV* will converge uniformly in probability to the *QV* as the sampling frequency of the underlying returns approaches infinity (Barndorff-Nielsen and Shephard, 2002):

$$QV_{t,t+\Delta} = \text{plim}_{n\to\infty} RV_{t,t+\Delta}. \quad (3.15)$$

Similarly, I employ a consistent, nonparametric measure of the sum over cross products of frequently sampled returns for the *IV*. I rely on the realized bipower variation (hereafter *BV*) measure developed by Barndorff-Nielsen and Shephard (2004) to estimate the *IV*:

$$(3.16)\quad \mathrm{BV}_{t,t+\Delta} = \frac{\pi}{2}\frac{n}{n-1}\sum_{i=2}^{n}\left|r_{t+\frac{i}{n}\Delta}\right|\left|r_{t+\frac{i-1}{n}\Delta}\right|.$$

Importantly, for increasingly finely sampled returns the *BV* measure becomes immune to jumps and consistently estimates the *IV*:

$$(3.17)\quad IV_{t,t+\Delta} = \mathrm{plim}_{n\to\infty} BV_{t,t+\Delta}.$$

Additionally, I also have empirical implementation issues for the *MF* implied volatility; option prices required for calculating the right hand side of eq. 3.8 are not available for all strike prices. In fact only a finite number of strike prices are traded in the market, so I have to approximate it from these limited observed option prices. I empirically implement the *MF* implied volatility using Jiang and Tian approach (2005):

$$(3.18)\quad MF_{t,t+\Delta} \approx 2\int_{K_{low}}^{K_{up}} \frac{C(t+\Delta,K)-\max(0,S_t-K)}{K^2}\,dK,$$

$$\approx \sum_{i=1}^{m}[g(t+\Delta,K_i)+g(t+\Delta,K_{i-1})]\Delta K,$$

where K_{up} and K_{low} are upper and lower truncation points of strike prices, a strike price increment $\Delta K = \frac{K_{up}-K_{low}}{m}$, $K_i = K_{low} + i\Delta K$ for $0 \le i \le m$, and $g(t+\Delta,K_i) = [C(t+\Delta,K_i)-\max(0,S_t-K_i)]/{K_i}^2$. The approximation method produces two measurement errors. One is truncation errors from a limited range of strike prices; the other is discretization errors due to numerical integration. Jiang and Tian (2005) showed that these two errors can be negligible if the truncation points are more than two standard deviations (SDs)

from S_t and the strike price increment $\Delta K \leq 0.35$ SDs. For options with the truncation range beyond the available maximum and minimum strike prices, I assume their implied volatilities are the same as endpoint implied volatilities and extrapolate their option values by using the endpoint implied volatilities. The endpoint implied volatilities are calculated by using the inverse *BS* formula.[35] These implied volatilities are translated into call prices with any unavailable strike prices by using the *BS* formula once more.

In the implementation, a further challenge is that even in a given limited range $[K_{low}, K_{up}]$, only a sparse set of discrete strike prices are listed for trading in the market. I apply a curving-fitting method to implied volatilities to interpolate between available strike prices. Likewise, the inverse *BS* formula is used to obtain estimates of implied volatilities of listed calls. The detailed implementation can be found in Jiang and Tian (2005).

3.3.3 The GMM Framework

The parameter vector ξ is estimated utilizing the moment conditions (3.11)-(3.13) after replacing unobservable variables with their respective estimates. Additionally, I employ the lagged value of *BV* and the *MF* implied volatility as instrumental variables to impose over-identifying restrictions. Therefore, the system of equations is:

[35] Note that this procedure does not assume that the *BS* model is the true model underlying option price process. It is merely used as a tool to provide a one-to-one mapping between option prices and implied volatilities (Jiang and Tian, 2005).

$$(3.19)\quad f(\xi) = \begin{bmatrix} BV_{t+\Delta,t+2\Delta} - \alpha_\Delta BV_{t,t+\Delta} - \beta_\Delta \\ \left(BV_{t+\Delta,t+2\Delta} - \alpha_\Delta BV_{t,t+\Delta} - \beta_\Delta\right)BV_{t-\Delta,t} \\ (BV_{t+\Delta,t+2\Delta} - \alpha_\Delta BV_{t,t+\Delta} - \beta_\Delta)MF_{t-\Delta,t} \\ BV_{t,t+\Delta} - A_\Delta MF_{t,t+\Delta} + A_\Delta \phi\Delta - B_\Delta \\ \left(BV_{t,t+\Delta} - A_\Delta MF_{t,t+\Delta} + A_\Delta \phi\Delta - B_\Delta\right)BV_{t-\Delta,t} \\ \left(BV_{t,t+\Delta} - A_\Delta MF_{t,t+\Delta} + A_\Delta \phi\Delta - B_\Delta\right)MF_{t-\Delta,t} \\ RV_{t,t+\Delta} - BV_{t,t+\Delta} - \varphi\Delta \\ \left(RV_{t,t+\Delta} - BV_{t,t+\Delta} - \varphi\Delta\right)BV_{t-\Delta,t} \\ \left(RV_{t,t+\Delta} - BV_{t,t+\Delta} - \varphi\Delta\right)MF_{t-\Delta,t} \end{bmatrix}$$

The population moment is $E_t\big(f(\xi)\big) = 0$. I estimate ξ via standard GMM estimation such that $\hat{\xi} = argmin\ g_T(\xi)'W g_T(\xi)$, where $g_T(\xi)$ refers to the sample means of the moment conditions $g_T(\xi) = 1/T \sum_{t=\Delta}^{T-2\Delta} f(\xi)$ and W denotes the weighting matrix. I use an efficient two-step GMM estimator in which the first estimator $\hat{\xi}_1$ is constructed using the covariance matrix of the instrument vector to weigh the moment conditions and the second estimator is chosen to minimize $g_T(\xi)'W(\hat{\xi}_1)g_T(\xi)$, where $W(\hat{\xi}_1)$ is the inverse of the asymptotic covariance-variance matrix of $g_T\big(\hat{\xi}_1\big)$. Empirically, I employ a heteroskedasticity and autocorrelation consistent robust covariance matrix estimator with a Bartlett-kernel in implementing $W(\hat{\xi}_1)$ (Newey and West, 1987). At parameter estimators the objective function times the number of observations is asymptotically χ^2 distributed with degrees of freedom equal to the number of over-identifying restrictions. The test statistic provides a straightforward method for testing over-identifying restrictions.

3.3.4 Simulation Analysis

To assess the finite-sample properties of the GMM estimators in the model, I conduct a Monte Carlo study for the specialized Bates (2000) version of the model. The dynamics of (3.2), (3.3), (3.4) and (3.5) are simulated with the Euler method. The parameter configurations are: $k = 2, \theta = 0.025, \delta = -1, \phi = 0.01596,$ and $\varphi = 0.0192$. The *MF* implied volatility is calculated using the above Jiang and Tian approach. *RV* and *BV* are constructed from the 5-minute returns according to the formula (3.14) and (3.16) to approximate *QV* and *IV*. Inside the simulations I also partition each five-minute interval into 5 smaller segments for the continuous-time record in order to calculate the true *QV* and *IV* (however, they are not observable in practice). I compare the GMM estimator using the "five-minute" *RV* and *BV* with the corresponding non-feasible estimator using the true *QV* and *IV*. The comparison assesses whether *RV* and *BV* constructed under the sampling frequency affect the estimation. The accuracy of the asymptotic approximations is illustrated by contrasting the results for sample sizes of 150 and 600. The Monte Carlo replications are 500. The detailed experimental design can be found in the Appendix G.

Table 3.1. Monte Carlo Simulation Results

	Mean	Median	RMSE	Mean	Median	RMSE
	T=150			T=600		
MF, *IV*, and *QV*						
k	2.2300	2.2200	0.8030	2.1400	2.1100	0.3432
θ	0.0254	0.0253	0.0020	0.0253	0.0252	0.0008
δ	-1.1200	-1.1100	1.0300	-1.0300	-0.9100	0.4500
ϕ	0.01530	0.01487	0.0050	0.01537	0.01501	0.0020
φ	0.1511	0.1501	0.0870	0.01522	0.0146	0.0370
MF,*BV*, and *RV*						
k	2.2600	2.2700	0.8950	2.1400	2.1200	0.4060
θ	0.0256	0.0255	0.0020	0.0253	0.0255	0.0008
δ	-1.1600	-1.1700	0.1305	-1.0200	-0.9100	0.6601
ϕ	0.01478	0.01463	0.0040	0.01557	0.01551	0.0017
φ	0.0143	0.0142	0.0870	0.0150	0.0146	0.0445

Note: the table reports the estimation results in the GMM framework (eq. 3.19). Monte Carlo replications are 500. The parameter configurations are: $k = 2, \theta = 0.025, \delta = -1, \phi = 0.01596,$ and $\varphi = 0.0192$. *MF*, *IV*, *QV*, *BV*, and *RV* refer to *MF* implied volatility, integrated volatility, quadratic variation, bipower variation, and realized volatility, respectively.

The results are summarized in Table 3.1. In addition to means and medians I also report the root-mean-square-errors (RMSEs). There are several points to be highlighted from Table 3.1. First, most parameter estimates using *RV* and *BV* are quite close to their corresponding true values, measured in terms of mean and median. RMSEs for the parameter estimates decrease roughly at the rate of 2 as the sample size goes from 150 to 600, showing the estimates converge at $\sqrt{T}$ speed. Second, the use of *RV* and *BV* achieves a similar RMSE as the true infeasible *QV* and *IV*. The results indicate the feasible estimator fares as well as the continuous-record *QV* and *IV*. In summary, the finite sample results indicate that the GMM method and nonparametric estimators for volatilities can recover the parameters of interest with reasonable precision.

3.4 Empirical Application

Our empirical analysis is based on *MF* implied volatilities, *BV*s and *RV*s for futures prices of corn, a major agricultural commodity. In recent years agricultural commodity markets have

witnessed extreme and unpredictable increases in price volatility. However, gauging the level of volatility risk and developing volatility-based tools in the agricultural commodity market has not received so much attention as their counterparts in stock and currency markets. Faced with volatility risk and lack of an instrument for hedging volatility, stakeholders in agricultural commodities have to urge regulators of futures market to consider regulations on position and trading limits. Against this backdrop, this application has significant implications not only for precisely forecasting corn futures volatility and testing the efficiency of the corn option markets, but also for developing volatility-based products in agricultural commodity markets. This section will detail how to construct the risk-adjusted implied volatility for the corn market based on a 23-year sample of daily options and high-frequency futures. The predictive power of the model will be evaluated in the next section.

3.4.1 Data

MF Implied volatilities are extracted from call options contracts traded from Feb 25, 1987 to June 30, 2010. The intervals for which volatilities are computed are based on the structure of expiration for corn futures and options. Corn futures contracts expire five times per year, that is, March, May, July, September, and December. The corresponding options contracts mature about one month ahead of futures expiration. Therefore, the five volatility intervals in each year are November to February, February to April, April to June, June to August, and August to November.[36] To extract the non-overlapping sample, I choose options on the

[36] Although corn futures and options contracts are listed every year, lengths of intervals of each year have slight date changes because the options expiration rules change and the number of days varies year to year.

Wednesday immediately following the expiration date of the previous options contract.[37] The intervals are either two or three months, resulting in a total of 118 observations. Call options are filtered to exclude options that violate the boundary conditions, for example, in-the-money options with a premium less than payoff for immediate exercise. Strike price increment is 10 cents and only options with strike prices inside the range of three SDs from S_t are used to calculate *MF* implied volatilities.[38] For comparison purposes I also calculate *BS* implied volatilities. *BS* implied volatilities are computed as the average of volatilities derived from two nearest-to-the-money call options by inverting the *BS* formula. The risk-free rate is calculated by compounding the corresponding three-month T-bill rate obtained from the Federal Reserve. *RV*s and *BV*s should be good approximations to the true continuous quadratic variation and integrated volatility measures. These are calculated based on the 5-minute returns on logarithmic corn futures for the period matching the maturity of the corresponding options in the *MF* implied volatility. For a typical trading day, I have 45 five-minute returns covering trading hours from 9:30 am to 1:15 pm. I also analyze the jump measure by calculating the difference between *RV*s and *BV*s. Finally, all volatility measures are annualized for comparisons across varying intervals and across years.

The upper panel of Table 3.2 presents summary statistics of all five volatilities in the form of standard deviations and shows that the *MF* is on average higher than the *RV*. The difference between *MF*s and *RV*s is sometimes used by market participants as a raw measure of

[37] I select the sample this way because option trading seems to be more active during the week following the expiration date and Wednesday has the fewest holidays among all weekdays.

[38] Since the trading volumes of corn options with a \$0.05 strike price increment (serial options) are too small, I discretize the range of integration into a grid of 10 points, which also meets the requirement that $\Delta K \leq 0.35$ SDs. The standard deviation of price movement before 2005 in the corm market is set at 20%, while it is set at 30% after 2005, because the market is more volatile in the latter period.

the volatility risk premium. But the difference is rather noisy and it is hard to determine its exact value. The *RV* is systematically higher than the *BV*, implying positive jumps across time.

Table 3.2: Summary Statistics for Volatilities, 1987-2010

	RV	*BV*	*MF*	*BS*	*JUMP*
Mean	0.236	0.196	0.253	0.221	0.040
Std. Dev.	0.088	0.067	0.082	0.092	0.028
Skewness	1.034	1.083	0.869	0.911	1.552
Kurtosis	3.913	4.057	3.814	3.981	5.229
Min	0.107	0.092	0.120	0.081	0.005
Max	0.534	0.422	0.579	0.590	0.148
Seasonality-mean					
Feb-Apr	0.200	0.173	0.215	0.187	0.027
Apr-Jun	0.248	0.209	0.269	0.235	0.040
Jun-Aug	0.311	0.241	0.335	0.310	0.071
Aug-Nov	0.224	0.190	0.238	0.200	0.034
Nov-Feb	0.194	0.164	0.204	0.170	0.030

Note: in total, there are 118 observations. All volatilities are annualized standard deviations. *RV*, *BV*, *MF*, and *BS* stand for realized volatility, bipower variation, *MF* implied volatility, and *BS* implied volatility. *JUMP* is computed as the difference between the *RV* and the *BV*.

Empirically, corn price volatility exhibits seasonality. It tends to increase during summer time as weather in this critical period causes uncertainty. Volatility is also sensitive to inventory levels which can be seasonal. Periods of systematically greater and smaller volatility are present in corn futures as depicted in Figure 3.1 and described in the lower panel of Table 3.2. For example, the June-August interval that covers the most critical growing season and where the weather effect is most pronounced displays the largest mean volatility, while the November-February interval during the non-growing period has the smallest mean volatility. The repeated movement pattern is embodied simultaneously in implied volatilities since market participants incorporate this information into option prices. In addition, jumps also occur more often in the June-August interval due to abrupt changes in weather conditions and supply forecasts.

Figure 3.1. Realized Volatilities (*RVs*), Bipower Variations (BVs), and MF Implied Volatilities (*MF*) in Annualized Standard Deviation

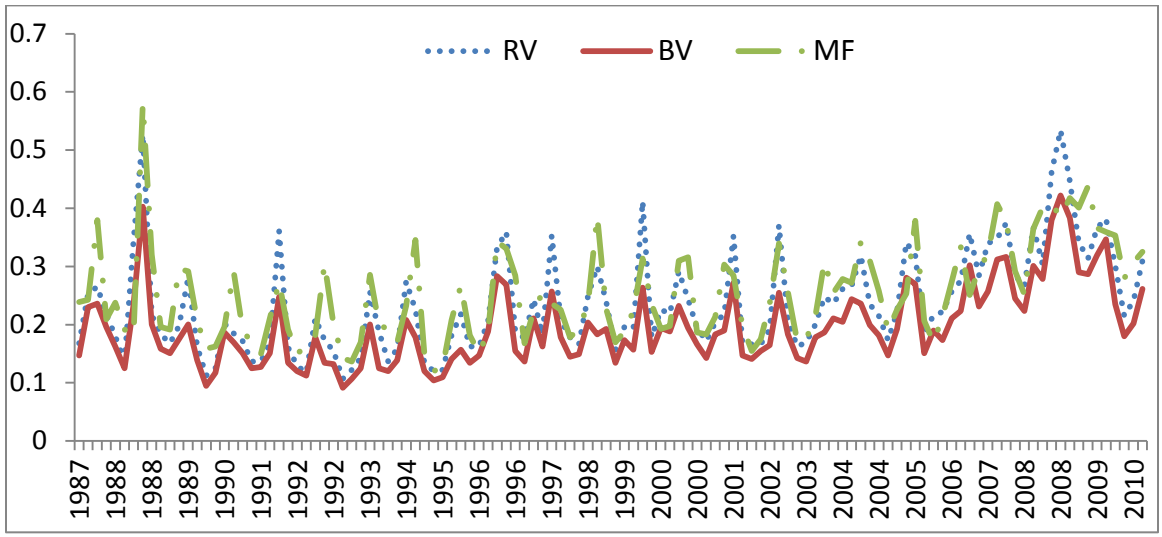

3.4.2 Estimation Results

I accommodate the seasonality feature in the empirical estimation by using four seasonal dummy variables to proxy seasonal components so that moment conditions 3.11 and 3.13 can be modified as:

$$E_t^P\left(IV_{t+\Delta,t+2\Delta}\right) = \alpha_\Delta E_t^P\left(IV_{t,t+\Delta}\right) + \beta_\Delta - b_1Q_1 - b_2Q_2 - b_3Q_3 - b_4Q_4, \quad (3.20)$$

$$E_t^P\left(QV_{t,t+\Delta}\right) = E_t^P\left(IV_{t,t+\Delta}\right) + \varphi\Delta - q_1Q_1 - q_2Q_2 - q_3Q_3 - q_4Q_4, \quad (3.21)$$

where Q_1 Q_2, Q_3, and Q_4 are dummies that take value 1 if volatility observations lie in Feb-Apr, Apr-Jun, Aug-Nov, and Nov-Feb intervals, respectively, and take value zero otherwise; b_i and q_i ($i = 1,2,3,4$) are the corresponding coefficients. I define observations in the Jun-Aug interval as the default.

Table 3.3: Parameter Estimates using the *RV, BV* and *MF*

Parameters	Estimates	Std. Err.	*p*-value
k	2.2450	0.6820	0.0010
θ	0.0909	0.0204	0.0000
δ	-4.4905	1.6034	0.0051
ϕ	0.0105	0.0062	0.0886
φ	0.0446	0.0042	0.0000
b_1	0.0046	0.0008	0.0000
b_2	0.0027	0.0009	0.0027
b_3	0.0014	0.0010	0.1408
b_4	0.0056	0.0012	0.0000
q_1	0.0055	0.0008	0.0000
q_2	0.0054	0.0008	0.0000
q_3	0.0038	0.0009	0.0000
q_4	0.0053	0.0007	0.0000
$\mathcal{X}^2$(d.o.f=8) (*p*-value)		6.7019(0.5691)	

Note: realized volatilities (*RVs*) and bipower variations (*BVs*) are computed based on 5-minute returns. The lag length in the Newey-West weighting matrix employed in the estimation is set at 5.

I estimate parameters of interest with two-month volatilities, that is, $\Delta = 1/6$. Three-month volatilities are converted to two-month ones using the adjustment coefficient $2/3$. The parameter estimates along with the corresponding asymptotic standard errors and *p*-values are reported in Table 3.3. As can be seen in the first row of the table, the estimate for the mean reversion parameter k is relatively high, suggesting a strong mean reversion pattern in volatility under the *P* measure. As expected, the long-run mean parameter (θ=0.0909) is close to the sample mean of *BV*. Also, the results show that most seasonal dummy estimates are positive and highly significant (d_1, d_2, d_4), implying that the *BV* in Jun-Aug is highest. The jump-adjusted parameter ϕ is statistically significant at the 10% level, which corroborates the difference between the *MF* implied volatility and the risk-neutral expected *IV* (i.e., the approximation error from Jiang and Tian (2005) is not negligible). The expected jump component in *RV*, φ, is also

significant (at the 1% level). All seasonal dummy variables in jumps are positive and highly significant, consistent with earlier statistical analysis.

The volatility risk premium estimate δ is negative and statistically significant at the 1% level. This finding is consistent with other studies that have found negative risk premiums on stochastic volatility in equity, currency, and energy markets. The magnitude of the estimated risk premium is so large that it makes the volatility process non mean-reverting under the *Q* measure. According to Gordon and St-Amour (2004), the stochastic volatility risk premium reflects the risk preferences of a representative investor. This negative stochastic volatility risk premium implies risk-aversion, which means that investors are willing to pay a risk premium to hedge the volatility risk. Finally, as can be seen in the last row of the table, the chi-squared test of overidentifying restrictions suggests that the overall specification is not rejected at conventional significance levels.

3.4.3 Robustness Analysis

It follows from equations 3.15 and 3.17 that higher frequency data should provide better possible estimates for *QV* and *IV* if the semi-martingale assumption is not violated. However, it should also be kept in mind that, along with the presence of market microstructure noise including price discreteness and bid-ask spread, ultra-high frequency returns may render the *RV* and *BV* measures inconsistent since the market microstructure noise will invalidate the semi-martingale assumption underlying equations 3.2 and 3.3 (Andersen, Bollerslev, and Huang, 2010). This prevents us from sampling too frequently while maintaining the fundamental semi-martingale assumption. In order to investigate the robustness of our findings based on the 5-minute returns, I first consider alternative volatility estimators constructed from more coarsely

sampled returns. This is a simple way to alleviate these contaminating effects, while maintaining most of the relevant information in the high-frequency data. I re-estimate the model with *RV* and *BV* constructed from 10-minute returns. As can be seen in Table 3.4, compared to the original results, the parameter estimates show little difference in signs and significance levels, although the volatility risk premium estimate falls a little from -4.4905 to -3.6993.

Table 3.4: Parameter Estimates using the *RV_10, BV_10* and *MF*

Parameters	Estimates	Std. Err.	*p*-value
k	1.9214	0.5847	0.0010
θ	0.1049	0.0233	0.0000
δ	-3.6993	1.3752	0.0071
ϕ	0.0166	0.0046	0.0003
φ	0.0384	0.0038	0.0000
b_1	0.0051	0.0007	0.0000
b_2	0.0027	0.0008	0.0012
b_3	0.0015	0.0009	0.0761
b_4	0.0061	0.0011	0.0000
q_1	0.0049	0.0007	0.0000
q_2	0.0044	0.0008	0.0000
q_3	0.0034	0.0008	0.0000
q_4	0.0044	0.0007	0.0000
$\mathcal{X}^2$(d.o.f=8) (*p*-value)	8.2051(0.4137)		

Note: RV_10 and *IV_10* refer to *RVs* and *BVs* constructed from 10-minute returns. The lag length in the Newey-West weighting matrix employed in the estimation is set at 5.

A better way to deal with the market microstructure noise is to construct a robust estimator. This has been the subject of intensive research efforts recently (Barndorff-Nielsen and Shephard, 2006; Barndorff-Nielsen et al., 2008). Barndorff-Nielsen and Shephard (2006) developed a new *BV* measure robust to certain types of market microstructure noise. The *BV* measure is the sum of the product of absolute returns and themselves lagged by two periods:

$$\text{(3.22)}\quad \mathrm{BV}_{t,t+\Delta} = \frac{\pi}{2}\left(\frac{n}{n-2}\right)\sum_{i=3}^{n}\left|r_{t+\frac{i}{n}\Delta}\right|\left|r_{t+\frac{i-2}{n}\Delta}\right|,$$

The staggering relative to the measure originally considered in eq. 3.16 alleviates the confounding influences of the market microstructure noise, resulting in empirically more accurate finite sample approximations (Huang and Tauchen, 2005). It is also shown that the measure converges in probability to the *IV* under the general assumption that the logarithmic price process is a semi-martingale. The results in Table 3.5 are produced using the new measure. The parameter estimates as well as their standard errors are generally close to the original results. Overall, the results clearly confirm the robustness of our previous findings with respect to market microstructure noise.

Table 3.5. Parameter Estimates using the *RV, BV_R* and *MF*

Parameters	Estimates	Std. Err.	*p*-value
k	2.5722	0.7214	0.0004
θ	0.0826	0.0172	0.0000
δ	-4.3618	1.6284	0.0074
ϕ	0.0152	0.0054	0.0050
φ	0.0487	0.0047	0.0000
b_1	0.0046	0.0007	0.0000
b_2	0.0026	0.0008	0.0010
b_3	0.0018	0.0008	0.0263
b_4	0.0052	0.0010	0.0000
q_1	0.0058	0.0008	0.0000
q_2	0.0059	0.0009	0.0000
q_3	0.0039	0.0011	0.0003
q_4	0.0057	0.0008	0.0000
$\mathcal{X}^2$(d.o.f=8) (*p*-value)		7.8308(0.4502)	

Note: BV_R refer to bipower variations robust to microstructure market noise by taking into account an additional stagger. The lag length in the Newey-West weighting matrix employed in the estimation is set at 5.

3.5 Forecast Evaluation

After estimating parameters of interest, it is straightforward to convert the risk-neutral *MF* implied volatility into an adjusted equivalent. Consistent with the literature (e.g., Christensen

and Prabhala, 1998; Egelkraut and Garcia, 2006), the predictive ability of the risk-adjusted *MF* implied volatility is assessed using three criteria: a) forecast unbiasedness, b) informational efficiency, and c) superior predictive power relative to alternative forecasts. Three alternative forecasts are considered: the *MF* implied volatility, the *BS* implied volatility, and a *HV* realized during the past year.

3.5.1 Testing the Unbiasedness Hypothesis

I examine unbiasedness of *AD* using a univariate regression:

(3.23) $\sigma_{RV,t} = \gamma_0 + \gamma_{AD}\sigma_{AD,t} + \epsilon_t,$

where σ_{RV} and σ_{AD} are the annualized *RV* and *AD*. Panel A in Table 3.6 summarizes the OLS regression results for *AD* and alternative volatilities. These parameters are estimated following a procedure robust to the presence of heteroscedasticity. The Durbin-Watson statistics are close to two in most regressions, indicating that the regression residuals exhibit little autocorrelation. In the regression of the *AD*, the slope coefficient is positive, significantly different from zero, insignificantly different from one, while the intercept is small and insignificantly different from zero. The Wald test shows that the null hypothesis of $\gamma_0 = 0$ and $\gamma_{AD} = 1$ cannot be rejected, implying that the new volatility estimate is an unbiased estimator for future realized volatility. This confirms our prediction that forecast bias of the risk-neutral *MF* implied volatility can be eliminated after making the risk premium adjustment. Results in other model specifications show that the unbiasedness hypothesis is strongly rejected and all the slope coefficient estimates are downward biased. This finding is consistent with previous research (e.g. Szakmary et al., 2003; Jiang and Tian, 2005) and supports our argument that investors' risk aversion brings forth a

negative volatility risk premium and, consequently, leads to higher volatilities implied in option prices than their observed counterpart.

Table 3.6. Testing Unbiasedness and Informational Efficiency

T	γ_0	γ_{AD}	γ_{MF}	γ_{BS}	γ_{HV}	Durbin-Watson	t-Test	Wald Test
Panel A								
118	0.010	0.936	--	--	--	1.874	0.92	0.710
	(0.470)	(0.000)					(0.340)	(0.495)
118	0.015	--	0.876	--	--	2.210	4.450	6.620
	(0.279)		(0.000)				(0.037)	(0.002)
118	0.068	--	--	0.760	--	2.200	18.9	20.060
	(0.000)			(0.000)			(0.000)	(0.000)
113	0.109	--	--	--	0.548	1.305	36.94	21.78
	(0.000)				(0.000)		(0.000)	(0.000)
Panel B								
118	0.027	0.594	--	0.296	--	2.063	2.160	0.950
	(0.142)	(0.034)		(0.209)			(0.145)	(0.419)
113	0.007	0.952	--	--	0.002	1.865	0.300	0.280
	(0.631)	(0.000)			(0.997)		(0.837)	(0.837)
113	0.025	0.583	--	0.318	0.005	2.066	2.260	0.630
	(0.190)	(0.038)		(0.181)	(0.946)		(0.136)	(0.641)
Panel C								
118	0.002	--	1.126	-0.228	--	2.166	0.160	5.040
	(0.926)		(0.001)	(0.435)			(0.693)	(0.003)
113	0.011	--	0.872	--	0.025	2.205	2.450	3.850
	(0.405)		(0.000)		(0.728)		(0.121)	(0.012)
113	0.000	--	1.080	-0.190	0.025	2.177	0.070	3.240
	(0.983)		(0.001)	(0.522)	(0.729)		(0.791)	(0.015)

Note: T is the sample size. The numbers in parentheses below the parameter estimates are p-values. Each regression is implemented with a robust procedure taking into account of heteroscedasticity. The t-test in Panel A is for the hypothesis: $\gamma_j = 1$ (j = AD, MF, BS, HV). The Wald test in panel A is for the null hypothesis: $\gamma_0 = 0$ and $\gamma_j = 1$ ($j = AD, MF, BS, HV$). The *t*-test in Panel B is for the hypothesis: $\gamma_{AD} = 1$. The Wald test in panel B is for the null hypothesis: $\gamma_0 = 0, \gamma_{AD} = 1$ and $\gamma_j = 0$ $(j = BS, HV)$, or $\gamma_0 = 0,\ \gamma_{AD} = 1, \gamma_{BS} = 0, and\ \gamma_{HV} = 0$. The *t*-test in Panel C is for the hypothesis: $\gamma_{MF} = 1$. The Wald test in panel C is for the null hypothesis: $\gamma_0 = 0, \gamma_{MF} = 1$ and $\gamma_j = 0$ $(j = BS, HV)$, or $\gamma_0 = 0, \gamma_{MF} = 1, \gamma_{BS} = 0, and\ \gamma_{HV} = 0$.

3.5.2 Testing Informational Efficiency

If *AD* is informationally efficient relative to alternative forecasts, the forecast will subsume all information contained in them. The hypothesis is assessed in encompassing regressions including two or more volatility forecasts as explanatory variables:

$$\sigma_{RV,t} = \gamma_0 + \gamma_{AD}\sigma_{AD,t} + \gamma_{BS}\sigma_{BS,t} + \gamma_{HV}\sigma_{HV,t} + \epsilon_t. \quad (3.24)$$

[39]

If the slopes of alternative forecasts are equal to zero, it means they provide no incremental predictive information. A total of three encompassing regressions involving *AD* are analyzed for different choices of volatility measures. As shown in Panel B of Table 3.6, the *t*-statistics cannot reject the hypothesis that the slope coefficient for *BS* or *HV* is zero at any conventional significance level. Furthermore, the joint test does not reject that both slope coefficients for *BS* and *HV* are zero. It implies that alternative volatilities are redundant and their information content has been subsumed in *AD*, supporting that *AD* is an efficient forecast for future realized volatility. In addition, I jointly tested unbiasedness and efficiency of *AD* by formulating a joint hypothesis as H_0: $\gamma_0 = 0, \gamma_{AD} = 1,$ and $\gamma_j = 0$ ($j = BS, HV$). The null hypotheses in all three specifications are not rejected. This provides further evidence that *AD* is unbiased and does subsume all information contained in both *BS* and *HV*.

For comparison purposes, I investigated the informational efficiency of the *MF* implied volatility relative to *BS* and *HV*. As can be seen in Panel C of Table 3.6, the slope(s) of *BS* and/or *HV* is statistically insignificant in all three specifications, suggesting that the *MF* implied volatility is also efficient. But the joint hypothesis of unbiasedness and efficiency is strongly rejected in all regression specifications due to the forecast bias.

[39] Regressions (3.24) are appropriately specified only if the variables are stationary. This has been confirmed by Egelkraut and Garcia (2006).

3.5.3 Testing Predictive Power

An unbiased forecast could increase its predictive power after the bias is removed. To further assess the difference in accuracy of volatility forecasts, we use the following two loss functions: mean absolute percentage errors (*MAPE*) and mean absolute errors (*MAE*)

$$(3.25)\quad MAPE = \frac{1}{T}\sum_{t=1}^{T}\left|\frac{\sigma_{j,t}-\sigma_{RV,t}}{\sigma_{RV,t}}\times 100\right|,$$

$$(3.26)\quad MAE = \frac{1}{T}\sum_{t=1}^{T}\left|\sigma_{j,t}-\sigma_{RV,t}\right|,$$

where $\sigma_{j,t}$ is a volatility measure (j =*AD*, *MF*, *BS*, or *HV*), T is the number of forecasts. The *MAPE* loss function measures the relative accuracy, while *MAE* measures the absolute one. In addition, they are generally more robust to the possible presence of outliers than the mean square errors, which is especially important for small samples. I assessed the statistical significance of difference in pairs of competing models by the Diebold-Mariano (*DM*) Test and one of its modifications. Such tests are based on the null hypothesis of no difference in accuracy of any two competing forecasts. I define the loss differential between two forecasts as $d_t = \left|e_{t,1}\right| - \left|e_{t,2}\right|$, where *e* is percentage forecast error or forecast error. The *DM* statistic is computed for one-step-ahead forecast as:

$$(3.27)\quad DM = \frac{\bar{d}}{\sqrt{\hat{V}(\bar{d})}},$$

where $\bar{d}$ is the sample mean loss differential. $\hat{V}(\bar{d})$ is an estimate of the asymptotic variance of $\bar{d}$, taking into account the autocorrelation of series d_t. Under the null hypothesis of equal forecast accuracy, the *DM* statistic has an asymptotic standard normal distribution. Since the *DM* test can be over-sized in small samples, I also consider a Modified DM (*MDM*) test, where *DM* is multiplied by the factor$\sqrt{(T-1)/T}$. The *MDM* test is useful for determining the significance of

differences in our competing forecasts because it does not rely on the assumption of forecast unbiasedness.

Table 3.7. Testing Predictive Power

	MAPE	DM	MDM	MAE	DM	MDM
AD	16.512			0.038		
MF	17.840	-1.715(0.086)	-1.740(0.092)	0.041	-1.120(0.263)	-1.110(0.269)
BS	18.915	-2.063(0.039)	-2.046(0.043)	0.045	-2.543(0.011)	-2.522(0.013)
HV	24.529	-3.995(0.000)	-3.962(0.000)	0.060	-4.334(0.000)	-4.297(0.000)

Note: the numbers in parentheses beside the statistics are *p*-values. *MAPE* and *MAE* are the mean absolute percentage errors and mean absolute errors. The *DM* and *MDM* tests are reported when the benchmark is the *AD* implied volatility, compared to each one of other forecasts.

Table 3.7 reports the *DM* and *MDM* tests when the benchmark is the *A*D forecast. The signs of the *DM* and *MDM* statistics are always negative, implying that the benchmark's loss is lower than any other forecast. The findings show that *AD* has the smallest forecast error among all volatility forecasts whether in *MAPE* or in *MAE*. For *MAPE* and for all models, I reject the null of equal predictive ability, suggesting that the *AD* benchmark fares the best. For *MAE* and for *BS* and *HV* forecasts, I reject the null of equal forecast accuracy, indicating that *AD* has superior predictive power over *BS* and *HV*. However, when the benchmark is compared to the second best (the *MF* implied volatility), I fail to reject the null of equal forecast accuracy. Overall, the *AD* implied volatility tends to have superior predictive power over alternative forecasts.

3.6 Conclusion

The extent to which implied volatilities provide unbiased forecasts of corresponding future realized volatilities has attracted a great deal of attention in recent years. In testing the unbiasedness hypothesis, the typical finding is an upward-bias predictor. Prior studies have argued that the volatility risk premium may be an important factor in explaining the documented

bias in volatility forecast. An intuitive method to eliminate the bias is to directly transform the risk-neutral implied volatility into an observational equivalent. Following Becker, Clements, and Coleman-Fenn (2009), I proposed a risk-adjusted implied volatility by converting a risk-neutral implied volatility using risk premiums. However, my approach extends Becker, Clements, and Coleman-Fenn by using jump-diffusion models, which are widely accepted as more plausible descriptions of asset returns than general diffusion processes. I explicitly derive the link between the *MF* implied volatility and the *QV* in the jump-diffusion process, which is the risk adjustment model. The model suggests that the jump risk premiums also contribute to the forecast bias. The GMM estimation framework of Bollerslev, Gibson, and Zhou (2010) was also extended to a jump-diffusion model. A Monte Carlo simulation study confirms that the framework performs well in recovering the parameters of interest.

I illustrated the procedure using volatilities implied in the two-month options on corn futures. Motivated by the success of the VIX index based on the liquid S&P500 index options, I calculated a *MF* implied volatility, "corn VIX", using Jiang and Tian (2005) method. This is the first time a *MF* measure has been used to gauge volatility in commodity markets. Such a *MF* measure may help facilitate volatility contracts in corn futures markets and expand risk management portfolio for corn market participants. In the empirical model specification, I accommodate seasonality characteristics in corn volatilities into the moment conditions and find statistically significant seasonality effects. I also find that a negative volatility risk premium exists in the corn futures, consistent with substantial evidence documented in the equity index and currency markets. After evaluating forecast performance of the *AD* implied volatility, I find that the adjusted implied volatility accurately reflects the patterns of realized volatility and provides an unbiased forecast. Although both the adjusted and unadjusted *MF* implied volatilities

are more efficient than *BS* and *HV*, the former tend to have superior predictive power with respect to relative accuracy.

Our method could be extended to equity and currency markets. Furthermore, while our specification for the futures price process is quite general, our method could be extended to many other continuous time models capturing more empirically relevant features of price and volatility dynamics, such as time-varying risk premiums and jumps in volatility. The recent study by Bollerslev, Gibson, and Zhou (2010) found significant evidence for temporal variation in the volatility risk premiums depending on macro-finance state variables. I leave further work along these lines for future research.

APPENDIX F

APPENDIX F: DERIVATION OF EQUATION 3.10

First, I construct the link between the *MF* implied volatility and the expected *IV* under the *Q* measure. Integrating eq. 3.4 over time and taking expectations, I have

$$E_t^Q(lnS_{t+\Delta}) = lnS_t - E_t^Q\left(\int_t^{t+\Delta}\frac{V_u}{2}du\right) + (\mu^* - \mu_J^*)\lambda^*\Delta.$$

Therefore,

$$E_t^Q\left(IV_{t,t+\Delta}\right) = 2\left(lnS_t - E_t^Q(lnS_{t+\Delta})\right) + 2(\mu^* - \mu_J^*)\lambda^*\Delta.$$

Jiang and Tian (2005) have proven that

$$\int_0^\infty \frac{C(t+\Delta,K)-\max(0,S_t-K)}{K^2}dK = lnS_t - E_t^Q(lnS_{t+\Delta}).$$

It is valid for a very general class of asset price processes including a jump-diffusion process because its derivation does not require any knowledge of the asset return process. The detailed derivation can be found in the appendix of Jiang and Tian (2005). Hence,

(F.1) $$E_t^Q\left(IV_{t,t+\Delta}\right) = MF_{t,t+\Delta} - \phi\Delta,$$

where $\phi = 2\lambda^*\left(\mu_J^* - \mu^*\right)$.

Second, following from the results in Bollerslev and Zhou (2006), I establish the link between the risk-neutral expectation of the *IV* and the expectation of the *IV* in the observed measure:

(F.2) $$E_t^P\left(IV_{t,t+\Delta}\right) = A_\Delta E_t^Q\left(IV_{t,t+\Delta}\right) + B_\Delta.$$

where

$$A_\Delta = \frac{\left(1-e^{-k\Delta}\right)k^*}{\left(1-e^{-k^*\Delta}\right)k},$$

$$B_\Delta = \theta\left[\Delta - \frac{1}{k}\left(1-e^{-k\Delta}\right)\right] - A_\Delta\theta^*\left[\Delta - \frac{1}{k^*}\left(1-e^{-k^*\Delta}\right)\right].$$

Finally, I derive the expression for the expected value of quadratic variation:

(F.3) $$E_t^P\left(QV_{t,t+\Delta}\right) = A_\Delta MF_{t,t+\Delta} - A_\Delta \phi\Delta + B_\Delta + \varphi\Delta.$$

APPENDIX G

APPENDIX G: MONTE CARLO EXPERIMENTAL DESIGN

I assume one year has 252 trading days, and I divide up a day into 45 artificial "5-minute" intervals.[40] I further partition each five-minute interval into 5 smaller segments for the continuous record. The horizon is fixed at two month. Without loss of the generality, I set the drift of the price dynamics in (3.2) to zero. The initial asset price is at 250 cents, and the initial latent stochastic volatility with a two-month maturity begins at 0.025. The parameter configurations in the *P* measure are: $k = 2$, $\theta = 0.025$, $\sigma = 0.1$, $\rho = 0.1$,$\lambda = 6$, $\mu_J = -0.025$, and $\sigma_J = 0.05$, while other parameter configurations in the *Q* measure are: $\mu_J^* = 0.01$, $\lambda^* = 6$, and the volatility risk premium $\delta = -1$.[41] With such parameter configurations, the composite parameters $\phi = 0.01596$ and $\varphi = 0.0192$. The *MF* implied volatility is calculated using the above Jiang and Tian approach. I only use call options with strike prices ranging three SDs from current asset price S_t. The strike price increment is 10 cents, which is close to the 0.35 SDs. Options valuation is based on the stochastic-volatility jump-diffusion model under the risk-neutral measure, eqs. (3.4) and (3.5). I resort to Monte Carlo simulation method for pricing options. The antithetic variable technique is adopted to reduce the standard error of the options value and improve the efficiency of the results. For a 2-month to expiration option, 9450 ($42\times 45 \times 5$) random shocks from a normal distribution are drawn for the price process. This procedure is replicated for the volatility process with drawing shocks from a Poisson process.

[40] In the empirical session, I will apply my method to corn futures. Corn futures trading hours are from 9:30 am to 1:15 pm at the trading floor. Therefore, it generates 45 5-minute returns each day.

[41] Several parameter values refer to parameter estimates of futures price dynamics in the existing agricultural commodity literature (Koekebakker and Lien, 2004).

The simulation sample path for options pricing is set to 10000. The option value for a call is then calculated as the average value across all paths.

REFERENCES

REFERENCES

A ť-Sahalia, Y., Kimmel, B. 2007. Maximum likelihood estimation of stochastic volatility models. Journal of Financial Economics 83, 413-452.

Andersen, T. G., Bollerslev, T. 1998. Answering the skeptics: yes, standard volatility models do provide accurate forecasts. International Economic Review 39, 885-905.

Andersen, T. G., Bollerslev, T., Huang, X. 2010. A reduced form framework for modeling volatility of speculative prices based on realized variation measures. Journal of Econometrics 160,176-189.

Barndorff-Nielsen, O. E., Shephard, N. 2002. Econometric analysis of realized volatility and its use in estimating stochastic volatility models. Journal of the Royal Statistical Society, Series B 64.

Barndorff-Nielsen, O. E., Shephard, N. 2004. Power and bipower variation with stochastic volatility and jumps. Journal of Financial Econometrics 2, 1-48.

Barndorff-Nielsen, O. E., Shephard, N. 2006. Econometrics of testing for jumps in financial economics using bipower variation. Journal of Financial Econometrics 4, 1-30.

Barndorff-Nielsen, O. E., Hansen, P. R., Lunde, A., Shephard, N. 2008. Designing realised kernels to measure the ex-post variation of equity prices in the presence of noise. Econometrica 76, 1481-1536.

Bates, D. 2000. Post-'87 crash fears in S&P500 future options. Journal of Econometrics 94, 181-238.

Becker, R., Clements, A. E., Coleman-Fenn, C. A. 2009. Forecast performance of implied volatility and the impact of the volatility risk premium. NCER working paper.

Bollerslev, T., Zhou, H. 2002. Estimating stochastic volatility diffusion using conditional moments of integrated volatility. Journal of Econometrics 109, 33-65.

Bollerslev, T., Zhou, H. 2006. Volatility puzzles: a simple framework for gauging return-volatility regressions. Journal of Econometrics 131, 123-150.

Bollerslev, T., Gibson, M., Zhou, H. 2010. Dynamic estimation of volatility risk premia and investor risk aversion from option-implied and realized volatilities. Journal of Econometrics 160, 235-245.

Britten-Jones, M., Neuberger, A. 2000. Option prices, implied price processes, and stochastic volatility. Journal of Finance 55, 839-866.

Canina, L., Figlewski, S. 1993. The informational content of implied volatility. Review of Financial Studies 6, 659-681.

Carr, P., Wu, L. 2009. Variance risk premiums. Review of Financial Studies 22, 1311-1341.

Chernov, M. 2007. On the role of risk premia in volatility forecasting. Journal of Business and Economic Statistics 25, 411-426.

Christensen, B. J., Prabhala, N. R. 1998. The relation between implied and realized volatility. Journal of Financial Economics 50, 125-150.

Doran, J. S., Ronn, E. I. 2008. Computing the market price of volatility risk in the energy commodity markets. Journal of Banking and Finance 32, 2541-2552.

Ederington, L. H., Guan, W. 2002. Is implied volatility an informationally efficient and effective predictor of future volatility? Journal of Risk 4, 29-46.

Egelkraut, T. M., Garcia, P. 2006. Intermediate volatility forecasts using implied forward volatility: the performance of selected agricultural commodity options. Journal of Agricultural and Resource Economics 31, 508-528.

Gordon, S., St-Amour, P. 2004. Asset returns and state-dependent risk preferences. Journal of Business and Economic Statistics 22, 241-252.

Heston, S. 1993. A closed-form solution for options with stochastic volatility with applications to bond and currency options. Review of Financial Studies 6, 327-343.

Huang, X., Tauchen, G. 2005. The relative contribution of jumps to total price variance. Journal of Financial Econometrics 3, 456-499.

Hull, J., White, A. 1987. The pricing of options on assets with stochastic volatilities. Journal of Finance 42, 281-300.

Jiang, G., Tian, Y. 2005. The model-free implied volatility and its information content. Review of Financial Studies 18, 1305-1342.

Jones, C. S. 2003. The dynamics of stochastic volatility: evidence from underlying and options markets. Journal of Econometrics 116, 181-224.

Jorion, P. 1995. Predicting volatility in the foreign exchange market. Journal of Finance 50, 507-528.

Koekebakker, S., Lien, G. 2004. Volatility and price jumps in agricultural futures prices: evidence from wheat options. American Journal of Agricultural Economics 86, 1018-1031.

Lamoureux, C. G., Lastrapes, W. D. 1993. Forecasting stock returns variances: towards understanding stochastic implied volatility. Review of Financial Studies 6, 293-326.

Newey, W. K., West, K. D. 1987. A simple positive semi-definite, heteroskedasticity and autocorrelation consistent covariance matrix. Econometrica 55, 703-708.

Pan, J. 2002. The jump-risk premia implicit in options: evidence from an integrated time-series study. Journal of Financial Economics 63, 3-50.

Szakmary, A., Ors, E., Kim, J. R., Davidson, W. N. 2003. The predictive power of implied volatility: evidence from 35 futures markets. Journal of Banking and Finance 27, 2151-2175.